Journal of the

ENGINEERING MECHANICS DIVISION

Proceedings of the American Society of Civil Engineers

CONTENTS

July, 1959

Papers

Journal of the
ENGINEERING MECHANICS DIVISION
Proceedings of the American Society of Civil Engineers

COMMENTARY ON PLASTIC DESIGN IN STEEL: BASIC CONCEPTS

Progress Report No. 1 of the Joint WRC-ASCE Committee on Plasticity Related to Design

FOREWORD

The Joint Committee has approved the publication of this Commentary on Plastic Design in Steel with a strong recommendation that it be read carefully by all structural engineers. It is based on a series of preliminary reports prepared for the Welding Research Council and the American Society of Civil Engineers by a research group at Fritz Engineering Laboratory, Department of Civil Engineering, Lehigh University.

Although much of the experimental and theoretical work reported was performed at Lehigh University, the WRC-ASCE Joint Committee has broadened this Commentary by including the results of research at other institutions, both here and abroad. The inclusion of this information and of certain unpublished data is gratefully acknowledged.

Among the recent books which should be consulted for a much fuller discussion than space permits here are Refs. 1.1 to 1.7. Problems associated with stability, connections, and design procedures are discussed in Refs. 1.1, 1.2 and 1.3.

SYNOPSIS

The evaluation of a considerable amount of research work has demonstrated the applicability of plastic analysis to structural design. For the type of structure to which its application is intended plastic design results in an overall balanced design, it makes for a more economical use of material, and compared with allowable stress ("elastic") methods it is a simpler design technique.

Note: Discussion open until December 1, 1959. Separate discussions should be submitted for the individual papers in this symposium. To extend the closing date one month, a written request must be filed with the Executive Secretary, ASCE. Paper 2091 is part of the copyrighted Journal of the Engineering Mechanics Division, Proceedings of the American Society of Civil Engineers, Vol. 85, No. EM 3, July, 1959.

This report documents the applicability of plastic analysis to design of structural steel beams and frames. Theoretical considerations involved in the plastic theory and in certain secondary design problems are given. Experimental verification is provided. Approximations in the form of "design guides" are suggested.

A separate and companion report[1.3] illustrates the procedures of the plastic method of design with specific reference to building construction, and supplies information to supplement clauses in a specification for plastic design.

This progress report covers only a portion of the subject matter. Other papers will follow and will cover "Additional Design Considerations" (shear force, local buckling, lateral buckling, repeated loading), "Compression Members", "Connections" and "Deflections".

The complete table of contents follows. Progress Report No. 1 includes Chapters 1, 2, 3, a set of definitions, and the Nomenclature for the entire Commentary.

COMMENTARY ON PLASTIC DESIGN IN STEEL

TABLE OF CONTENTS

CHAPTER 1. INTRODUCTION

1.1 Structural Design

An engineering structure is satisfactorily designed if it can be built with the needed economy and if, throughout its useful life, it carries its intended loads and otherwise performs its intended function. In the process of selecting the members for a steel frame structure it is necessary first to make a general analysis of structural strength and, second, to examine certain details (usually covered by codes or specifications) to assure that premature local failure does not occur.

The design load of a steel frame may be controlled by a number of criteria, any one of which may actually constitute a "Limit of Structural Usefulness." These are:

1. Hypothetical attainment of a specified minimum yield-point stress (design based on allowable stress)
2. Attainment of maximum plastic strength (assuming idealized behavior)
3. Excessive deflections
4. Instability
5. Fatigue

Item 1 in conjunction with Items 4 and 5 has, for many years, been the basis for structural design which uses the "allowable stress" concept. Certain provisions also are included in specifications which are intended to insure that the capacity is not otherwise limited. Under certain adverse conditions steel may fracture in a brittle manner; and although no specific rule has been available, the occurrence of such fractures has been reduced to a minimum by proper attention to material, design details, and fabrication procedures.

Strictly speaking, a design based on any one of the five criteria tabulated above could be referred to as a "Limit Design," although the term usually has been applied to determination of maximum strength according to Items 2 and 4. "PLASTIC DESIGN," as an aspect of limit design, embraces primarily Item 2 (attainment of maximum plastic strength) and is especially applicable to continuous beams and frames. It is based upon the maximum load the structure will carry, as determined from an analysis of strength in the plastic range (that is, a plastic analysis). Whereas "elastic design" is performed by assuming working loads and a working unit stress, plastic design is based on the concepts of ultimate loads, obtained by applying an appropriate load factor, and ultimate (or capacity) moments.

1.2 Plasticity and Design—Some Advantages and Limitations

It has long been known that an indeterminate steel frame has a greater load-carrying capacity than indicated by the allowable stress concept. Such frames are able to carry increased loads above the yield value because structural steel has the capacity to yield. While the allowable stress concept is satisfactory for simple structures, its extension to indeterminate steel structures has overemphasized the importance of stress rather than strength as a guide in engineering design. Furthermore it has introduced a complexity that is unnecessary for a large number of structures.

Indeed, there is no basis for an assumption that at no time should the stress in a steel structure go beyond the elastic range. If this premise were sound, then much current practice would have to be abandoned. As a matter of fact it is necessary to consider plasticity in all structural design. An actual structure is a very complex body with an extremely complicated state of stress. It is an assembly of many individual members joined together to form a working unit. The individual structural elements such as the beams and columns come from the mills with residual stresses which are often over one-half the yield stress. In connecting the parts together local stresses are produced by welding and misfits, and there are over-all assembly stresses. The structure is pierced by many holes, reinforcements of all kinds are present such as cover plates and stiffeners, and many secondary stresses arise owing to continuity of the structure; for example because of the deformations caused by the loading, bending and torsion may occur in what are assumed to be simple tension members, and axial force and torsion may occur in beams. As a consequence of these factors (the combination of unknown initial stress, stress concentration and redistribution due to discontinuities of the structure), it is inevitable that local plastic flow will take place in the best of designs. An examination of actual load-deflection curves presented later in this report will demonstrate this conclusively.

Numerous examples can be given in which the benefits of plasticity are used, consciously or unconsciously, in allowable stress design. By permitting a bending stress of 30,000 psi in a round pin, advantage is being taken of the considerable plastic reserve of strength (70%) that such a shape possesses. Similarly the 20% increase in allowable working stress permitted at points of interior support in continuous beams represents another case in which some advantage has been taken of the redistribution which results from ductility in design.

From the foregoing discussion it is evident that local yielding undoubtedly occurs in most steel frames the first time full service loads are reached. Furthermore parts of these structures will enter appreciably into the plastic range before reaching their assumed limit of carrying capacity.

This situation will also exist in a structure designed on the basis of plasticity. Nevertheless it is important to note that at working load, the plastically designed structure is normally in the so-called "elastic" range. A plastic design is based on a load which is equal to the working load multiplied by a load factor. Any local inelastic deformation at working load occurs only at first loading, precisely as it does in an elastically designed structure. This produces a state of residual stresses such that subsequent reapplication of the working load will produce purely elastic stresses.

Knowledge of the ductile behavior of steel also permits the designer to eliminate costly details intended to provide actual hinges that would be required only in case the construction material were brittle. With modern welding techniques, full capacity splices are often less expensive than mechanical hinges or other details that would allow more or less free rotations. With a knowledge of behavior in the plastic range, the designer will realize that the elimination of hinges simply results in a stiffer structure with a strength at least equal to that calculated for the same structure with hinges. The saving in fabrication costs that result due to a better design of details based on an understanding of ductile behavior may be very great indeed.

An exact plastic design which considered strain-hardening would be a formidable task. However, if the behavior of structural steel is idealized,* so that it is either completely elastic or perfectly plastic, then there is obtained a simple and yet a reasonably satisfactory approximation termed plastic design.** Within this simplification, the structure is assumed to reach its maximum predictable strength at a definite load called the "plastic limit load" or "ultimate load." For a large majority of continuous beams and frames, a design based upon a reasonable factor of safety (load factor) against this ultimate load provides a more appropriate structure than a design based upon allowable stresses and elastic stress computations.

As was intimated at the outset, there are a number of design factors to which consideration must be given over and beyond the selection of members on the basis of plasticity. One such factor is the effect of repeated loading. Another is the onset of buckling before full plasticity is reached and, in general, any other effect by which the weakening or strengthening effect of deformation prior to failure is large. Brittle fracture is another problem, of equal importance both to elastic and to plastic design. Ultimate load computations for continuous frames are based on the assumption that "plastic hinge moments" are developed at points of maximum moment in the structure and maintained during the subsequent loading. Thus design criteria for the stability of details, which under allowable stress design merely guard against the initiation of buckling prior to first yielding, require re-examination in plastic design where plastic buckling must be controlled during hinge deformation. The magnitude of the deflection at working load may constitute still another design criterion. All of these problems are discussed in more detail later; however, it is emphasized here that in principle the problems of plastic design are no different from that which exists in any design procedure.

A Hungarian, Gabor Kazinczy, first applied the plasticity concepts to the design of some apartment-type buildings in 1914.[1.8,1.9] Other early tests were made in Germany by Maier-Leibnitz.[1.10] Since that time, significant contributions have been made to the plastic theory of structures both in this country and abroad.*** Plastic design is already a part of certain specifications (it is widely used in Britain) and engineers in this country are now making use of it.

It is emphasized that plastic design is not a technique that is intended to replace all other design procedures. Factors such as fatigue and buckling may become the design criteria. As an example of a limitation that comes about because of column buckling, most trusses would be excluded from plastic design (with the exception of the Vierendeel type); the method discussed herein requires that "hinges" form, and chord members would not exhibit the necessary deformation capacity in compression. In ordinary building construction, limitations such as fatigue and buckling are usually the exception and not the rule. Therefore plastic design is finding considerable application in continuous beams and frames where the members are stressed primarily in bending.

---

*See Chapter 2.

**More precisely "plastic limit design" but referred to hereafter by the shorter term.

***See Refs. 1.1, 1.4, 1.6 and 1.11 to 1.17, inclusive.

CHAPTER 2. BASIC PRINCIPLES

2.1 Behavior of Material and Structural Elements

Plastic design takes advantage of an important and unique property of structural steel, namely its ductility. Evidence of this ductility may be seen by examining a stress-strain curve obtained from a simple tension or compression test. This curve may be represented in idealized form by two straight lines as shown in Fig. 2.1. Up to the yield stress level the material is elastic. After the yield stress has been reached the strain increases greatly without any further increase of the stress. From this it follows that the attainment of a maximum fiber stress equal to the yield value does not result in failure of a bent beam. Rather, the section has a plastic reserve in strength which depends on the shape of the cross section.

Fig. 2.2 shows the stress distribution at five stages as bending moment is applied to a member of rectangular cross section. It is assumed that each fiber behaves as shown in Fig. 2.1 and that plane sections before bending remain plane after bending. The moment-curvature relationship for this beam is shown in Fig. 2.3; the numbered points correspond to the five stages in Fig. 2.2. Stage 2 corresponds to the yield moment My and stage 5 corresponds to the plastic moment, Mp. The exact shape of the moment-curvature diagram between stages 2 and 5 depends on the cross-sectional form, but the moment rapidly approaches the value of the full plastic moment corresponding to stress distribution 5 (Fig. 2.2). The "rapid approach" to this limiting plastic moment is the essence of simple plastic theory. In most calculations

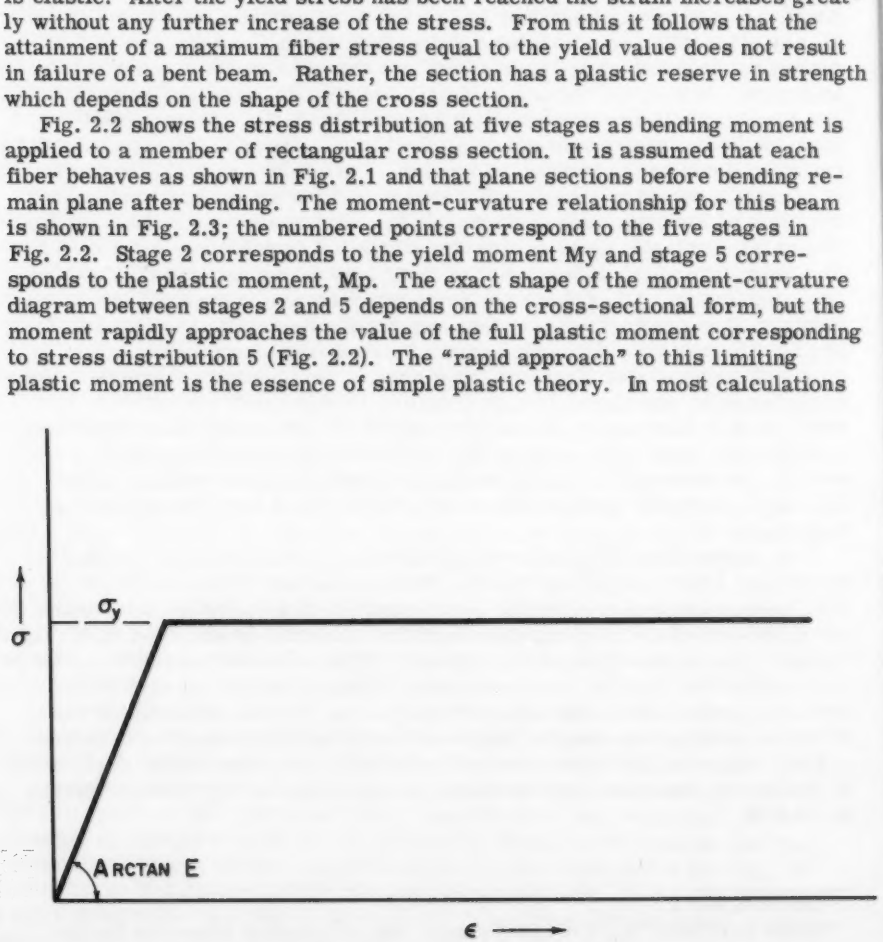

Fig. 2.1. Stress-Strain Curve for Uniaxial Tension or Compression

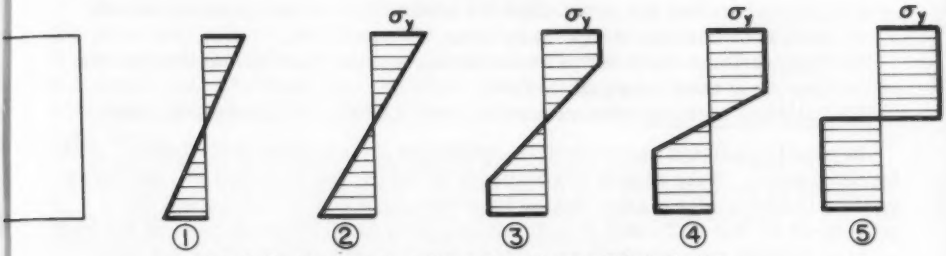

Fig. 2.2. Successive Stages of Stress Distribution

the moment-curvature relationship is approximated by two straight lines as shown partially dotted in Fig. 2.3.

The process of successive yielding of fibers as bending moment is increased (stage 2 to stage 5 of Fig. 2.3) is called plastification of the cross section. At the section(s) where yielding occurs, relatively large rotations are possible without a significant increase or decrease of moments; in other words, "plastic hinges" develop. The plastic hinge thus formed permits redistribution of moments in statically indeterminate beams and frames. Thus, further increases of the loads are carried by other less heavily stressed parts of the structure, until a sufficient number of plastic hinges are formed and the structure starts to behave as a mechanism. Thereafter deflections increase rapidly while the loads remain practically constant. In other words, the ultimate load has been reached.

In summary, a structure will reach its ultimate load as determined by simple plastic theory only if the sections or connections where plastic hinges are to form attain the predicted moment and subsequently are able to undergo sufficiently large rotations. An exception, of course, is the plastic hinge which forms last, for which no inelastic rotation is required after the plastic moment has been reached.

2.2 Plastic Theory

Conditions

In the elastic analysis of an indeterminate structure one must consider three conditions:

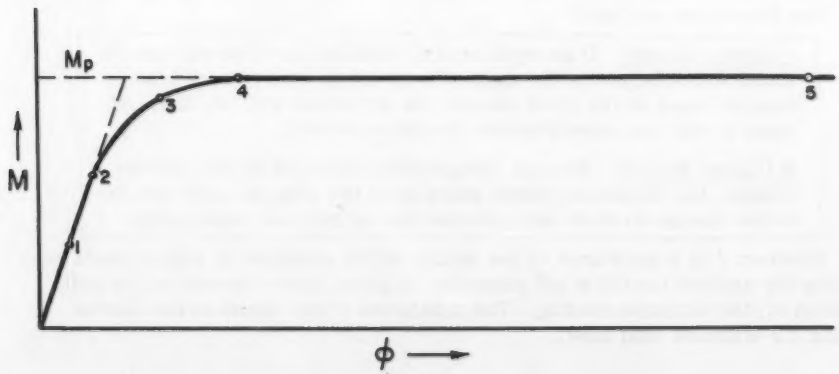

Fig. 2.3. Moment-Curvature Relationship for Beam in Bending

1. Continuity—the deflected shape is assumed to be a continuous curve, and thus "continuity equations" may be formulated.
2. Equilibrium—the summation of the forces and moments acting on any free body must be equal to zero.
3. Limiting Moment—the moment at first yield is the limiting moment.

In plastic analysis three similar conditions (or modifications thereof) must be considered. With regard to continuity of slope, the situation is just the reverse: theoretically plastic hinges interrupt such continuity, so the requirement is that sufficient plastic hinges form to allow the structure (or part of it) to deform as a mechanism. This could be termed a mechanism condition. The equilibrium condition is the same as in elastic analysis. Instead of initial yield, the limit of usefulness is the attainment of plastic hinge moments, not only at one cross section but at each of the sections involved in the mechanism motion; this requirement will be termed a plastic moment condition. A corollary to this is the obvious fact that moments in excess of the plastic bending strength cannot be resisted. The three conditions that must be satisfied in plastic analysis are, therefore,

1. Mechanism Condition
2. Equilibrium Condition
3. Plastic Moment Condition

When all three of these conditions are satisfied, then the resulting analysis for ultimate load is correct because the two limit theorems basic to the plastic method are satisfied. These theorems will now be discussed.

Limit Theorems

A general treatment of structures requires consideration of the plastic limit theorems of Drucker, Greenberg, and Prager[1.14,2.1,2.2] which have provided concise and rigorous formalization of intuitively known concepts of structural failure. According to the concepts discussed in Art. 2.1, structural steel may be idealized as an elastic-perfectly plastic material (Fig. 2.1). Therefore when changes in geometry are neglected (as is done in most elastic solutions) it can be shown that failure occurs under constant load and at constant stress. In Art. 2.1 this was stated in a different way, namely, that the ultimate load is reached when a sufficient number of sections have attained their "limit" or "plastic hinge" moment. Only plastic strains take place as deformation occurs at constant load.

The theorems are then:

> I (Lower Bound). If an equilibrium distribution of stress can be found which balances the applied load and is everywhere less than or equal to the yield stress, the structure will not fail. At most it will just have reached the ultimate load.
>
> II (Upper Bound). For any compatible pattern of plastic deformation, the structure cannot stand up if the rate at which the external forces do work exceeds the rate of internal dissipation.

Theorem I is a statement of the ability of the material to adjust itself to carry the applied load if at all possible. It gives lower bounds on, or safe values of, the ultimate loading. The maximum lower bound is the plastic limit, or ultimate load itself.

Theorem II is a formal statement of the fact that if a path to failure exists, the structure will not stand up. Thus a load computed on the basis of an assumed mechanism will always be greater than (or at least equal to) the true ultimate load. The theorem, therefore, deals with upper bounds on, or unsafe values of, the plastic limit load. The minimum upper bound is the ultimate load itself.

Plane frames and continuous beams are simple enough to permit "exact" calculations of the ultimate load. Almost all of this Commentary is devoted to a consideration of such frames and beams because of the important position they occupy in civil engineering structural practice.

An actual, therefore three-dimensional, building frame usually is treated as a collection of two-dimensional frames. This procedure is equivalent to setting a number of secondary interaction bending moments and torques equal to zero and is on the safe side according to Theorem I.

For complicated structures it may well be that "exact" ultimate loads cannot be found due to involved geometry of parts or of the complete structure. These two theorems enable the bracketing of the answer closely enough for practical engineering purposes.

The simplicity of plastic analysis opens the way to direct plastic design, as contrasted with the trial-and-error procedure which is normally necessary in allowable stress design of indeterminate structures. Some steps that have been taken along these lines will be outlined.

There are numerous methods by which the maximum strength of a continuous steel structure may be determined. In the semi-graphical ("statical" or "equilibrium") method, an equilibrium moment diagram is drawn such that the moment is nowhere greater than Mp. It thus automatically satisfies the lower bound theorem. The resulting ultimate load is correct only if sufficient plastic hinges were assumed to create a mechanism (thus satisfying the upper bound theorem). In the mechanism method a mechanism is assumed and the resulting virtual work equations are solved for ultimate load. This value is correct only if the plastic moment condition is also satisfied.

CHAPTER 3. ANALYSIS AND DESIGN

The purpose of this chapter is to indicate the important assumptions of the simple plastic theory and to describe the essential features of plastic analysis by the "Statical" and the "Mechanism" methods. It is not intended to present a complete discussion of all the various methods available for analysis and design; Refs. 1.1, 1.2, 1.3, 1.4, 1.5, 1.6, 3.1, 3.2 and 3.3 may be consulted for this purpose. However, by presenting in Arts. 3.2 and 3.3 a brief outline of two frequently-encountered methods, it is hoped that the significance of the basic principles and assumptions will become evident.

3.1 Assumptions

The important concepts and assumptions with regard to the plastic behavior of structures according to the "simple plastic theory" are as follows:

1. The material is ductile. It has the capacity of absorbing plastic deformation without the danger of fracture.
2. Each beam shape has a maximum resisting moment (the plastic moment Mp), a moment that is attained through plastic yield of the entire cross section (plastification).
3. Because of the ductility of steel, rotation at relatively constant moment will occur through a considerable angle; in other words, a plastic hinge will form.
4. Connections proportioned for full continuity will transmit the calculated plastic moment.
5. As a result of the formation of plastic hinges at connections and other points where the moments under elastic condition were the critical ones, redistribution of moment will occur, allowing the formation of plastic hinges elsewhere, where the moments under elastic condition were less than critical.
6. The ultimate load may be computed on the basis that a sufficient number of plastic hinges have formed to create a mechanism.
7. The deformations are so small that the equilibrium equations can be formulated for the undeformed structure (as in ordinary elastic analysis).
8. No instability will occur prior to the attainment of the ultimate load.
9. The influence of normal force and shearing force on the plastic moment is neglected.
10. The loading is proportional, i.e., the ratios between different loads remain constant during loading.

The experimental verification of some of these assumptions is presented later in this report (Chapters 5 and 8). Other assumptions may need implementation to assure that the appropriate requirements are met, and this is the concern of portions of Chapter 4 and of Chapters 6 and 7 which will appear in later Progress Reports.

3.2 Statical Method of Analysis

The statical method of analysis is suitable for continuous beams and for frames in which the number of redundants does not exceed two or three. As described in Art. 2.2 the objective of this method is to draw a possible moment diagram in such a way that the plastic moment condition is not violated ($M \leq M_p$) but with sufficient plastic hinges being formed to create a mechanism. An example follows.

Suppose it is desired to determine the total load W_u in span L that may be carried by a beam of given moment capacity in a multi-span structure. One of the interior spans A-C is shown in Fig. 3.1a.

As the load W increases from zero, there are peak moments at the two supports and a peak moment within the span. In general the moments at the two supports will be unequal, and a typical moment diagram at the elastic limit is shown in Fig. 3.1b. The maximum moment within the span is not at the span center line but is near it. As the load increases still further, the greater end moment (C) attains M_p and a plastic hinge forms there. As the load further increases, the other support moment (A) attains M_p, and the maximum moment within the span increases as shown by curve 2 in Fig. 3.1c. There now being a hinge at each end of the span, the point of maximum moment has shifted to the center of the span and the moment curve 2 is symmetrical. Finally a plastic hinge also forms at the center, and this corresponds to the ultimate load condition. The moment diagram at ultimate load W_u is shown by curve 3 in Fig. 3.1d.

The maximum ordinate of the statical moment diagram must be $\frac{W_u L}{8}$. Thus, referring to sketch d,

$$\frac{W_u L}{8} = M_p + M_p \tag{3.1}$$

or

$$W_u = \frac{16 M_p}{L} \tag{3.2}$$

As described in Art. 4.6, the plastic moment of any beam cross section may be computed from a knowledge of the yield stress level and the cross section geometry. Thus the ultimate load W_u is determined. Alternatively, if the required ultimate load is given by the terms of the problem, the required Mp for the beam may be calculated and the beam selected. It will be seen from Fig. 3.1d that the plastic solution for a uniform, restrained beam may be expressed as follows:

> Draw the statical moment curve for load W_u on a beam of the same span but with hinged ends. Draw a new base line for zero moments (a "fixing line") at the mid-height of this curve. Equate the three maximum moments thus found to M_p.

This completes the solution for an interior span of a continuous beam with restraining moments at least as great as the strength of the beam selected. The same reasoning as followed above for a uniform load will lead to the same solution method for other loading types, such as partial uniform or concentrated.

Of course, where a smaller beam adjoined an interior span or in the case of an end span with simple exterior support, the fixing line would not be drawn

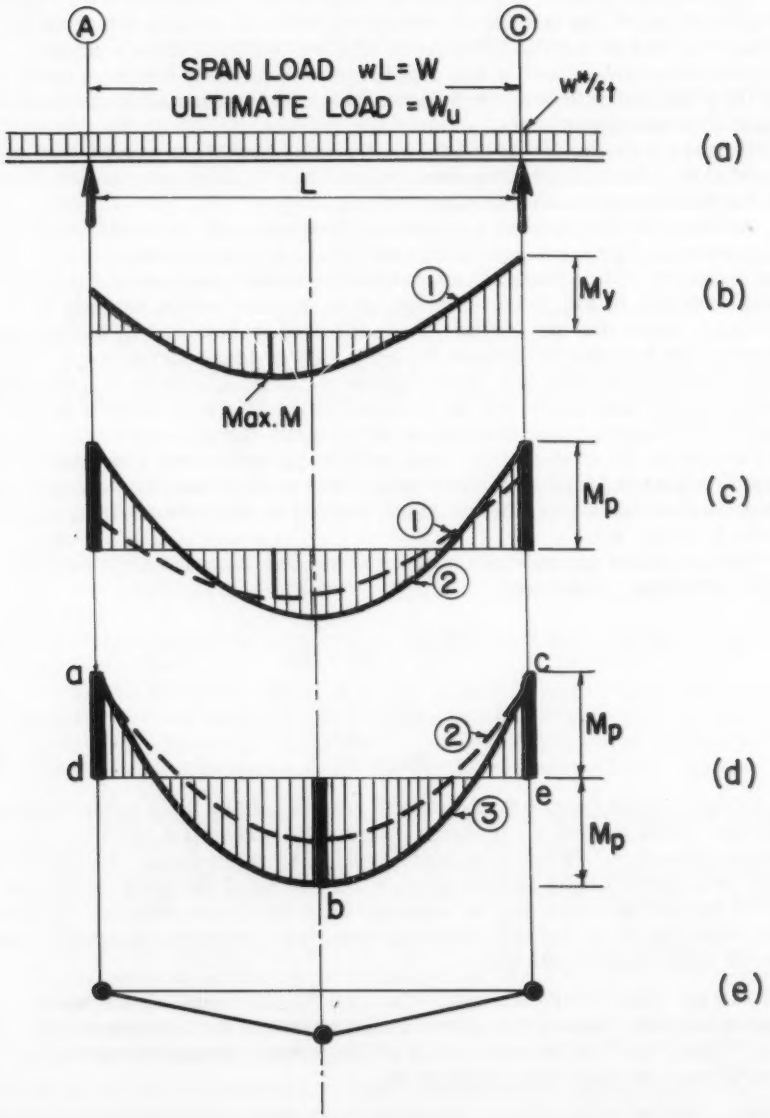

Fig. 3.1. Statical Method of Analysis Applied to a Continuous Beam

at mid-height of the determinate moment diagram. The position of the fixing line reflects the moment capacity at the points of peak moment. In essence, then, the failure moment diagram is drawn in such a way that a mechanism forms. Curve 3 of Fig. 3.1d satisfies this requirement, of course, because the three plastic hinges at a, d, and e result in the mechanism shown in Fig. 3.1e.

In plastic design of continuous beams and frames it is unnecessary to consider the elastic distribution of moments such as that shown in Fig. 3.1b or the behavior under increasing load. A systematized procedure for the general case would simply involve the construction of a determinate moment diagram (corresponding to curve a-b-c of Fig. 3.1d) which is then combined with a redundant moment diagram (a-d-e-c) in such a way that a mechanism is formed.

3.3 Mechanism Method of Analysis

Although the matter of personal preference is frequently involved in the selection of a particular method of analysis, when the number of redundants in a frame exceeds two or three the mechanism method usually will be found most suitable. As intimated in Art. 2.2, the objective in the mechanism method is to select from all the possible modes of failure the one that corresponds to the lowest possible "ultimate" load. A check is provided through the construction of the moment diagram to make sure that the plastic moment condition is not violated ($M \leq M_p$). In essence, therefore, the mechanism method gives an upper bound solution that is the correct value of the ultimate load when it also satisfies the lower bound theorem. An example follows.

Analysis of Rectangular Portal Frame

Suppose it is required to find the ultimate load for the structure shown in Fig. 3.2. The section is of uniform moment capacity M_p throughout.

The first step in the mechanism method is to find the position of possible plastic hinges. These hinges may form at points of peak moment (that is, where the shear passes through zero at such places as concentrated load points, connections, etc.); and therefore the possible plastic hinge locations are at sections 1, 2, 3, 4 and 5.

The next step is to select for investigation the various possible failure mechanisms. Three of these are shown in Fig. 3.2. Mechanism 1 corresponds to the action of vertical load P and is called a "beam" mechanism. Mechanism 2 corresponds to the action of the horizontal load P and is often referred to as a "sway" or "panel" mechanism. Mechanism 3, on the other hand, is a composite mechanism representing the action of both loads; it is a combination of mechanisms 1 and 2 that eliminates a plastic hinge at section 2.

The correct failure mechanism will be the one which results in the lowest load since any greater load would mean that the plastic moment condition would be violated. The load that corresponds to each mechanism may be computed by the principle of virtual displacements and is illustrated as follows: Referring to Fig. 3.2b, suppose that after the ultimate load is reached the beam is allowed to move through a virtual displacement Δ. For equilibrium, the external work (W_E) done by the load as it moves through this small displacement must equal the internal work (W_I) absorbed at each hinge as it rotates through a corresponding small angle, or

$$W_E = W_I \tag{3.3}$$

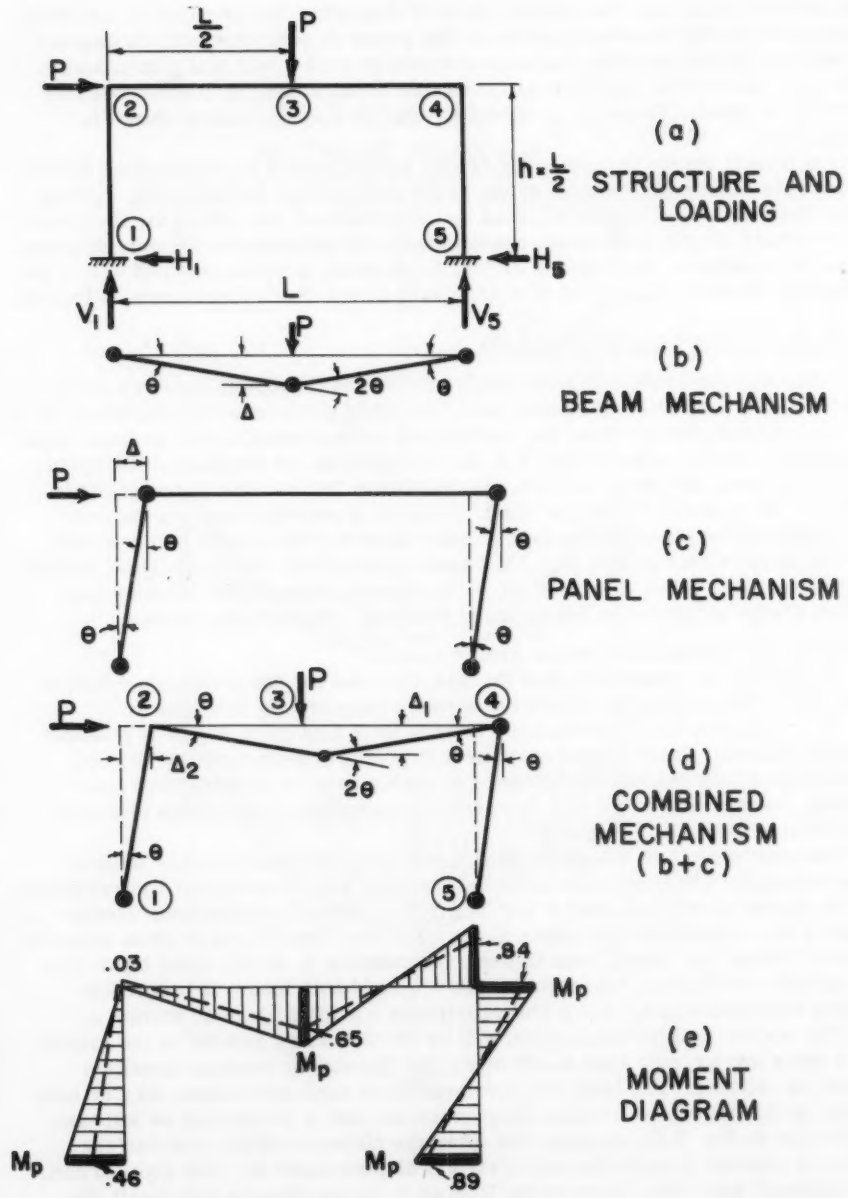

Fig. 3.2. Mechanism Method of Analysis Applied to a Fixed-Ended Rectangular Portal Frame

For mechanism 1 the external work is given by

$$W_E = P\Delta = P\frac{L}{2}\theta \tag{3.4}$$

The internal work is given by

$$W_I = M_p\theta = M_p 2\theta + M_p\theta = 4M_p\theta \tag{3.5}$$

Making use of Eq. (3.3),

$$P\frac{L}{2}\theta = 4\,M_p\theta$$

$$P_1 = \frac{8M_p}{L} \tag{3.6}$$

Similarly, for mechanism 2,

$$P\frac{L}{2}\theta = M_p(\theta + \theta + \theta + \theta)$$

$$P_2 = \frac{8\,M_p}{L} \tag{3.7}$$

and for mechanism 3,

$$P\Delta_1 + P\Delta_2 = M_p(\theta + 2\theta + 2\theta + \theta)$$

$$P\frac{L}{2}\theta + P\frac{L}{2}\theta = 6\,M_p$$

$$P_3 = \frac{6\,M_p}{L} \quad \leftarrow \boxed{P_u} \tag{3.8}$$

Since the lowest value is P_3, this is assumed to be the true ultimate load.

It is desirable to check to make sure that some other mechanism was not overlooked. This may be done by examining the plastic moment condition through construction of the moment diagram. The complete diagram is shown in Fig. 3.2e, the moment at each section being determined by statics (the moments are plotted on the tension side of the member). It is found that $M \leq M_p$ throughout, and thus the answer determined above is verified. It is only a coincidence that the moment at section 2 is equal to zero.

The dotted line in Fig. 3.2e traces the moment diagram at the stage at which the hypothetical yield moment would first be reached in the frame—namely at section 5, where the moment is shown as M_y. The first plastic hinge would form there, followed by hinges at sections 4, 3, and finally at 1.

3.4 Other Methods

The two previous articles have presented in simplified form the most important steps in two methods of plastic analysis. References 1.1 through 1.6, 3.1, 3.2 and 3.3 may be consulted for complete systematized procedures of analysis and design using these methods.

In addition to the Statical and Mechanism methods of analysis, other techniques are available for determining the ultimate load a structure will support. Two of these are the "Method of Inequalities" and the "Plastic Moment Distribution" method. References 1.13 and 3.4 cover these methods which have a particular application for certain structural problems.

Just as in elastic design, where the engineer has available certain charts, tables and formulas with which to analyze standard cases, so also it has been

possible to develop convenient design aids for the rapid selection of member sizes. The designer may use such techniques to shorten the design time even further, but discussion of these aids is not within the scope of this report. Many such techniques have been illustrated on practical design examples in Ref. 1.3.

ACKNOWLEDGMENT

The Joint Committee acknowledges the work of a research group at Fritz Engineering Laboratory, Department of Civil Engineering, Lehigh University. This group has been engaged through the Institute of Research in an investigation entitled "Welded Continuous Frames and Their Components". The results of that investigation were the basis of preliminary reports which were later revised and supplemented by the Joint WRC-ASCE Committee. The staff members at Fritz Laboratory included L. S. Beedle, G. C. Driscoll, Jr., T. V. Galambos, R. L. Ketter, T. Kusuda, G. C. Lee, T. Lee, L. W. Lu, A. Ostapenko and B. Thurlimann. Wm. J. Eney is Director of Fritz Laboratory and Head of the Civil Engineering Department.

The organizations that supported the research projects out of which the preliminary reports were prepared were the following: American Institute of Steel Construction, American Iron and Steel Institute, Column Research Council, the Navy Department (Office of Naval Research, Bureau of Ships, Bureau of Yards and Docks) and the Welding Research Council.

Respectfully submitted,

A. Amirikian
Lynn S. Beedle
J. M. Crowley
F. H. Dill
Samuel Epstein
LaMotte Grover
William H. Jameson
Bruce G. Johnston
Jonathan Jones
R. L. Ketter
Carl Kreidler
H. W. Lawson
Nathan M. Newmark
R. M. Stuchell
John Vasta

T. R. Higgins, Chairman

Lehigh Project Subcommittee

Structural Steel Committee
Welding Research Council

Frank Baron
John M. Biggs
Daniel C. Drucker
John D. Griffiths
William J. Hall
T. R. Higgins
Harry N. Hill
Eivind Hognestad
Robert L. Janes
Bruce G. Johnston
William H. Munse, Jr.
Egor P. Popov
John B. Scalzi
Paul S. Symonds
Bruno Thurlimann
George Winter
Douglas T. Wright
Lynn S. Beedle, Chairman

Committee on Plasticity Related to Design
Engineering Mechanics Division
American Society of Civil Engineers

Definitions

Ultimate Load or Plastic Limit Load.—The load attained when a sufficient number of yield zones have formed to permit the structure to deform plastically without further increase in load. It is the largest load a structure will support, when perfect plasticity is assumed and when such factors as instability, strain-hardening and fracture are neglected.

Allowable Stress Design—A design method which defines the limit of structural usefulness as the load at which a calculated stress equal to the yield point of the material is first attained at any point (usually disregarding local stress raisers).

Plastic Design.—A design method for continuous steel beams and frames which defines the limit of structural usefulness as the "ultimate load." (The term, "plastic" comes from the fact that the ultimate load is computed from a knowledge of the strength of steel in the plastic range).

Factor of Safety.—As used in elastic (allowable stress) design, it is a factor by which the yield stress is divided to determine a working or allowable stress for the most highly stressed fiber.

Load Factor.—In plastic design, a factor by which the working load is multiplied to determine the ultimate load. This choice of terms serves to emphasize the reliance upon load-carrying capacity of the structure rather than upon stress.

Yield Moment.—In a member subjected to bending, the moment at which an outer fiber first attains yield point stress.

Plastic Moment.—The resisting moment of a fully-yielded cross-section.

Plastification.—Gradual penetration of yield stress from the outer fiber towards the centroid of a section under increasing moment. Plastification is complete when the plastic moment, M_p, is attained.

Plastic Modulus.—The modulus of resistance to bending of a completely yielded cross section. It is the combined statical moment about the neutral axis of the cross-sectional areas above and below that axis.

Shape Factor.—The ratio M_p / M_y, or Z/S, for a cross-section.

Plastic Hinge.—A yielded zone which forms in a structural member when the plastic moment is applied. The beam rotates as if hinged, except that it is restrained by the moment M_p.

Hinge Angle.—The angle of rotation through which a yielded segment of a beam must sustain its plastic moment value.

Rotation Capacity.—The angular rotation which a given cross-sectional shape can sustain at the plastic moment value without prior local failure.

Mechanism.—An articulated system able to deform without a finite increase in load. It is used in the special sense that the linkage may include real hinges and/or plastic hinges.

Redistribution of Moment.—A process which results in the successive formation of plastic hinges until the ultimate load is reached. As a result of the

formation of plastic hinge, less-highly stressed portions of a structure may carry increased moments.

Proportional Loading.—All loads increase in a constant ratio, one to the other.

Nomenclature

A = Area of cross-section.

A_f = Area of two flanges of WF shape, $A_f = 2bt$.

A_p = Cross-sectional area of plate.

A_w = Area of web, $A_w = wd$.

a = Column height to span length ratio of gable frame (column height = aL).
= Distance between centroids of cross-sectional area above and below neutral axis.
= Distance from end of cantilever to critical section of beam.

b = Flange width.
= Breadth of rectangular cross section.
= Roof rise to span length ratio of gable frame (roof rise = bL).

C = Overturning moment parameter (windward side).

C_f = Correction factor due to end fixity (restraint) for determining critical length for lateral buckling.

c = Distance from neutral axis to the extreme fiber.

D = Overturning moment parameter (leeward) side.

d = Depth of section.

d_f = Distance between centers of two flanges.

d_p = Distance between two cover plates.

d_w = Web depth of WF shape ($d - 2t$).

E = Young's modulus of elasticity.

E_{st} = Strain-hardening modulus.

E_t = Tangent modulus.

e = Eccentricity.

F = Load factor of safety.

f = Shape factor $= \frac{M_p}{M_y} = \frac{Z}{S}$.

G = Modulus of elasticity in shear.

G_{st} = Modulus of elasticity in shear at onset of strain-hardening.

G_t = Tangent modulus in shear.

g_A = Moment ratio in adjacent segment.

H = Hinge angle required at a plastic hinge.
= Horizontal reaction.

H_B = Portion of hinge angle that occurs in critical (buckling) segment of beam.

h = Story height in multi-story frame.

I = Moment of inertia; subscripts denote axis.
= Number of redundants remaining in a structure at ultimate load.

I_e = Moment of inertia of elastic part of cross-section.

I_p = Moment of inertia of plastic part of cross-section.

I_w = Warping constant.

K = Torsion constant.

KL = Effective (pin-end) length of column. K = Euler length factor.

k = Distance from flange face to end of fillet.
= Plastic moment ratio.
= Stiffness factor of a beam.

L = Span length.
= Actual column length.
= Length of bar.

L_B = Length of buckling (critical) segment.

ℓ = Length of segment (slope-deflection equation).

L_{cr} = Critical length for lateral buckling.

L_ℓ, L_s = Critical length (with C = 1.0) of adjacent spans; subscripts ℓ and s denote larger and shorter critical lengths, respectively.

ΔL = Equivalent length of connection.
= Length of plastic hinge.

M = Bending moment.
= Number of plastic hinges necessary to form a mechanism.

M_{cr} = Critical moment for lateral buckling of a beam.

M_h = Moment at the haunch point.

M_{max} = Maximum moment.

M_o = Column end moment; a useful maximum moment.

M_p = Plastic Moment.

M_{pc} = Plastic hinge moment modified to include the effect of axial compression.

M_{ps} = Plastic hinge moment modified to include effect of shear force.

M_s = Maximum moment of a simply-supported beam.

M_w = Moment at working (service) load.

M_y = Moment at which yield point is reached in flexure.

M_{yc} = Moment at which initial outer fiber yield occurs when axial thrust is present.

N = Number of possible plastic hinges.
= Normal force.

n = Number of possible independent mechanisms.
= Shift of neutral axis.

P = Concentrated load.

P_e = Euler buckling load.

P_{max} = Maximum load.

P_s = Stabilizing ("shakedown") load.

P_t = Tangent modulus load.

P_u = Ultimate load (theoretical).

P_w = Working (allowable) load.

P_y = Axial load corresponding to yield stress level; $P = A\sigma_y$. Load on beam when yield point is reached in flexure.

Q = b/a = roof rise ÷ column height.

R = Rotation capacity.
= Radius of curved haunch.

r = Radius of gyration; subscripts denote flexure axis.

S = Section modulus, I/c.

S_e = Section modulus of elastic part of cross section.

s = Length of compression flange of haunch.

T = Force.
= Horizontal load applied at eaves which produces overturning moment about the base of structure equivalent to that of horizontal distributed load.

t = Flange thickness; subscripts c and t denote compression and tension.

t_s = Stiffener thickness.

t_{tr} = Transverse stiffener thickness.

V = Shear force.

V_{max} = Maximum allowable shear force.

u, v, w = Displacements in x, y, and z directions.

W = Total distributed load.

W_E = External work due to virtual displacement.

W_I = Internal work due to virtual displacement.

w = Distributed load per unit of length.
= Web thickness.

X = Number of redundancies in original structure.

x = Longitudinal coordinate.
= Distance to position of plastic hinge under distributed load.

y = Transverse coordinate.

y_o = Ordinate to furthest still-elastic fiber.
= Distance from midheight to neutral axis.

$\bar{y}$ = Distance from neutral axis to centroid of half-area.

Z = Plastic modulus, $Z = \frac{Mp}{\sigma_\gamma}$

Z_e = Plastic modulus of elastic portion of cross-section.

Z_p = Plastic modulus of plastic portion of cross-section.

Z_t = Trial value of Z, neglected axial force.

z = Lateral coordinate.

α = Central angle between points of tangency of curved connection.

β = Angle between two non-parallel flanges.

Δ = Virtual displacement.

δ = Deflection. Subscripts, u, w, y denote deflection at ultimate, working, and yield load respectively.

ϵ = Strain.

ϵ_{max} = Elongation at fracture.

ϵ_{st} = Strain at strain-hardening.

ϵ_y = Strain corresponding to theoretical onset of plastic yielding.

θ = Measured angle change, rotation.
= Mechanism angle.

μ = Poisson's ratio.

ρ = Radius of curvature.

σ = Normal stress.

σ_{ly} = Lower Yield point.

σ_p = Proportional limit.

σ_r = Residual stress.

σ_{ult} = Ultimate tensile strength of material.

σ_{uy} = Upper yield point.

σ_w = Allowable (working) stress.

σ_y = Yield stress level.

τ = Shear stress.

τ_y = Shear yield stress.

ϕ = Rotation per unit length, or average unit rotation; curvature.

ϕ_p = M_p/EI.

ϕ_{st} = Curvature at strain-hardening.

ϕ_y = Curvature corresponding to first yield in flexure.

REFERENCES

Chapter 1

Books

1.1 Baker, J. F., Horne, M. R., Heyman, J., "The Steel Skeleton, Vol. 2", Cambridge University Press, Cambridge, England, (1956).

1.2 Beedle, L. S., "Plastic Design of Steel Frames", John Wiley and Sons, New York, (1958).

1.3 AISC, "Plastic Design in Steel", AISC, New York, (1959).

1.4 Heyman, J., "Plastic Design of Portal Frames", Cambridge University Press, Cambridge, England, (1957).

1.5 Hodge, P. G., Jr., "Plastic Analysis of Structures", McGraw-Hill Book Company, New York, (1959).

1.6 Neal, B. G., "The Plastic Methods of Structural Analysis", John Wiley and Sons, New York, (1956).

1.7 Prager, W., "Introduction to Plasticity", to be published, in English, by Addison-Wesley Press.

Additional References

1.8 Kazinczy, G., "Kiserletek Befalazott Tartokkal", ("Experiments with Clamped Girders"), Betonszemle, 2(4) p. 68 (1914); 2(5) p. 83 (1914); 2(6) p. 101 (1914).

1.9 Hoff, N. J., Discussion of Ref. 1.13, Welding Journal, 33(1), p. 14-s (1954).

1.10 Maier-Leibnitz, H., "Contribution to the Problem of Ultimate Carrying Capacity of Simple and Continuous Beams of Structural Steel and Timber", Die Bautechnik, 1(6) (1927).

1.11 Van Den Broek, J. A., "Theory of Limit Design", John Wiley and Sons, (1948).

1.12 Roderick, J. W., Phillipps, I. H., "Carrying Capacity of Simply Supported Mild Steel Beams", Engineering Structures, Academic Press, New York, (1950), p. 9.

1.13 Horne, M. R., "A Moment Distribution Method for the Analysis and Design of Structures by the Plastic Theory", Proceedings, Inst. of Civil Engineers, p. 51, (April, 1954).

1.14 Greenberg, H. J., Prager, W., "Limit Design of Beams and Frames", ASCE Transactions, p. 447, Vol. 117 (1952).

1.15 Symonds, P. S., Neal, B. G., "Recent Progress in the Plastic Methods of Structural Analysis", J. Franklin Institute, 252, 383-407, 469-492, (1951).

1.16 Winter, G., "Trends in Steel Design and Research", Building Research Congress, Div. I, Part II. pp. 81-88, (1951).

1.17 Johnston, B. G., Beedle, L. S., Yang, C. H., "An Evaluation of Plastic Analysis as Applied to Structural Design", Welding Journal, 32(5), p. 224-s (1953).

Chapter 2

2.1 Drucker, D. C., Greenberg, H. J., Prager, W., "The Safety Factor of an Elastic-Plastic Body in Plane Strain", Transactions, ASME, Vol. 73, pp. 371-378 (1951).

2.2 Drucker, D. C., Greenberg, H. J., Prager, W., "Extended Limit Design Theorems for Continuous Media", Quarterly of Applied Mathematics, Vol. 9, pp. 381-389 (January, 1952).

Chapter 3

3.1 Beedle, L. S., Thurlimann, B., Ketter, R. L., "Plastic Design in Structural Steel", (Lecture Notes), Lehigh University, (Bethlehem Pa.) and AISC (New York) (September, 1955).

3.2 Dolphin, J. W., Wright, D. T., Nelson, H. M., "Plastic Design of Steel Structures", Royal Military College and Queen's University Publication, (May, 1956).

3.3 Ketter, R. L., Thurlimann, B., "Analysis and Design for Ultimate Strength", (To be published by McGraw-Hill Book Company, New York).

3.4 Neal, B. G., Symonds, P. S., "The Calculation of Collapse Loads for Framed Structures", Journal, Inst. of Civil Engineers, Vol. 35, p. 20, (1950).

Journal of the

ENGINEERING MECHANICS DIVISION

Proceedings of the American Society of Civil Engineers

COMMENTARY ON PLASTIC DESIGN IN STEEL: GENERAL PROVISION AND EXPERIMENTAL VERIFICATION

Progress Report No. 2 of the Joint WRC-ASCE Committee on Plasticity Related to Design

FOREWORD

This paper is the second in a series of reports on Plastic Design emanating from a Joint Committee of the Welding Research Council and the American Society of Civil Engineers. Reference should be made to the First Progress Report (Proc. Paper 2091) for the Foreword, Definitions, and Nomenclature. Chapters 4 and 5 are included in this present paper.

Note: Discussion open until December 1, 1959. Separate discussions should be submitted for the individual papers in this symposium. To extend the closing date one month, a written request must be filed with the Executive Secretary, ASCE. Paper 2092 is part of the copyrighted Journal of the Engineering Mechanics Division, Proceedings of the American Society of Civil Engineers, Vol. 85, No. EM 3, July, 1959.

CHAPTER 4. GENERAL PROVISIONS

4.1 Introduction

This chapter will discuss some of the basic conditions that should be satisfied in establishing a plastic design procedure. This includes questions regarding types of construction, materials, structural ductility (avoidance of brittle fracture), the yield stress level to be used, the plastic moment, the loads and forces that would be considered as applied to the structure, and the load factor.

In each case the suggested provision will be given first, followed by pertinent discussion.

4.2 Types of Construction

The following types of construction are suitable for plastic design:

(a) Continuous Beams
(b) One and two-story, single- and multi-span continuous type building frames
(c) Multi-story tier buildings with sidesway prevented by walls and/or diagonal bracing.

Plastic design is not recommended as a substitute for allowable stress design for structures that are essentially pin-connected. It is intended for structures which depend upon continuity for their ability to carry the computed ultimate load.

The necessary continuity may be achieved by welding, riveting, or bolting. The background and justification for design guides for the use of such connecting devices is discussed elsewhere in this report (see Chapter 7).

4.3 Material

Material with the characteristics of ASTM A7 steel for bridges and buildings should be used, with modifications, when needed, to insure weldability and ductility at lowest expected service temperature.

It is not the intent to specify any one steel, but to indicate that the important property that is required of a material is ductility at service temperature. As was shown in Ref. 3.1, many of the high strength steels exhibit stress-strain characteristics similar to those of ASTM A7 steel except with a higher yield stress level. It is reasonable to expect that plastic design may be applied to structures in which such steels are used, providing they meet design guides similar to those suggested in this report, but appropriate to the particular material.

4.4 Structural Ductility

> Fabrication processes should be such as to retain ductility. At plastic hinge locations unfinished sheared edges and punched holes in tension flanges should not be permitted. Sub-punched and reamed holes for connecting devices would be satisfactory if the reaming removes the cold-worked material.
>
> In design, triaxial states of tensile stress set up by geometrical restraints should be minimized.

This provision together with Art. 4.3 is intended to assure that brittle fracture will not prevent the formation of a plastic hinge. The assumption of ductility is an equally important aspect of elastic design and numerous design assumptions rely upon it.

In plastic design the engineer should be guided by the same principles that govern the proper design of an all-welded structure designed by the allowable stress methods, since ductility is of equal importance to both. Thus the proper material must be specified to meet the appropriate service conditions, the fabrication and workmanship must meet high standards, and design details should be such that the material is as free to deform as possible.(4.3)

With respect to fabrication, due to the severe cold working involved, punched holes and sheared edges should not be permitted in parts that might be subjected to the yield stress in tension at ultimate load. Punched holes would be permitted here if followed by sufficient reaming to remove the cold-worked material. In Ref 4.5 the effect of various edge conditions on the brittle failure of steel has been studied.

4.5 Yield Stress Level

> For ASTM A7 steel,
>
> Normal stress, σ_y = 33.0 ksi
> Shear stress, τ_y = 19.0 ksi

A yield stress level of 33.0 ksi corresponds to the minimum yield point permitted in a mill-type acceptance test of ASTM A7 steel. Such a test differs from the test conducted in the laboratory because of a number of factors, one of the most important of which is strain rate. An extensive investigation into the yield stress level has been conducted(4.1) using as the test specimen a complete cross-section of a rolled WF shape. The loading was carried out in a manner that simulates "static" loading. By such a test procedure it was possible to include such effects as differences in web and flange strength, strain rate, and size, since representative cross sections from the very smallest to the largest rolled shapes were included in the program.

According to the data available at that time, this investigation showed that the most probable value of the yield stress level is 34.1 ksi, with variations ranging from 24.6 ksi to 43.0 ksi. (According to the usual acceptance-type test, the most probable value of the yield stress level would be 42.6 ksi). Fig. 4.1 shows the histogram of the ratio of yield stress level determined from a stub column test as compared with the value obtained in a mill-type acceptance test.

While 33.0 ksi is the minimum yield stress permitted in acceptance tests, it turns out that it is very close to the average basic yield stress level of this material. Thus the factor of safety includes the possibility of variation below

this average value, because the design is actually based on an average, not a minimum. This situation has always existed in design, and therefore represents no departure from past practice.

4.6 Plastic Moment

$$M_p = \sigma_y Z \qquad (4.1)$$

σ_y = yield stress level

Z = plastic modulus

As pointed out in Art 2.1, the formation of plastic hinges is of basic importance to plastic design. Fig. 2.3 shows the characteristic moment-rotation curve of a beam under bending, and the moment at "stage 5" shown in Figs. 2.2 and 2.3 is called the plastic moment. It is computed according to Eq. (4.1).

The plastic modulus Z is a geometrical function analogous to the section modulus. It is the modulus of resistance to bending of a completely yielded cross section and is calculated by taking the combined statical moment about the neutral axis of the cross-sectional areas above and below that axis.

As will be evident in Chapter 5, it is frequently observed in tests that the moment-deformation behavior is not exactly like that shown in Fig. 2.3 (See Fig. 5.4, for example). Because of strain-hardening, the resisting moment is

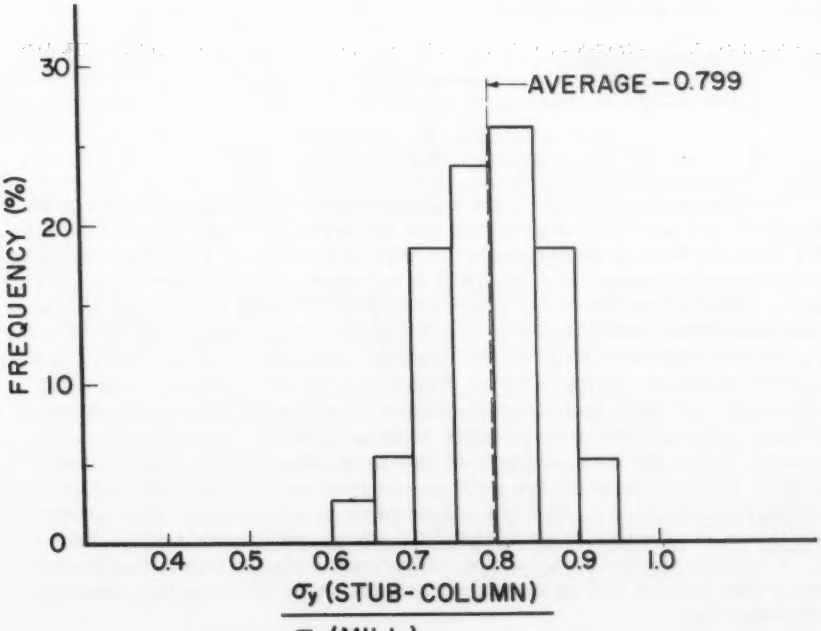

Fig. 4.1. Frequency Distribution of the Ratio $\frac{\sigma_y \text{ (Stub-Column)}}{\sigma_y \text{ (Mill)}}$

greater than the value computed according to Eq. (4.1). However, no present simple theory can take this additional reserve in strength into account without undue complications.

For material whose characteristics are not similar to A7 steel, but which exhibits continuous strain-hardening, it might be desirable to arrive at a semi-empirical value for the "plastic hinge" moment. Studies would have to be made on the particular material (including bending tests and tests of indeterminate structures) to arrive at a suitable approximation for the plastic moment.

4.7 Loads

The loads to be provided for (allowable loads) should be those that are customary for the particular type of construction. These loads are increased by a load factor to obtain an ultimate loading. Members are selected on the basis of their plastic strength to resist the most critical condition of ultimate loading.

$$P_u = F\,P_w \qquad (4.2)$$

F = Load factor

P_u = Ultimate load

P_w = Allowable (working) load

A margin of safety is achieved in elastic design by the use of allowable unit stresses obtained from a unit stress level assumed to represent failure and which has been reduced by a "factor of safety." In plastic design safety is achieved by multiplying the given service loads by a "load factor" as discussed in Art. 4.8.

The use of plastic design does not involve any changes in the magnitude of the service loading P_w specified for a given structure. The difference is that, in the case of plastic design, members are selected so that the structure will just support the computed ultimate load P_u. In elastic design the members are so selected that allowable unit stresses will not be exceeded at service load P_w. (As used here P is the critical combination of given independently variable loads used as the basis for the design by either method.)

The loading conditions that would be investigated for building construction are:

1. Dead load plus live load
2. Dead load, plus live load, plus wind or earthquake forces.

It is assumed that the live loading is static and proportional, even for the characteristic fluctuations of live load found in buildings. For unusual conditions, deflection stability would be investigated (see Art. 6.4).

In the design of structures to resist the dynamic loading resulting from blast forces, plastic design concepts generally are used. However selection of the loading and the type of design are largely a matter of judgment and are based on studies of vulnerability, consequences of failure, and required radiation protection. In making the design it is necessary to consider the nature of the loading, increased dynamic yield strength of the material, effective load duration, distribution of mass, effective mass, and natural period of the structure, as well as other factors not commonly considered in structural design.

In designing for earthquakes most building codes provide for the application of equivalent lateral static loads to produce a desired level of earthquake resistance. In conformity with such practice, the specified loads can be multiplied by a load factor to yield design ultimate loads.

Concepts of plastic analysis are currently being considered for design to resist earthquake forces using procedures that take into account the elastic-plastic response of the structure as a function of time. Here, the variation and random nature of earthquake loading require that consideration be given to loading approximations used in the design, as well as to many of the factors noted above as of importance in designing for blast forces. Greater refinement in design procedures using these concepts must await further study. The complex nature of such an approach makes it almost mandatory to use digital computers in the analysis.

4.8 Load Factors

Dead load plus live load,	F = 1.85
Dead load plus live load plus wind or earthquake,	F = 1.40

It should be noted that the factor of safety implicit in allowable stress design and the load factor used in plastic design are not concerned alone with the possibility of overloading. Other factors which influence the selection of an appropriate margin of safety are:

1. Approximations and uncertainties in the method of analysis
2. Quality of workmanship
3. Presence of residual stresses and stress concentrations*
4. Under-run in physical properties of material
5. Under-run of cross-sectional dimensions of members
6. Location and intended use of structure.

Depending upon the type of structure and its intended use, the importance of any one of the above factors, as compared with the others, can vary somewhat. One might arrive at a precise over-all load factor F in each case if sufficient statistical data were available to weigh properly the importance of its various constituent parts; but any resulting departure from current practice would be equally applicable to the allowable stresses specified for use in elastic designs. Since such statistical data are not available, it would seem logical to draw upon the vast experience gained from allowable stress design to obtain a single average value, applicable throughout the range of building construction.

Such a value can be obtained by considering the plastic strength of simple beams in the light of the allowable stress for which these beams were proportioned, there being no necessity for requiring any greater margin of safety merely because the structure is redundant. For simple beams the load factor is equal to the ratio of the ultimate load P_u to the working load P_w; thus F equals P_u/P_w. Since here the bending moment varies linearly with the load

$$F = \frac{P_u}{P_w} = \frac{M_p}{M_w}$$

*While this factor contributes to uncertainty as to the precise stress level, the discussion in Arts. 1.2, 5.1 and 5.3 shows that it may not influence ultimate load-carrying capacity (excepting column buckling, of course).

Substituting for M_p and M_w

$$F = \frac{\sigma_y Z}{\sigma_w S} = \frac{\sigma_y}{\sigma_w} f$$

where f is the shape factor.

Since adoption of its Standard Specification for Structural Steel for Buildings by the American Institute of Steel Construction in 1923, and to a limited extent even before that, the basic allowable working stress in building design in the United States has been 0.6 of the specified minimum unit yield stress of the steel furnished. Restated, the load factor against the guaranteed minimum ultimate capacity of these beams has not exceeded

$$F = \frac{30{,}000 \text{ psi}}{18{,}000 \text{ psi}} f = \frac{33{,}000 \text{ psi}}{20{,}000 \text{ psi}} f = 1.65f \qquad (4.3)$$

The formulation of a satisfactory load factor is therefore dependent only upon the determination of a shape factor representative of the simple beams now in service.

The variation of the shape factor for WF beams and columns, and for American Standard beams is shown in Fig. 4.2. For WF shapes normally used as beams listed in the "section economy" table[4.4] the shape factor varies from 1.10 to 1.18 with an average value of 1.134 and a mode (most frequently observed value) of 1.12. For WF shapes normally used as columns that appear in the "column" tables of Ref. 4.4 the shape factor varies from 1.10 to 1.23 with an average value of 1.137 and a mode of 1.115. The shape factor distribution of American Standard beams is shown in the lower portion of Fig. 4.2. The minimum is 1.14 and the maximum is 1.23, the average being 1.18.

The following table shows several possible values of the load factor, depending on the choice of the shape factor.

SHAPE FACTOR	FACTOR OF SAFETY*	LOAD FACTOR
1.10 — Minimum Value	1.65	1.81
1.12 — Mode for WF beams	1.65	1.85
1.14 — Average for WF beams and Columns	1.65	1.88
1.18 — Average for American Standard I beams	1.65	1.95
1.23 — Maximum Value	1.65	2.03

The two most reasonable values for the load factor are 1.85 and 1.88. The former would seem appropriate because it represents the shape factor that will recur most frequently in beams. The value 1.88 implies an accuracy in our knowledge of the general problem of safety that is not justified.

In the case of gravity loading in combination with wind or earthquake forces, allowable stress design specifications permit a one-third increase in

*Yield stress divided by working stress.

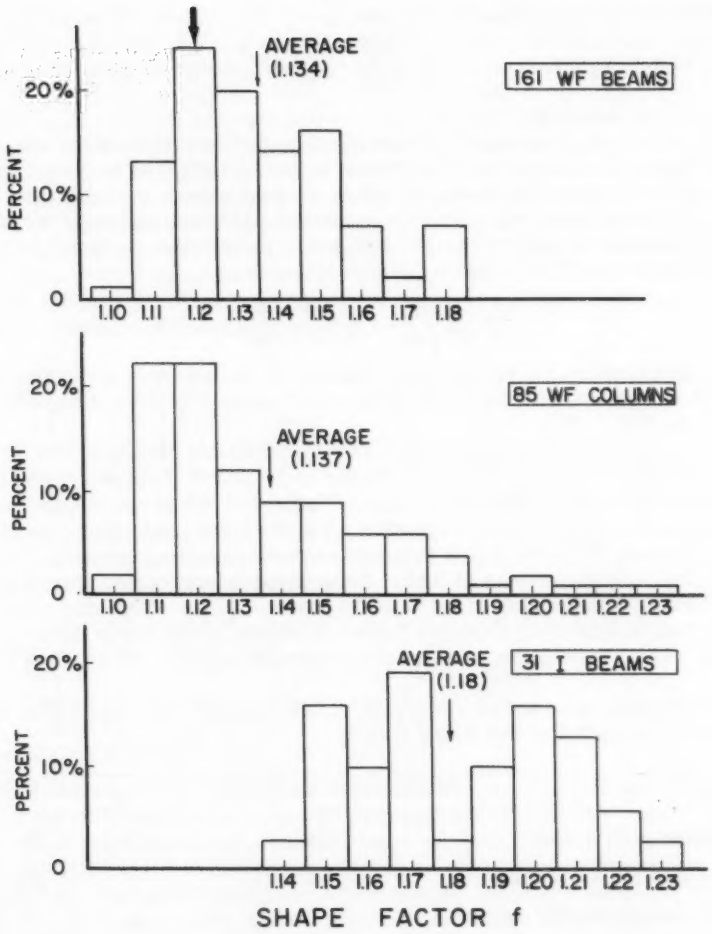

Fig. 4.2. The Variation of Shape Factor for WF Beams and Columns and American Standard Beams

computed stresses. Consistent with this allowance, the value of F for combined dead, live, and wind or earthquake loading would be 3/4 x 1.85 = 1.40.

CHAPTER 5. VERIFICATION OF PLASTIC THEORY

In this chapter it is shown that the actual behavior of structures under test verifies the predictions of plastic theory. In Art. 5.1 it is demonstrated that structural steel exhibits the ductility assumed, and that plastic hinges will form and allow the necessary redistribution of moment. Article 5.2 presents the results of continuous beam tests, and finally Art. 5.3 shows how tests of rigid frames verify plastic theory.

5.1 Basic Concepts

Ductility of Steel

Fig. 5.1 shows the tensile stress-strain curves obtained from two coupons cut from two separate locations of an 8WF40 beam. They are typical of the behavior of ASTM-A7 steel. The steel deforms plastically about 15 times the

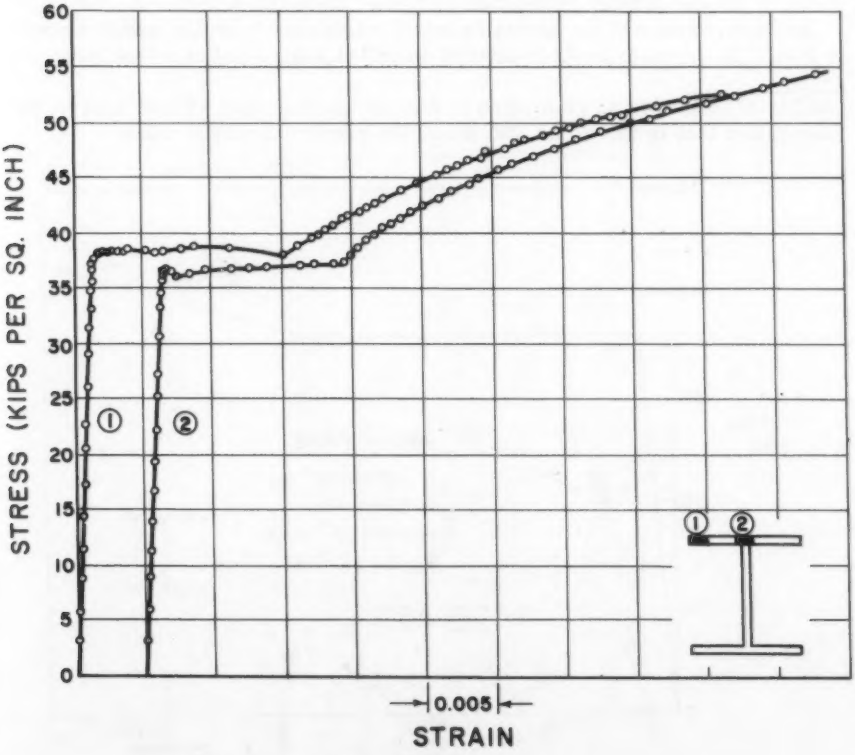

Fig. 5.1. Stress Strain Relationship of Tensile Coupons of ASTM A7 Steel(5.3)

strain at the elastic limit and then commences to strain harden.* Although the data is plotted well into the strain-hardening range, the strains shown are still considerably less than those at ultimate strength (tensile strength). The compressive and the tensile stress-strain relationships are quite similar. In fact the properties in compression are practically identical with those in tension. Fig. 5.2 shows in idealized form the stress-strain relationships for ASTM-A7 steel drawn according to average values obtained in laboratory tests.

The Plastic Moment and the Plastic Hinge

As a demonstration that the plastic moment is attained through plastification of the cross section, Fig. 5.3a shows a typical M-ϕ curve obtained from a beam, a portion of which is in pure bending.(5.1) The dotted line is the idealized curve and the solid line through the circles shows the results of a test. The theoretical stress distributions (according to the simple plastic theory) at different stages of bending are shown in Fig. 3b. Below these in Fig. 5.3c are shown the corresponding stress distributions as determined from SR-4 gage measurements. It will be seen that plastification of the cross section does occur, and that the bending moment corresponding to this condition is the full plastic moment as computed from the equation $M_p = \sigma_y Z$.

Although there will be inevitable minor variations from the result shown in Fig. 5.3a the many tests conducted on rolled shapes indicate that most

*ASTM-A7 requires an elongation in 2 in. of not less than 24% at failure, an elongation that is more than 200 times the maximum elastic value.

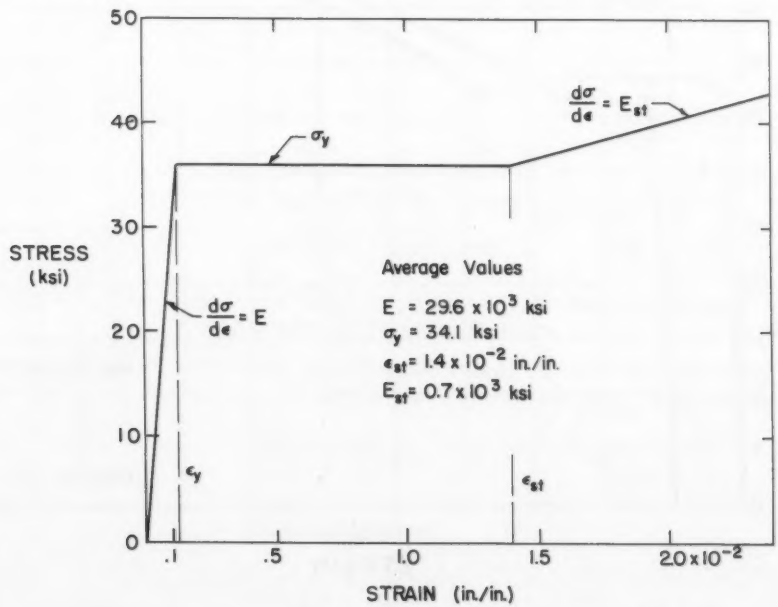

Fig. 5.2. Idealized Stress-Strain Relationship for ASTM A7 Steel

hot-rolled wide-flange beams will develop the strength predicted by the plastic theory and that a plastic hinge (characterized by rotation at near-constant moment) does actually form.

To be sure, a somewhat unrealistic loading condition has been taken since "pure moment" is a condition not likely to be encountered in actual structures. Usually there will be a gradient in moment, as when a single concentrated load is applied to a beam. In such a case the deformation tends to be concentrated under the load point (the point of maximum moment). Because the plastic deformation is more localized, the strain-hardening region is reached at a lesser deflection; consequently, the beam tends to develop a moment greater than the plastic moment. Typical of the behavior of a beam under moment gradient is that shown in Fig. 5.4.(5.2) The theoretical load-deflection curve with and without the inclusion of strain-hardening is shown by dashed lines. The results of a test of such a beam are shown as a solid line. It will be noted that as a result of the strain-hardening phenomenon, there is an increase in load-carrying capacity as the deformation continues beyond the yield level. The decrease in measured resistance, which occurred after a large hinge rotation at the center, resulted from local buckling of the flanges followed by lateral buckling.

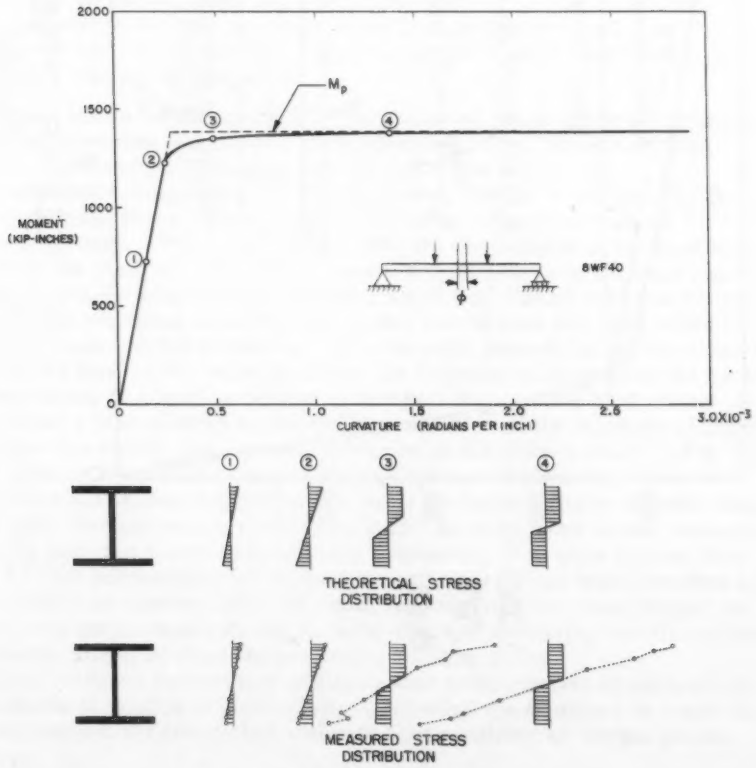

Fig. 5.3. Experimental Verification of the Moment-Curvature Relationship Theoretical and Computed Stress Distributions

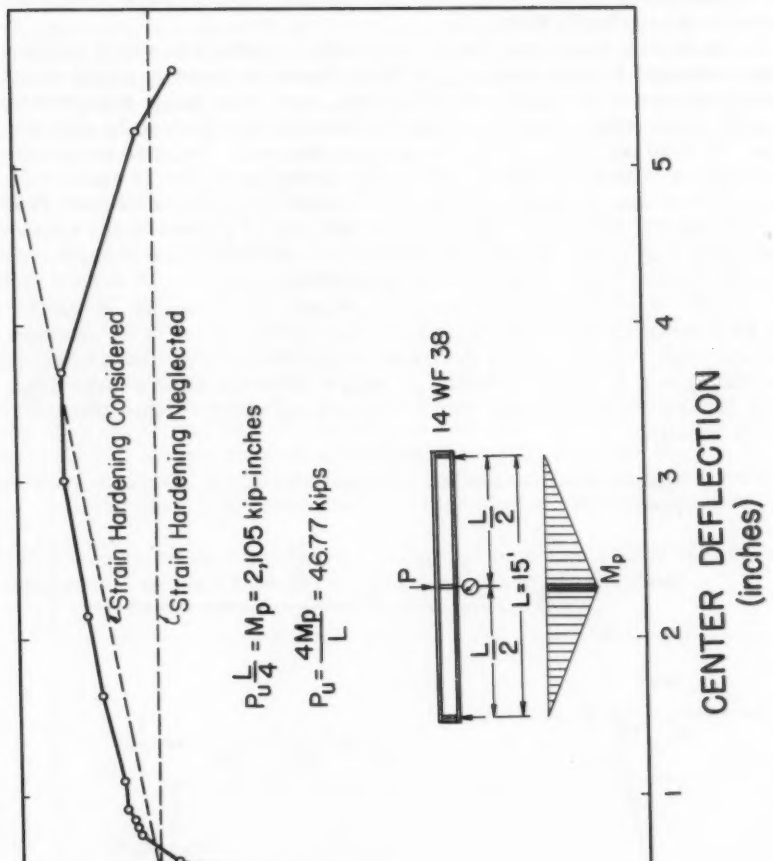

Fig. 5.4. Load vs. Center Deflection Relationship of a 14WF38 Beam

Thus strain-hardening improves the moment-carrying capacity of a beam. Although it is neglected in the simple plastic theory (except for checking a beam for stability against buckling) this additional reserve strength is still present in most ordinary structures, and this contributes to an actual factor of safety that is greater than the value assumed in the simple plastic theory.

Redistribution of Moment

From the previous section it is seen that plastic hinges may be depended upon to form at connections and at concentrated load points. Development of the plastic moment is one of the sources of reserve strength in structural steel beyond the elastic limit. Another source is the redistribution of moment in continuous structures.

In Fig. 5.5 is shown a picture of the redistribution process—as predicted theoretically and as obtained experimentally. A test was made on a continuous beam to simulate the condition of third-point loading on a fixed-ended span;[5.3] thus experimental data was available to compare with the theoretical predictions. The fixed-ended beam and its various components are shown in four stages:

Stage 1—at the computed elastic limit
Stage 2—after the plastic hinges have formed at the ends and the load has increased towards its ultimate value
Stage 3—when the theoretical ultimate load is first reached, and
Stage 4—after deformation has been continued through an arbitrary additional displacement.

The figure shows (a) the loading, (b) the deflected shape at the four stages, (c) the moment diagram, (d) the load-deflection curve, and the moment-curvature relationship near the ends (e) and at the center (f).

In the elastic range (stage 1) it will be seen that the beam behaves just as assumed by the theory, the moment at the center being one-half the moment at the fixed ends. (Figs. 5.5c, 5.5e, 5.5f). As the moment at the ends approaches the yield moment, the curvature ϕ commences to increase more rapidly; a plastic hinge begins to form (Fig. 5.5e). Because of this "hinge action", the additional moments due to increase in load are distributed between the ends and the center in a different ratio beyond the elastic range than before. As long as the beam is elastic the increase in moment at the center corresponding to a load increment is one-half the increase at the ends. However, after a plastic hinge forms at the ends, most of the increase of moment occurs at the center; the moment increment at the ends is small. (Fig. 5.5e, 5.5f) This is the process known as redistribution of moment.

As a result of plastification at the ends, the beam actually behaves somewhat more flexibly than before. (Fig. 5.5d) At stage 2 the elastic moment capacity near the center is practically exhausted. It is quite evident from Fig. 5.5 that substantially all of the moment capacity has been absorbed by the time stage 3 is reached (ultimate load). Beyond this, the beam simply deforms as a mechanism with the moment diagram remaining largely unchanged, the plastic hinges at the ends and center rotating further.

Clear evidence is therefore available that redistribution of moment occurs through the formation of plastic hinges, allowing the structure to reach (and usually exceed) the theoretical ultimate load predicted by simple plastic theory.

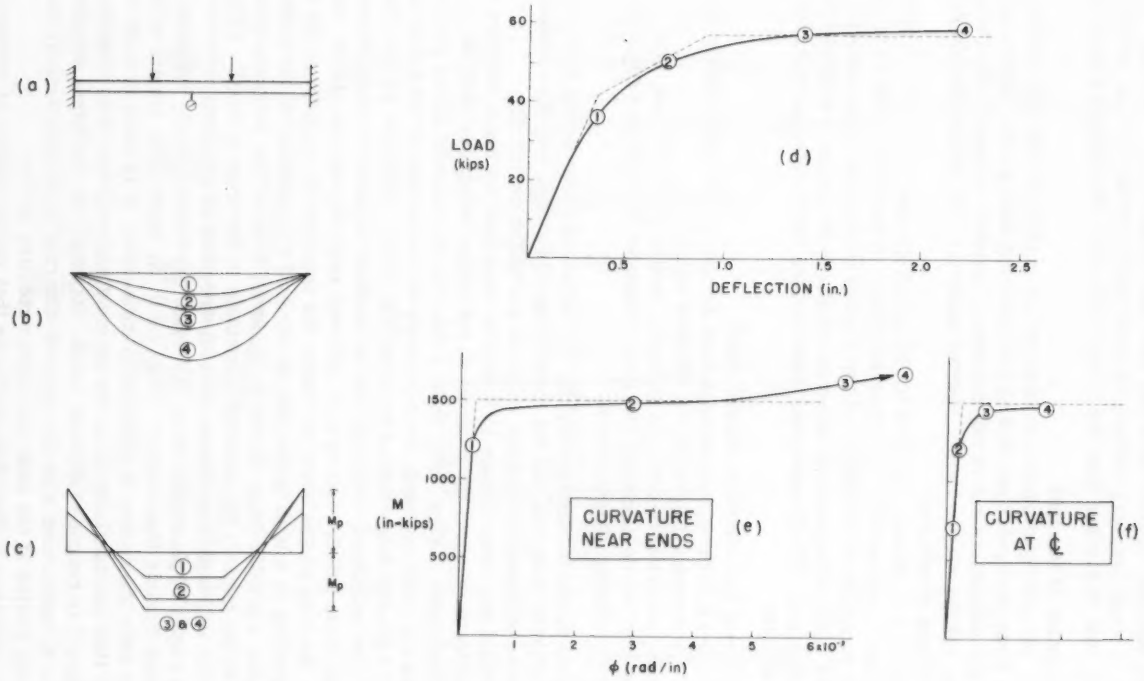

Fig. 5.5. Redistribution of Moment as Revealed by Test on a Fixed-Ended Beam

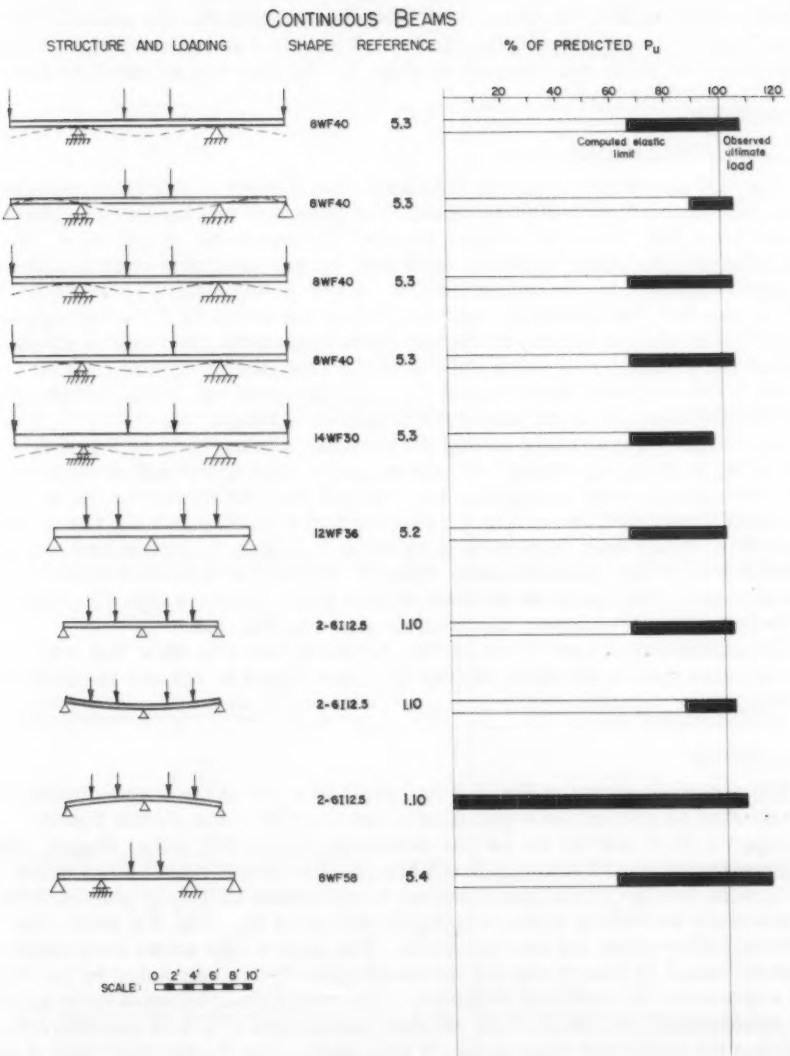

Fig. 5.5. Redistribution of Moment as Revealed by Test on a Fixed-Ended Beam

Fig. 5.6. Summary of Beam Test Results Showing Correlation with Predictions of Plastic Theory

Incidentally, sketch (d) of Fig. 5.5 illustrates the gradual transition from the elastic to the inelastic range that is typical for continuous steel beams and frames. Theoretically, upon first loading the structure should remain elastic up to stage 1. However, because of the combination of unknown initial stress conditions and discontinuities, local plastic flow takes place at a lower load than that which corresponds to stage 1. But there is no effect whatever upon the ultimate load.

5.2 Continuous Beams

Fig. 5.6 shows the results of continuous beam tests in which the members were fabricated from rolled sections. The structure and loading are shown to scale at the left. Next, the size of member (or members) is indicated. To the right is a bar graph on which is plotted the per cent of predicted ultimate strength exhibited by the test structure. A test result plotted to the "100%" line shows that the structure reached the load predicted by the simple plastic theory. The shaded portion of the bar chart represents the reserve strength beyond the elastic limit, since the end of the unshaded portion of each bar graph is the computed elastic limit (on a non-dimensional basis) and the end of the shaded portion is the observed maximum strength.

Particularly remarkable among the continuous beam tests of Fig. 5.6 is one conducted by Maier-Leibnitz[1.10] shown as the next to the last structure. In this experiment, prior to applying the vertical load, he raised the center support until the allowable working stress was just reached, with the result that application of the first increment of external load was, in fact, a load greater than allowed by the specifications. In spite of this, the computed ultimate load was attained. The observed ultimate load in this test was within 3% of that of the two structures shown immediately above in Fig. 5.6.

The continuous beams shown in Fig. 5.7 were tested to show that members of otherwise inadequate strength may be cover-plated to achieve the desired load-carrying capacity.

5.3 Frames

The structure shown in Fig. 5.8 is typical of some of the frames tested in this country as part of the experimental verification of the plastic theory. The span is 40 ft and the frame was fabricated of 12WF36 rolled shapes. Not only has the computed ultimate load been reached at the stage shown in the photograph, but the frame has absorbed considerable additional plastic deformation while sustaining a load slightly in excess of P_u. Fig. 5.9 shows the load-deflection curve for this structure. The dashed line shows the predicted behavior based on theory and the series of open circles connected by the solid line represents the observed behavior. This result demonstrates once again that inelastic action (due to local effects) commences at a load considerably less than the predicted yield value. It also shows that the ultimate load is not affected by such initial conditions.

It is of interest that at ultimate load the excess of actual deflection above the computed value for this frame was no greater than that observed at the predicted yield load. This means that the methods for computing such deflections are as dependable as the elastic deflection calculations.

Figs. 5.10, 5.11, 5.12, and 5.13 show frames tested both in this country and abroad, and represent some of the structures which have been tested to maximum load capacity prior to 1958. As before, the unshaded portion of each bar

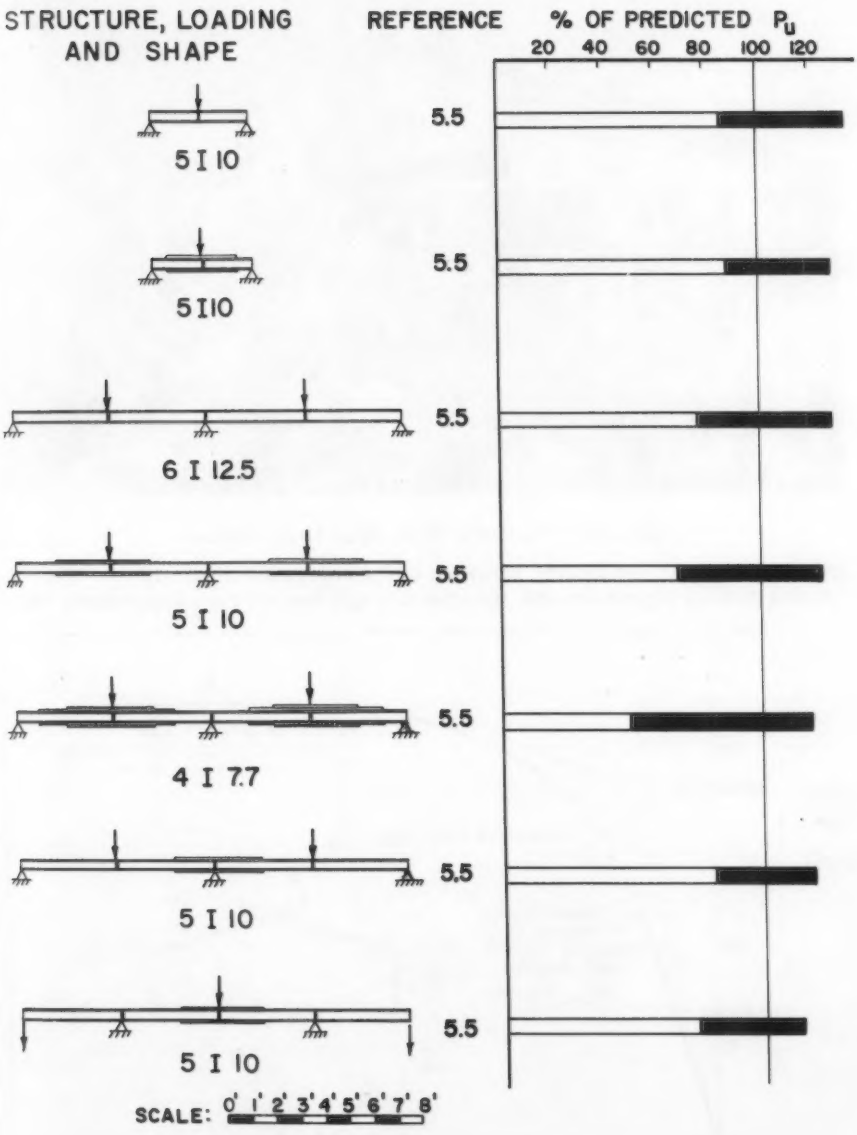

Fig. 5.7. Summary of Beam Test Results Showing Correlation with Predictions of Plastic Theory

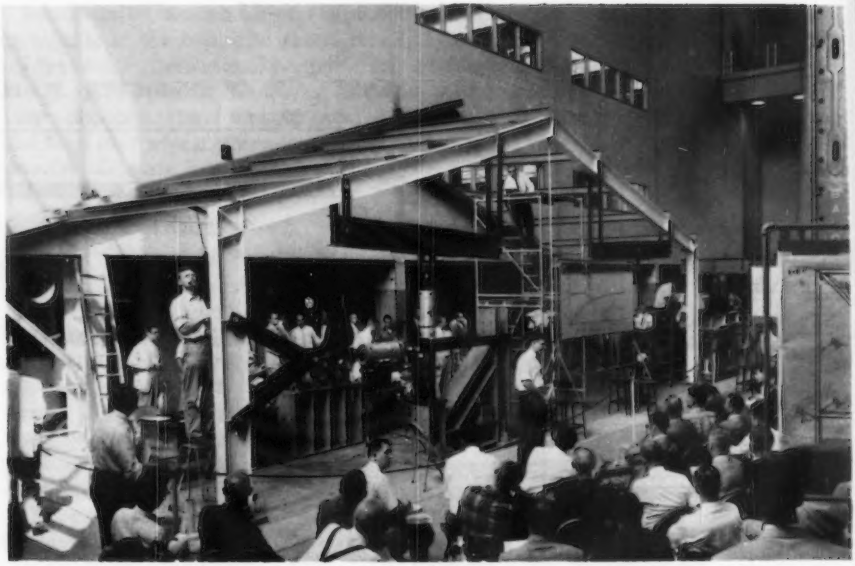

Fig. 5.8. Test of a 40-ft. Span Gable Frame

graph represents the loading range up to the computed elastic limit. The shaded portion represents the reserve strength beyond the elastic limit, the

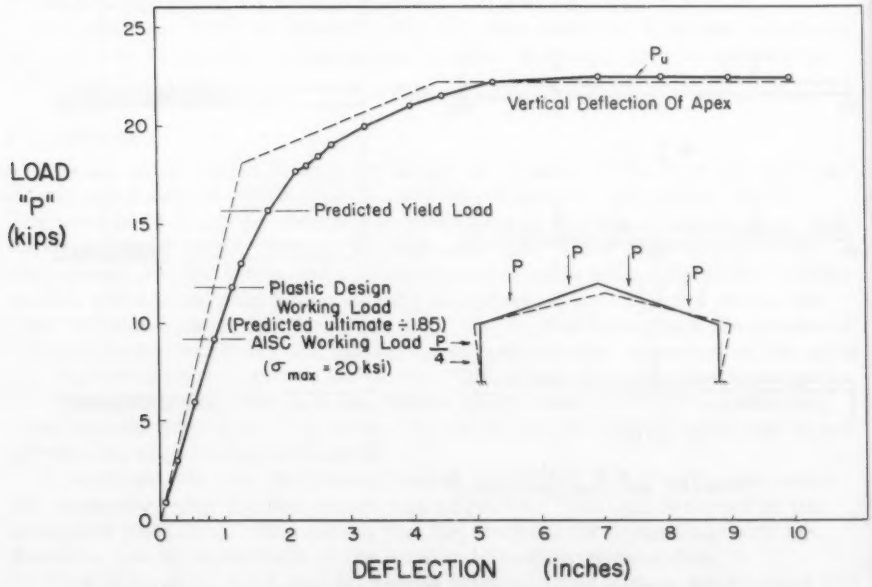

Fig. 5.9. Load vs. Center Deflection Diagram of Test Frame Shown in Fig. 5.8

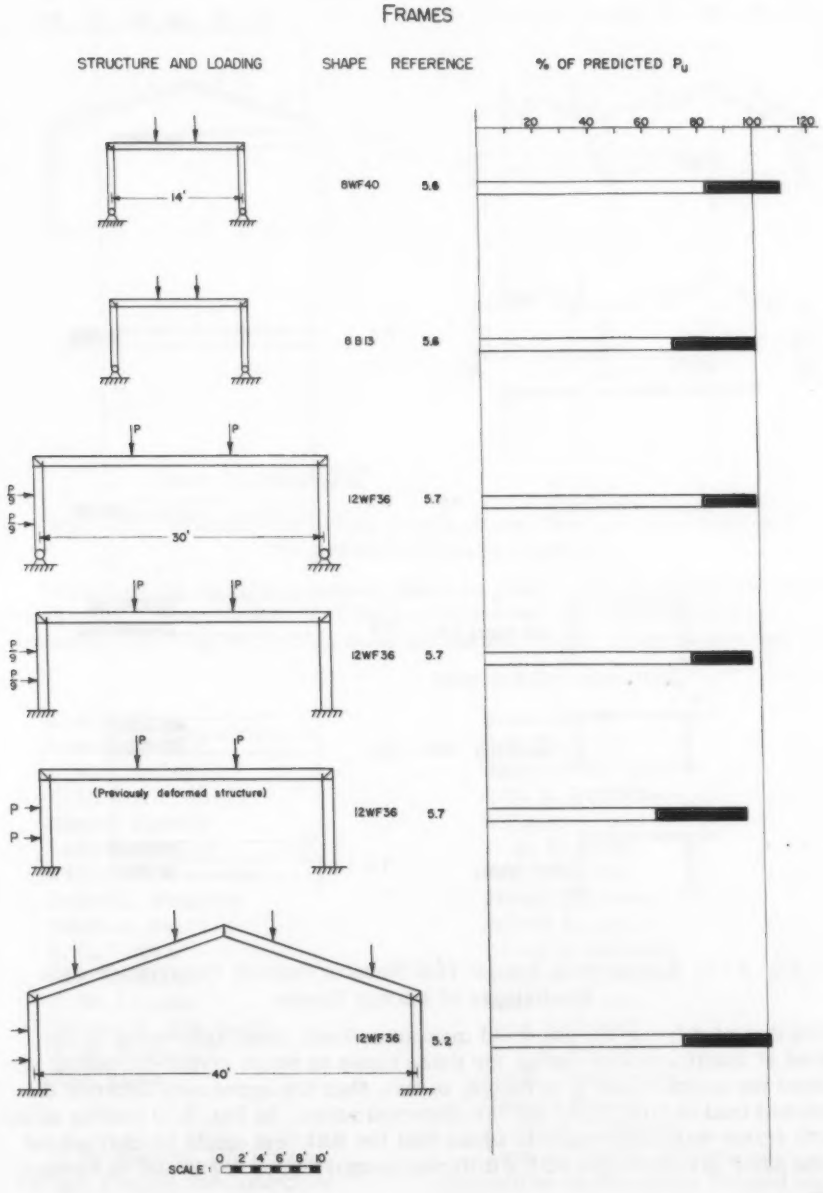

Fig. 5.10. Summary of Frame Test Results Showing Correlation with Predictions of Plastic Theory

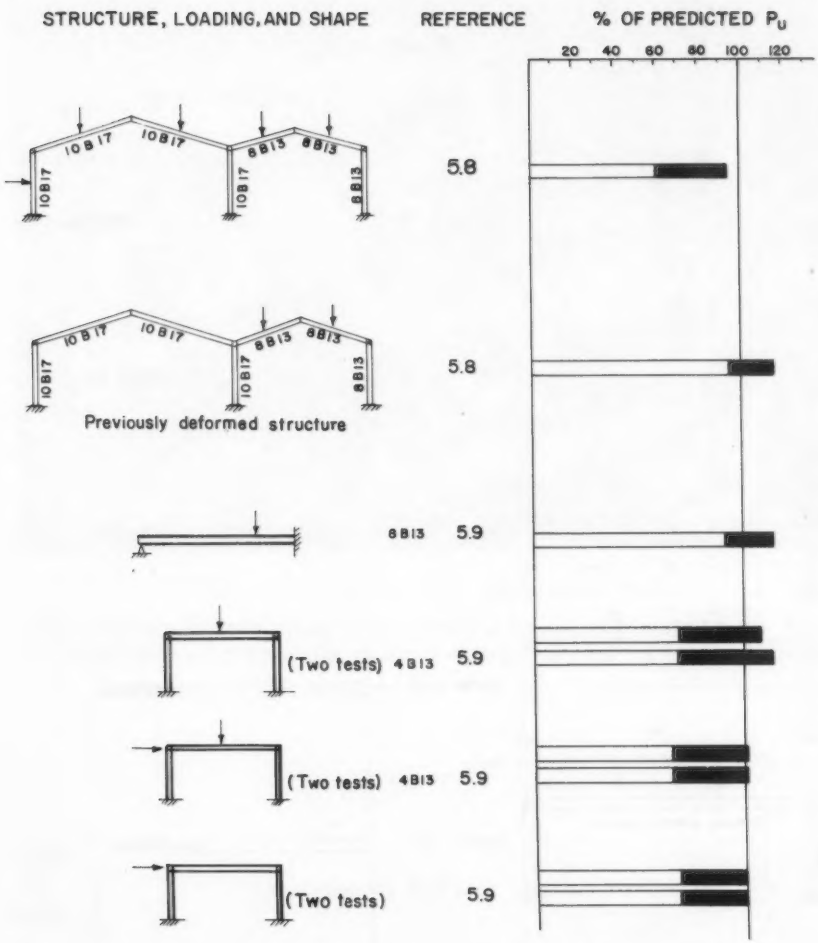

Fig. 5.11. Summary of Frame Test Results Showing Correlation with Predictions of Plastic Theory

end of that part being the observed maximum load. Good agreement is observed at maximum load except for those cases in which strain-hardening accounted for an increase; it is better, in fact, than the agreement between the predicted load at first yield and the observed value. In Fig. 5.10 testing of the fourth frame was interrupted in order that the fifth test might be carried out on the same structure but with a different proportion of horizontal to vertical load.

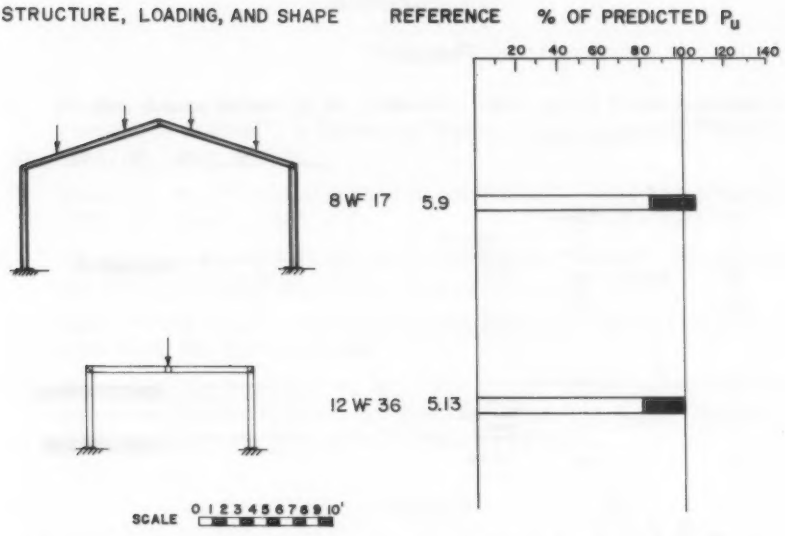

Fig. 5.12. Summary of Frame Test Results Showing Correlation with Predictions of Plastic Theory

In view of the notable agreement between plastic theory and the results of these tests, the applicability of the plastic method to structural design problems involving continuous steel beams and frames is demonstrated.

Respectfully submitted,

A. Amirikian
Lynn S. Beedle
J. M. Crowley
F. H. Dill
Samuel Epstein
LaMotte Grover
William H. Jameson
Bruce G. Johnston
Jonathan Jones
R. L. Ketter
Carl Kreidler
H. W. Lawson
Nathan M. Newmark
R. M. Stuchell
John Vasta

T. R. Higgins, Chairman
Lehigh Project Subcommittee

Structural Steel Committee
Welding Research Council

Frank Baron
John M. Biggs
Daniel C. Drucker
John D. Griffiths
William J. Hall
T. R. Higgins
Harry N. Hill
Eivind Hognestad
Robert L. Janes
Bruce G. Johnston
William H. Munse, Jr.
Egor P. Popov
John B. Scalzi
Paul S. Symonds
Bruno Thurlimann
George Winter
Douglas T. Wright
Lynn S. Beedle, Chairman
Committee on Plasticity Related to Design
Engineering Mechanics Division
American Society of Civil Engineers

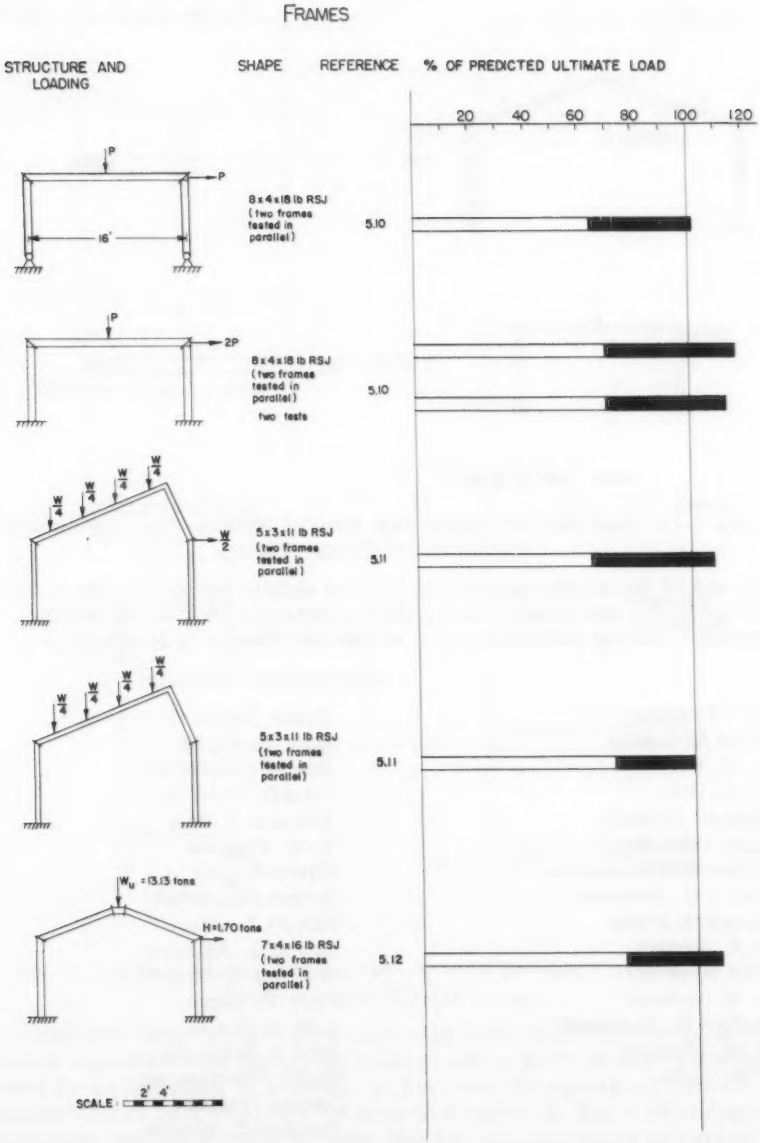

Fig. 5.13. Summary of Frame Test Results Showing Correlation with Predictions of Plastic Theory

REFERENCES

Chapter 4

4.1. Beedle, L. S., Huber, A. W., "Residual Stress and the Compressive Properties of Steel", A Summary Report, Fritz Laboratory Report 220A. 27, (July, 1957).

4.2. Huber, A. W., "Residual Stress Measurement", Fritz Laboratory Report 220A. 17, (March, 1955).

4.3. Thurlimann, B., "Modifications to the Plastic Theory", Proceedings of the AISC National Engineering Conference, p. 50, (1956).

4.4. AISC, "Steel Construction", American Institute of Steel Construction, New York, 5th Edition, (1950).

4.5. Harris, L. A., Newmark, N. M., "The Effect of Fabricated Edge Conditions on Brittle Fracture of Structural Steel", A.R.E.A. Bulletin, 59 (538), pp. 247-289, (September-October, 1957).

Chapter 5

5.1. Luxion, W., Johnston, B. G., "Plastic Behavior of Wide-Flange Beams", Welding Journal, 27(11) p. 538-s (November, 1948).

5.2. Driscoll, G. C., Jr., Beedle, L. S., "The Plastic Behavior of Structural Members and Frames", Welding Journal, 36(6) p. 275-s (June, 1957).

5.3. Yang, C. H., Beedle, L. S., Johnston, B. G., "Residual Stress and the Compressive Strength of Steel Beams", Welding Journal, 31 (4), p. 205-s (April, 1952).

5.4. Hall, W. J., Newmark, N. M., "Shear Deflection of Wide-Flange Steel Beams in the Plastic Range", Transactions of the ASCE, 122 p. 666 (1957).

5.5. Popov, E. P., Willis, J. A., "Plastic Design of Cover-Plated Continuous Beams", ASCE Journal, 84 (EM1), Paper No. 1494 (January, 1958).

5.6. Knudsen, K. E., Ruzek, J., Johnston, E. R., Beedle, L. S., "Welded Portal Frames Tested to Collapse", Welding Journal, 33 (9) p. 469-s, (September, 1954).

5.7. Schilling, C. G., Schutz, F. W., Jr., Beedle, L. S., "Behavior of Welded Single-Span Frames Under Combined Loading", Welding Journal 35(5) p. 234-s (May, 1956).

5.8. Driscoll, G. C., Jr., "Test of Two-Span Gabled Portal Frame", AISC National Engineering Conference Proceedings, p. 74 (1956).

5.9. Nelson, H. M., Wright, D. T., Dolphin, J. W., "Demonstrations of Plastic Behavior of Steel Frames", ASCE Proceedings, Paper No. 1390, (October, 1957).

5.10. Baker, J. F., Roderick, J. W., "Tests on Full-Scale Portal Frames", Proceedings of the Inst. of Civil Engineers (January, 1952).

5.11. Baker, J. F., Eickhoff, K. G., "The Behavior of Saw-Tooth Portal Frames", Conference on the Correlation between Calculated and Observed Stresses and Displacements in Structures. Inst. of Civil Engineers, p. 107, (1955).

5.12. Baker, J. F., Eickhoff, K. G., "A Test on a Pitched Roof Portal", Preliminary Publication, IABSE, Fifth Congress, Lisbon (1956).

5.13. Blessey, W. E., A letter report from Mr. Walter E. Blessey, Tulane University, (February 7, 1958).

Journal of the
ENGINEERING MECHANICS DIVISION
Proceedings of the American Society of Civil Engineers

STRATIFIED FLOW INTO A LINE SINK

Walter R. Debler[1]

SYNOPSIS

The discharge of a stratified fluid (with a stable linear density variation at infinity) through a horizontal slot at the end of a channel has been experimentally investigated. The experiments show that when the densimetric Froude number is less than 0.28 the flow pattern is divided into two horizontal regions: an upper, essentially stagnant, region and a lower region in which the entire discharge is concentrated. The specific results obtained are useful for the solution of many engineering problems involving stratified flows.

INTRODUCTION

The experimental investigation of a stratified fluid flowing along a horizontal channel into a line sink was undertaken to gain additional insight into the mechanics of stratified fluid flows. The practical application of this problem, and those similar to it, is encountered in the cooling of thermoelectric generating stations. In such installations it has been observed that the coolant discharge water flowed, by virtue of its lower density, into the proximity of the coolant inlet where it was subsequently pumped through the cooling system with an attendant loss in operating efficiency.

Other examples in which stratification phenomena are present are in the drawing off of crude petroleum from underground reservoirs, and the removal of salt water that has encroached upon a supply of fresh water. This latter problem has assumed considerable importance to agriculture in Holland.

The analysis of Yih(1) for the type of flow under consideration predicts the flow patterns for large densimetric Froude numbers, but ceases to be valid for Froude numbers equal to or less than a critical value of $1/\pi$. His results show that there is no tendency for flow separation (i.e., discharge of the

Note: Discussion open until December 1, 1959. To extend the closing date one month, a written request must be filed with the Executive Secretary, ASCE. Paper 2093 is part of the copyrighted Journal of the Engineering Mechanics Division, Proceedings of the American Society of Civil Engineers, Vol. 85, No. EM 3, July, 1959.

1. Prof., Dept. of Eng. Mechanics, Univ. of Michigan, Ann Arbor, Mich.

heavier fluid to the exclusion of the lighter portions) for Froude numbers greater than $1/\pi$. Any separation would be expected to occur when the Froude number was equal to or less than this critical value.

The present work was undertaken to determine the critical Froude number experimentally and to compare its magnitude with the value obtained analytically. In addition, information was sought to correlate the degree of flow separation with the Froude number, and also to observe the flow patterns that accompany such separation.

Theory

The mathematical solution for the two-dimensional problem of a stratified fluid in a horizontal channel flowing into a line sink was obtained by Yih.[1] An abridgement of this work follows in order to give a complete background for the experimental work that was undertaken.

The density variation in the channel at a section far from the sink is considered to be linear and of the form:

$$\rho = \rho_0 - \beta y \qquad \beta = \frac{\rho_0 - \rho_2}{d_2} \tag{1}$$

in which y is measured vertically from the bottom, d_2 is the depth of fluid in the channel, ρ_0 is the density at the bottom, and ρ_2 is the density at the top. In this discussion x will be measured horizontally from the sink and only steady flows are considered. The fluid is incompressible and changes in density due to diffusion are excluded as being negligible.

The fact that the fluid density will be constant along a streamline can be expressed as

$$u\rho_x + v\rho_y = 0 \tag{2}$$

in which u and v are the respective velocity components in the x and y direction, and the subscripts denote partial differentiation. Eq. (2) permits the continuity equation to be written in the usual form

$$u_x + v_y = 0 \tag{3}$$

and the use of the stream function ψ so that

$$u = -\psi_y , \qquad v = \psi_x \tag{4}$$

Yih shows that the equations of motion are simplified if a new stream function ψ' is introduced such that

$$\psi' = \int_0^{\psi} \rho^{1/2} \, d\psi \tag{5}$$

The equations of motion can then be written in terms of ψ' as

$$\nabla^2\psi' + g\rho \frac{d\rho}{d\psi'} = H_1(\psi') \tag{6}$$

in which ∇^2 is the Laplacian operator in rectangular cartesian coordinates, g is the acceleration constant, and $H_1(\psi')$ is a function that must be determined.

This determination is accomplished by utilizing the conditions that exist far upstream. If the fluid originates from a large quiescent reservoir and flows horizontally into the channel, it can be shown that far upstream

$$\psi_0' = -Ay \tag{7}$$

in which the subscript on ψ' designates the upstream condition and A is a positive constant. One can also deduce directly that if U(y) is the velocity far upstream in the actual flow, then

$$U\rho^{1/2} = A \tag{8}$$

With Eqs. (1), (7) and (8), Eq. (6) becomes

$$\nabla^2\psi' + \frac{g\beta}{A^2}\psi' = -\frac{g\beta}{A}y \tag{9}$$

This equation along with the appropriate boundary conditions can be solved by the separation of variables technique so that

$$\psi' = -Ay - \frac{2}{\pi}Ad_2\sum_{n=1}^{\infty} e^{a_n x/d_2}\sin\frac{n\pi y}{d_2} \tag{10}$$

in which

$$a_n^2 = n^2\pi^2 - F^{-2} \tag{11}$$

and

$$F = (\text{Froude Number}) = \frac{A}{d_2\sqrt{g\beta}} \tag{12}$$

Eq. (10) is valid as long as

$$F > F_{cr} = \frac{1}{\pi} = 0.318$$

This follows from the fact that the solution yields an eddy, above the line sink, which becomes more and more elongated as the Froude number is reduced. At $F = 1/\pi$ the eddy reaches infinitely far upstream and invalidates the boundary conditions necessary for the evaluation of $H_1(\psi^1)$ in Eq. (6). The flow pattern for F = .35 is shown in Fig. 1.

The conclusion is reached in the original analysis that when the Froude number is greater than $1/\pi$, it is impossible to separate parts of the fluid in the discharge process. However, the question concerning the nature of the flows at Froude numbers equal or less than $1/\pi$ remained to be answered. To answer this question an experimental program was initiated.

Dimensional Analysis

For the case of stratified flow for which there is a separation of the flow pattern into two regions—an upper, essentially stagnant region and a lower region in which the flow is concentrated—the following variables can be selected to define the problem (see Fig. 9):

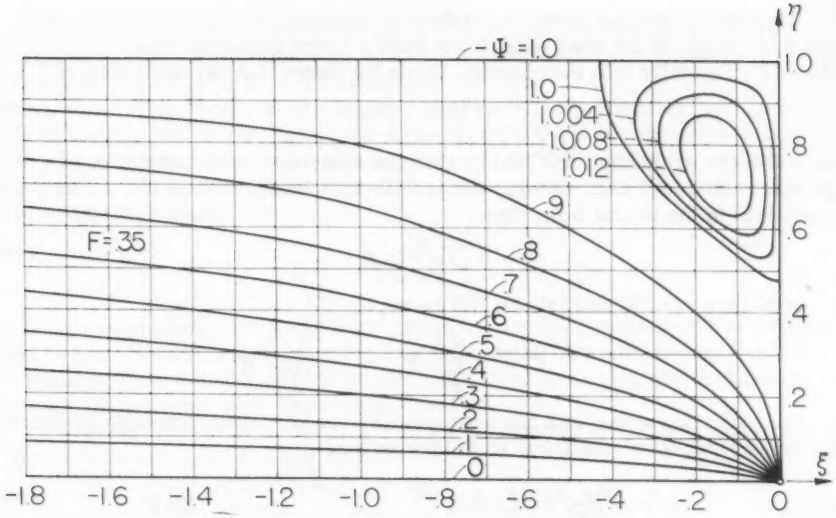

Fig. 1. Streamline pattern predicted by analysis for F = .35 (after Yih[1])

q = Volumetric discharge per unit width

d_1 = Height of zone in which flow is concentrated

d_2 = Depth of liquid in the channel

ρ_0 = Density of the liquid at the channel bottom

$\Delta\rho = \rho_0 - \rho_2$ = Density difference between the liquid at the bottom of the channel and that at the surface

g = Gravitational constant

μ = Viscosity of liquid in channel

Only one viscosity term has been included since for small $\Delta\rho$ the differences in viscosity throughout the liquid are exceedingly small and can be neglected.

The selected variables can be combined to form dimensionless parameters so that

$$\frac{d_1}{d_2} = \phi_1\left[\frac{q^2}{g d_2^3},\ \frac{\Delta\rho}{\rho_0},\ g\frac{\rho_0}{\mu}\right] \tag{13}$$

in which ϕ_1 is some function to be determined. By introducing the densimetric Froude number

$$F_2 = \frac{q}{d_2^2}\sqrt{\frac{\rho_0}{g\,\Delta\rho/d_2}} \tag{14}$$

the required expression becomes

$$\frac{d_1}{d_2} = \phi_2\left[F_2,\ \frac{\Delta\rho}{\rho_0},\ g\frac{\rho_0}{\mu}\right] \tag{15}$$

The experiment shows F_2 to be the predominant variable in the function. The parameter $\Delta\rho/\rho_0$ is important only when it is not small, and the Reynolds number, $q\rho_0/\mu$ is of secondary importance for the type of flow under consideration.

In the section devoted to a theoretical development and where separated flows were not considered, the Froude number was defined by Eq. (12) as

$$F = \frac{A}{d_2\sqrt{g\beta}}$$

This expression results from non-dimensionalizing the differential equation governing the flow. If the derived velocity distribution given by Eq. (8) is used and small differences in density are considered, the constant A can be eliminated so that

$$F = \frac{q}{d_2^2}\sqrt{\frac{d_2\rho_0}{g\Delta\rho}}$$

which is the same result as that obtained by dimensional analysis considerations alone.

When the Froude number is defined for the case of separated stratified flow, it is possible to employ as the characteristic length the height of the region in which the flow is concentrated, d_1, rather than the channel depth, d_2. If this is done the expression

$$F_1 = \frac{q}{d_1^2}\sqrt{\frac{\rho_0}{g\beta}} \qquad (16)$$

results, in which β is the upstream density gradient defined by Eq. (1). F_1 is related to F_2 by the multiplier $(d_1/d_2)^2$, and the significance of considering F_1 as a variable will be seen when the experimental results are discussed in the section under Results.

Experiment

The experimental work was carried out in a flume at the Hydraulics Laboratory of the National Bureau of Standards. This flume is 18 feet long, 2 feet high, and 1 foot wide (see Fig. 6). An eight foot long partition was placed in the flume in order to obtain a uniform channel of 6 inch width for a considerable distance upstream of the horizontal orifice. In this way it was possible to reduce the total quantity of discharge and to minimize the effects of the associated decrease in head pressure. The discharge orifice (see Fig. 6) with its rounded entrance to eliminate the formation of eddys was 11/16" in width and is judged to be narrow enough to approximate the line sink considered in the theoretical development.

The flume was filled with 15 distinct layers of salt-water, each with a different density, to a height of 22.85 inches (58 cm.). The alternate layers of water were dyed with a small amount of nigrosine prior to admission into the flume so as to delineate the flow pattern during the discharge of the flume. This technique for marking the flow was very satisfactory, and was prompted by the theoretical consideration that the streamlines would be lines of constant density. The densest solution was first added to the channel and then each succeeding lighter layer was floated onto the previous one. The equipment

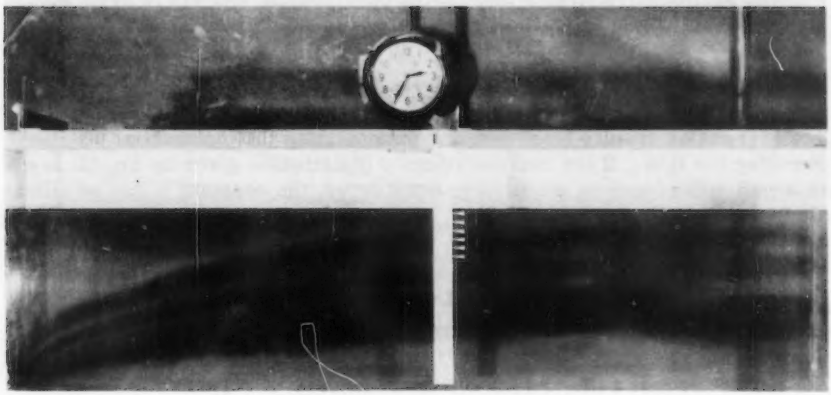

Fig. 2. Flow pattern obtained for F = .347 (Test 1).

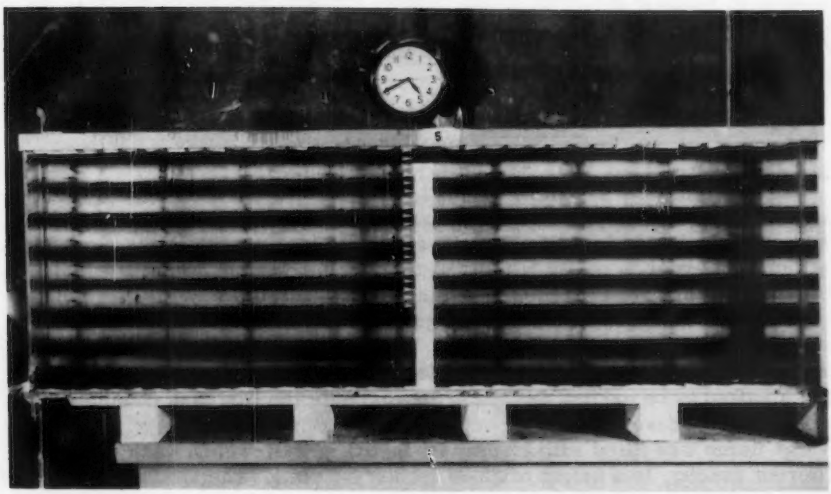

Fig. 3. Photograph of flume immediately prior to test. (The dye in the horizontal layers has not diffused appreciably in 17 hours. The vertical dye streaks, added just prior to taking the photograph, can also be seen.)

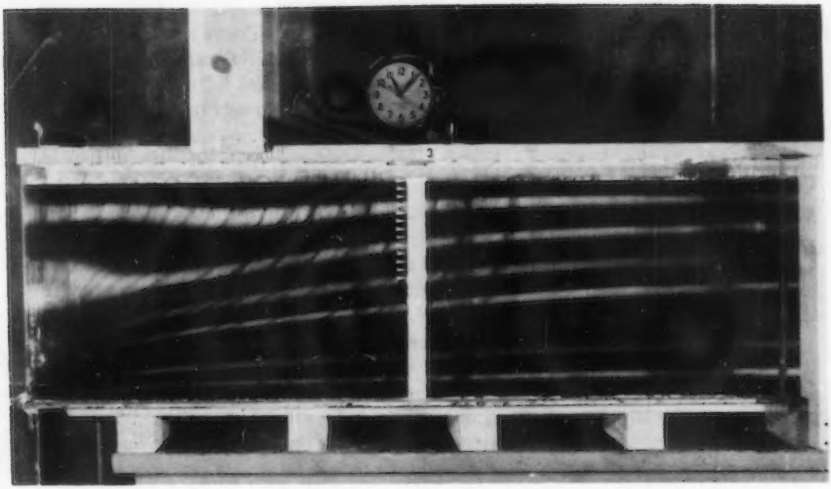

Fig. 4. Flow pattern for $F_1 = 0.262$ (Test 3). (Bulge in third layer from top appeared during the initiation of flow and was not significantly displaced during the test.)

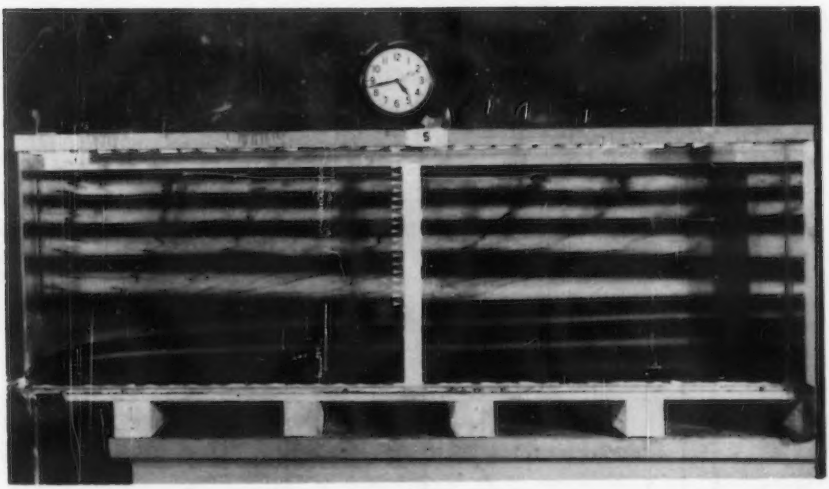

Fig. 5. Flow pattern for $F_1 = 0.245$ (Test 5). (The effects due to flow initiation are less pronounced but some wave motion exists in the upper region.)

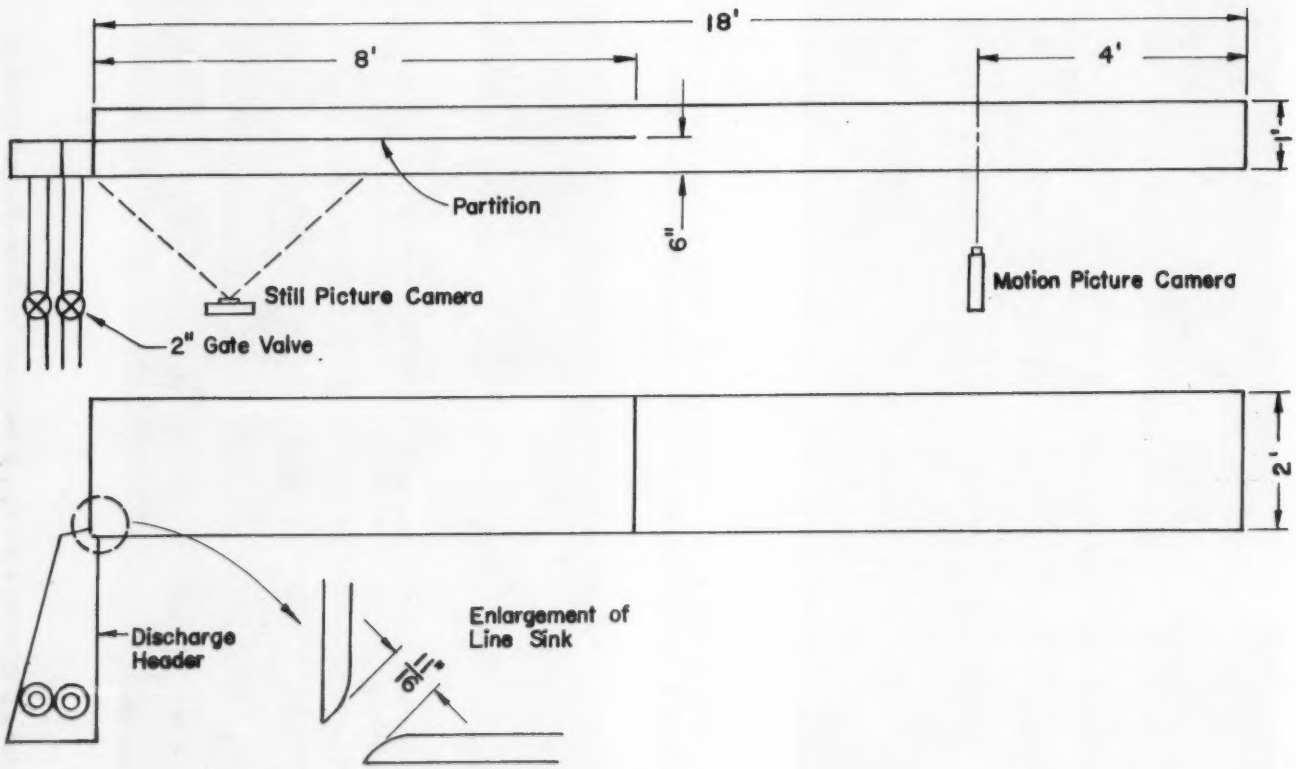

Fig. 6. Plan and elevation views of flume used for tests.

used for this floating process is shown in Fig. 7. With this apparatus there resulted a stream of liquid that was uniform across the breadth of the flume and which, when the rate of liquid addition was sufficiently low, yielded almost no disturbance of the liquid interface.

A period of about 18 hours elapsed between the time that the flume was completely filled and the time that the experiment (i.e. emptying the flume) was performed. This period of time permitted the diffusion process to smooth out the abrupt density differences between adjacent layers and thereby promoted the establishment of the desired linear density distribution. To this end the layers were made as narrow as practicable, 4 cm. However, the top and bottom layers were made 3 cm. high in order to compensate for the absence of diffusion at the upper and lower surfaces of the channel.

After the overall density difference for a particular test was decided upon, the prescribed density of the individual layers was obtained by adding quantities of sodium chloride, the required weight of which was determined from appropriate tables. An effort was made to obtain a qualitative picture of the density distribution after diffusion had taken place by using an electric probe that measured the conductivity of the solution between two platinum electrodes. This apparatus was calibrated with solutions of known salinity and the current recorded for a given voltage. A traverse was then made of the filled flume to determine the density profile. The results obtained with this probe verify the establishment of a continuous linear density profile from the original discrete or staircase distribution. Fig. 8 demonstrates the results of a density traverse made before one of the experiments. The change in the density distribution—from staircase to linear—is clearly evident even though the second set of density (i.e., conductivity) readings is consistently greater than the first set. The cause for the apparent, but unrealistic, increase in density between the two traverses was investigated but no complete explanation was obtained. With the linearity of the density profile established, the magnitude of the gradient used in the computations was determined from the channel depth and the difference in density of the liquid at the top and bottom of the channel. The values for these two densities were obtained by knowing the weight of dissolved sodium chloride in the top and bottom layers and using the aforementioned tables which relate solution density and the amount of solute used.

The flume was emptied by opening a gate valve that was located downstream of the sink. Different valve settings gave the various discharge rates used in the experiment. The discharge rate itself was determined by observing the time required for the free surface in the flume to drop 1 cm. in height.

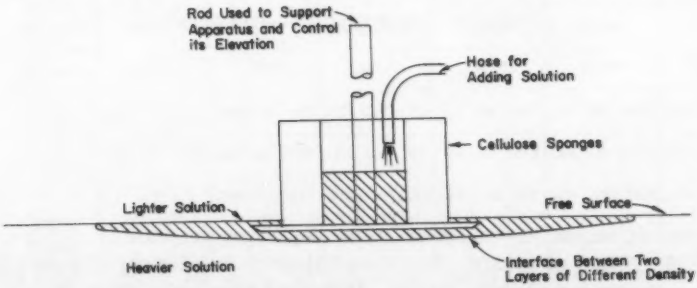

Fig. 7. Schematic drawing of apparatus used to fill flume.

Fig. 6. Plan and elevation views of flume used for tests.

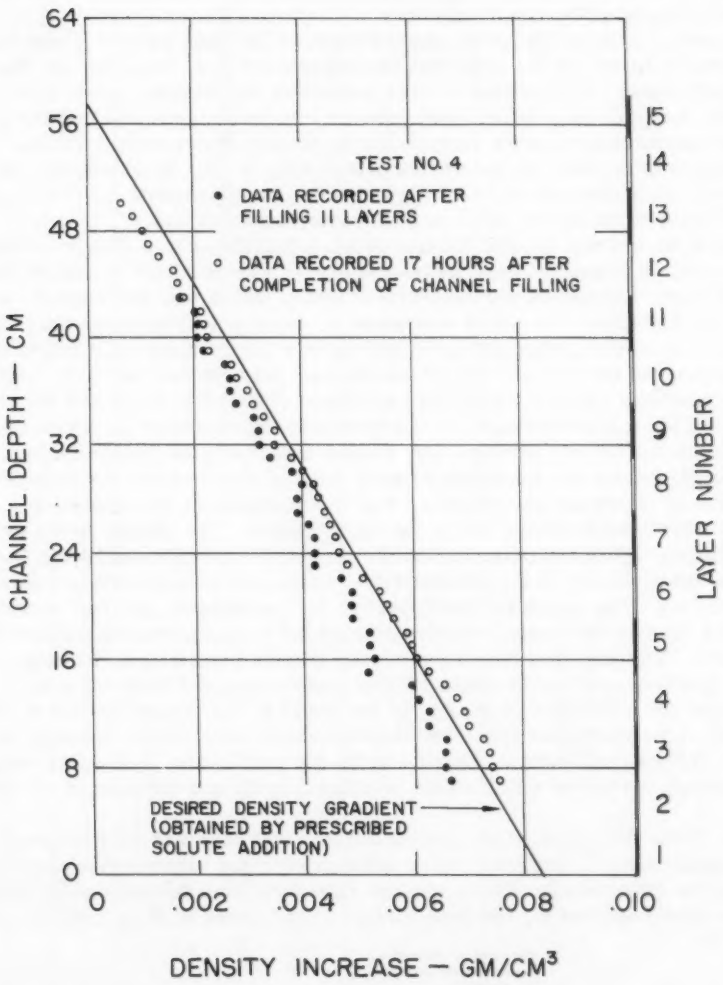

Fig. 8. Effect of sodium chloride addition on the density of solutions at various channel depths. Densities shown are those in excess of fresh water.

The liquid depth was measured with a multi-pronged hook gauge, and a recording chronograph was used to note the various time intervals.

Photographs of the flow pattern were taken in the vicinity of the discharge orifice whenever the free surface dropped 1 cm. in elevation (see Figs. 2, 3, 4 and 5), and motion pictures were taken near the upstream end of the flume in order to record the flow "at infinity".

The alternately dyed layers were effective in showing the flow pattern but they did not give much information regarding the magnitude and direction of the velocity components within the layers. In order to overcome this difficulty, vertical dye streaks were introduced by dropping potassium permanganate crystals into the flume just prior to the experiment. These dye trails along with a grid placed upon the side of the flume enabled the experimenter to observe more thoroughly the motion of the liquid.

Results

The most significant result of the experiment was the discovery of the separation of the flow pattern into two regions for densimetric Froude numbers below a critical value. The division in the flow pattern was horizontal and extended the full length of the flume. The upper region contained liquid which did not flow out of the discharge orifice while the lower region consisted entirely of liquid that flowed out of the channel. As the Froude number was decreased the region occupied by the upper, or relatively static portion became increasingly greater. The pertinent data for the six tests that were conducted are contained in Table I and summarized in Fig. 9.

The location of the dividing streamline was obtained by examining and measuring the photographs that had been taken. Several successive photographs for each test were used which accounts for the presence of more than one data point in Fig. 9 for a particular test. The data presented were gotten from those photographs that were taken after the unavoidable inertial effects due to flow initiation had subsided.

TABLE I
SUMMARY OF EXPERIMENTAL DATA

TEST	1			2			3			4			5			6		
q c.f.s./ft. width	.454			.214			.256			.127			.046			.052		
ρ_o gm./cm.^{3}	1.0132			1.0132			1.0132			1.0048			1.0048			1.0465		
$\Delta\rho$ gm./cm.^{3}	.0167			.0167			.0167			.00833			.00833			.050		
d_1 ft.	1.74	1.71	1.67	1.35	1.31	1.28	1.39	1.35	1.36	1.18	1.14	1.09	.719	.721	.696	.535	.526	.554
d_2 ft.	1.74	1.71	1.67	1.84	1.81	1.77	1.84	1.81	1.77	1.84	1.81	1.77	1.84	1.81	1.77	1.87	1.84	1.81
d_1/d_2	1	1	1	.733	.723	.723	.755	.747	.766	.64	.63	.617	.391	.399	.393	.286	.286	.306
$F_1 = \frac{q}{(d_1)^2}\sqrt{\frac{d_2\rho_o}{g\Delta\rho}}$	.273	.280	.289	.220	.232	.239	.249	.262	.262	.239	.255	.274	.235	.230	.245	.203	.209	.187
$F_2 = \frac{q}{(d_2)^2}\sqrt{\frac{d_2\rho_o}{g\Delta\rho}}$	.273	.280	.289	.118	.121	.125	.142	.146	.151	.098	.101	.104	.036	.037	.038	.017	.017	.017

EM 3

It was intended to investigate more thoroughly the flow for Froude numbers in the neighborhood of $1/\pi$. However, the quantity of flow that was needed to achieve this Froude number was so great, and the accompanying drop in head so fast, that an extensive investigation was not considered justified with the available equipment. Therefore, only a preliminary experiment was made for F near $1/\pi$. However, a comparison between the flow pattern predicted by Yih for F = .35 (Fig. 1) and the experimental result for F = .347 (Fig. 2) shows a striking agreement. The bulk velocity is 0.31 f.p.s. in this photograph which was taken 35 seconds after the initiation of flow.

The data presented in Fig. 9 indicates that separation of the flow pattern commences for a Froude number of 0.28. This agrees quite well with the value of 0.318 (i.e., $1/\pi$) suggested by the analysis as being the critical Froude number—in the sense that a significant change of flow pattern is to be expected. The experimental curve has been drawn to pass through the origin. This can be expected, not only from the data, but also from another consideration. Yih[2] has shown analytically and experimentally that as a horizontal disturbance in a stratified fluid becomes infinitesmal in strength, the vertical extent of the induced fluid motion is confined to a region equal to the vertical height of the disturbance. Thus, as the discharge is reduced to zero, it can be expected that the region of flow, hence d_1, will approach the height of the line sink, and consequently zero.

Fig. 9 also shows the curve $(d_1/d_2)^2 = \pi F_2$. It is proposed that this curve represents the results that would be obtained with an inviscid fluid. The two end points of the curve can be justified, and the form of the curve is consistent with the observed data and the expected influence of viscosity on the flow. The proposed relationship also supports the conjecture that F_1 would be nearly constant if plotted against d_1/d_2 and that F_1 may be the more significant parameter when dealing with stratified flows of the type under discussion. Fig. 10 represents the accumulated data with F_1 as the independent variable.

It was observed in the course of the experiment that there were horizontal velocity components in the upper region (i.e., above the dividing streamline). These components were small in magnitude and would reverse their direction as the flume was emptying. The direction of the motion was occasionally opposite at different elevations in this region of the flow. There was some indication of wave motion within the upper portion, but there was no evidence whatsoever of mixing of the liquid. Thus, compared to the lower region, the upper is considered to be stagnant.

With the motion pictures it was intended to substantiate the upstream velocity distribution utilized by Long[3,4] and Yih in their theoretical analyses. However, the differences in densities that were employed were not sufficiently large to conclude anything significant regarding the velocity law. The motion pictures did verify the region of flow separation as shown by the still photographs taken at the other end of the flume.

CONCLUSION

It has been demonstrated for the flow of a stratified fluid with a linear density variation into a line sink at the end of a horizontal channel, that a critical densimetric Froude number exists, below which the flow pattern divides into two distinct regions. There is an upper region composed of fluid that does not flow into the sink and which remains relatively motionless, and

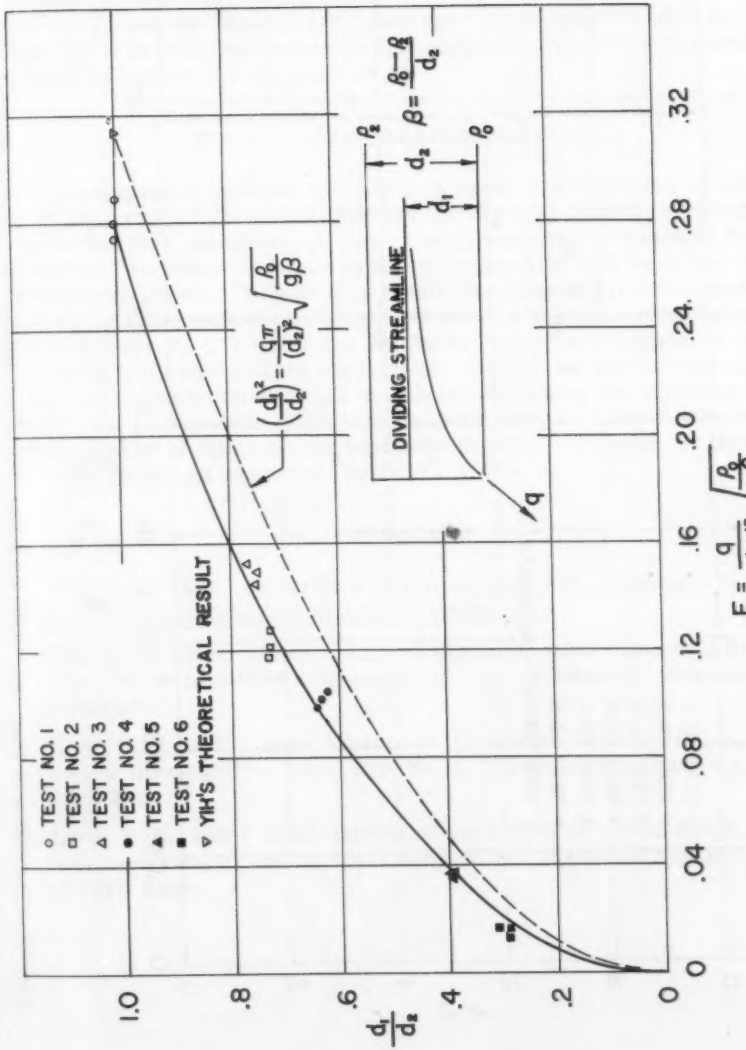

Fig. 9. The extent of flow separation as a function of the densimetric Froude number, F_2.

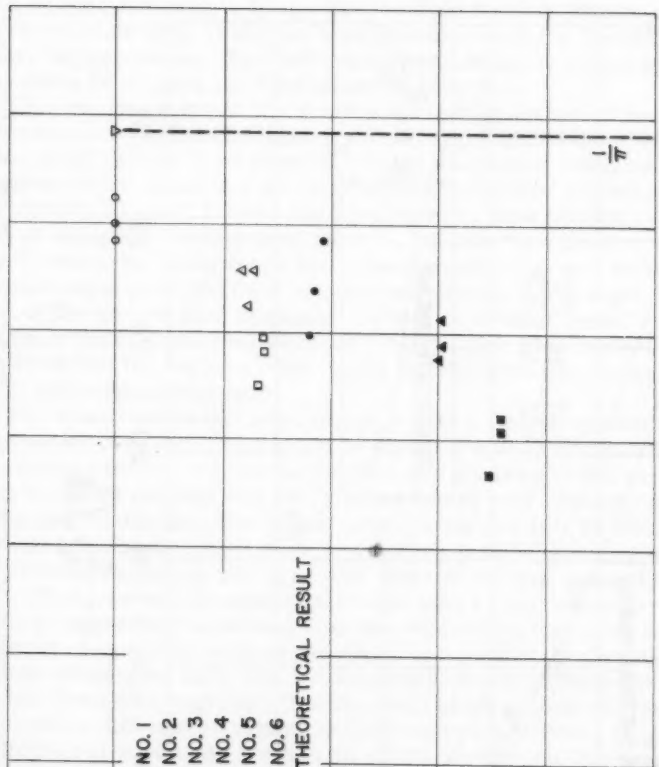

Fig. 10. The extent of flow separation as a function of the densimetric Froude number, F_1.

a lower region in which all of the discharging fluid is concentrated. As the Froude number is decreased to zero the height of this region of discharge, d_1, is also reduced to zero. The variation of d_1 with the Froude number is given in Figs. 9 and 10 which show the critical Froude number to be approximately 0.28.

The experimentally determined critical Froude number is somewhat less than the theoretical value of $1/\pi$ based upon the assumption of an inviscid fluid, but it is sufficiently close to give support to the theoretical analysis developed for higher Froude numbers.

ACKNOWLEDGEMENT

The experiment on which this paper is based was conducted by the author at the Hydraulics Laboratory, National Bureau of Standards, Washington, D. C. Without the kind permission of Drs. G. Schubauer and G. Keulegan to use the Laboratory facilities and their generous cooperation this work would not have been accomplished. The author is greatly indebted to Dr. Keulegan for the interest and suggestions that he offered during the course of the experiment and to Messrs. L. Carpenter and W. Plummer for their assistance during the setting up and running of the experiment. Finally, the author wishes to express his appreciation to Dr. C.-S. Yih for suggesting the experiment and for reading the manuscript. This work has been done for a research project at the University of Michigan, sponsored by the Office of Ordnance Research of the U. S. Army and supervised by Dr. C.-S. Yih.

REFERENCES

1. Yih, C.-S., 1958: On the flow of a stratified fluid. Presented to the Third U. S. National Congress of Applied Mechanics.
2. Yih, C.-S., 1958: Effect of a gravitational or electromagnetic field on fluid flow. To be published in Quarterly of Appl. Mechanics. Experiment unpublished.
3. Long, R. R., 1953: Some aspects of the flow of stratified fluids, I. A theoretical investigation, Tech. Rep. No. 2, The Johns Hopkins Univ., Dept. of Civil Engr.
4. Long, R. R., 1955: Some aspects of the flow of stratified fluids, III. Continuous density gradients, Tech. Rep. No. 6, The Johns Hopkins Univ., Dept. of Civil Engr.

Fig. 10. The extent of flow separation as a function of the densimetric Froude number, F_1.

Journal of the
ENGINEERING MECHANICS DIVISION
Proceedings of the American Society of Civil Engineers

A METHOD OF COMPUTATION FOR STRUCTURAL DYNAMICS

Nathan M. Newmark,[1] F. ASCE

This paper is one of the group of papers which were the bases for oral presentations at the Joint ASCE-IABSE Meeting, New York, October 1958. The entire group, including those published in CIVIL ENGINEERING, will be reprinted in one volume.

SUMMARY

This paper describes a general procedure for the solution of problems in structural dynamics. The method is capable of application to structures of any degree of complication, with any relationship between force and displacement ranging from linear elastic behavior through various degrees of inelastic behavior or plastic response, up to failure. Any type of dynamic loading such as that due to shock or impact, vibration, earthquake motion, or blast from a nuclear weapon, can be considered.

A method of numerical integration is described which for simpler cases and for a relatively small number of degrees of freedom is suitable for use with desk calculators. However the method is developed particularly for use with high-speed digital computers. Consideration is given to various types of damping, and to nonlinear behavior. A description is given of a method of treatment of elasto-plastic members in flexure, including the development of yield hinges. By suitable means of application of the loading, and with the introduction of enough damping to prevent indefinite oscillatory motion, the procedure can be used to determine the "static" behavior of a structure as it progresses through various degrees of inelastic behavior up to collapse.

Although the general procedure described is suitable for use in the study of the response of structures to earthquake motions, a modified procedure is described for handling the problem of a structure having time-dependent boundary conditions, which permits the direct calculation of displacements in

Note: Discussion open until December 1, 1959. Separate discussions should be submitted for the individual papers in this symposium. To extend the closing date one month, a written request must be filed with the Executive Secretary, ASCE. Paper 2094 is part of the copyrighted Journal of the Engineering Mechanics Division, Proceedings of the American Society of Civil Engineers, Vol. 85, No. EM 3, July, 1959.

1. Head, Dept. of Civ. Eng., Univ. of Illinois, Urbana, Ill.

the structure relative to the ground displacement, for convenience in interpreting earthquake phenomena.

The paper discusses the problem of structures with curved members and describes in detail a method of dealing with arched or curved structures in which the members are not permitted to change in length. The treatment of such inextensible structures presents some difficulties in the general treatment but methods are available for modifying the general procedure by introducing a series of constraint relations which reduces the number of degrees of freedom permitted in the motion of the structure.

The methods described herein have been used for the computation of the dynamic response of structures of various degrees of complexity including arches, domes, stiffened rings, framed structures, and simple spring-mass systems, subjected to various types of loading including nuclear bomb blast, earthquake foundation motions, random shock disturbances, wave action, and impact and dynamic effects from moving vehicles. However, examples of these applications are not given.

The work on which this paper is based was supported at the University of Illinois by the Mechanics Branch of the Office of Naval Research.

INTRODUCTION

Only general principles and methods for dynamic analysis are considered in this paper. The basic method of analysis is a general step-by-step method of integration of the equations of motion, and is applicable to any structure consisting of a group or series of concentrated or "lumped" masses supported on a deformable structure. For convenience, the structure may be considered to be a framework with joints or "nodes" at which forces may be applied, or at which masses may be placed. Any finite number of degrees of freedom may be considered, but it is essential in the procedure that the forces required to produce a pattern of deflection of the framework must be determinable when the deflections of the nodes at which masses are placed are specified. It is not necessary that the framing behave elastically.

Because in an actual structure the mass is not really divided into separate component parts connected together by flexible elements, the structure which is analyzed is only an approximation to the actual structure. However, a reasonable approximation can usually be made. For the actual structure, with distributed masses, the number of degrees of freedom of motion of the structure is infinitely large. The replacement of the distributed mass by a number of concentrated masses reduces the number of degrees of freedom and affects the response of the structure in the higher modes.

The simplification of a structure for the purpose of making a dynamic analysis involves engineering judgment. One must select the essential elements of resistance of the structure so as to arrive at an adequate and reasonably accurate expression of the resistance of the structure to motion. Also one must evaluate the masses of the structure and "lump" them together at places where they can be considered to act. In general the number of masses which should be considered depends on the accuracy which one wishes to achieve in the calculations.

The structure may be made up of individual members connected together at joints which would then be considered as the nodes of the structure.

However, the structure may be an integral one, either a solid body or an assemblage of plates and other elements, in which the nodes may only define points on the structure for convenience in the placement of loads and masses. It is necessary that the nodes be so chosen that the resistance of the structure to displacement of the nodes can be determinable, and that, if desired, the influence of inelastic behavior or plastic behavior can be taken into account. The structure is considered to be supported at its foundations at nodes also.

Although the method of analysis can take into account a situation in which the masses change with time or with displacement, the procedure is presented herein for masses which remain constant. No major change in concept or in procedure is required to deal with the case of a variable mass-time relationship.

Method of Analysis

Step-by-Step Integration Procedure

Consider the plane structure shown in Fig. 1 which is made up of weightless but deformable elements supporting lumped masses. The deformable elements of the structure in this particular instance are shown as either beams or bars which act under axial loading. However, much more complex structural types can be considered. All the elements shown are deformable and consequently each mass such as M, C, D, E, can move in both the vertical and horizontal direction. The points of support, such as at A and B, may also move both vertically and horizontally. In particular, these points may move in such a way that deformations and stresses are introduced in the structure by relative motion of the points of support on the foundation. Any of the masses may have acting on it a force in any direction, or component forces in the horizontal and vertical directions.

The mass at M in Fig. 1 is shown removed from the structure in Fig. 2. In Fig. 2a the point of attachment of the mass is indicated, and the positive directions of the resisting force exerted by the structure, R, and the displacement of the structure, x, are indicated. In Fig. 2b the mass is shown as a free body with the positive directions of P, R, and x indicated. Although this mass is shown as being acted on by only a horizontal force, in general it could have a vertical component of force acting on it also in which case it would have a component of motion and a component of resistance in the vertical direction. The sign convention that is chosen is determined by the arbitrary choice of the positive direction of the force P. The positive directions of x and of the resisting force R acting on the structure are taken as the same as for P, and the positive direction for the resisting force R acting on the free body mass M is opposite in sense to that of the resisting force R acting on the structure.

The positive directions of the acceleration a, the velocity v, and the displacement x are all the same. In general we will have for each possible component of direction of motion of the mass a displacement, velocity, acceleration, resisting force, and applied force. The resisting forces R at any instant of time are defined in such a way as to be that system of forces which are required to pull the weightless deformable structure into a deflection configuration defined by the instantaneous values of the displacement x at the same instant of time.

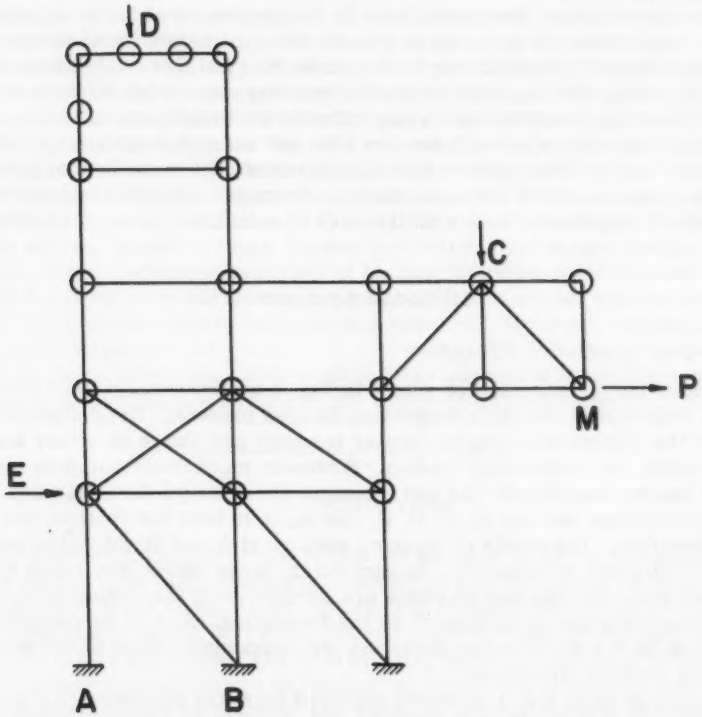

Fig. 1. General Type of Structure and Loading

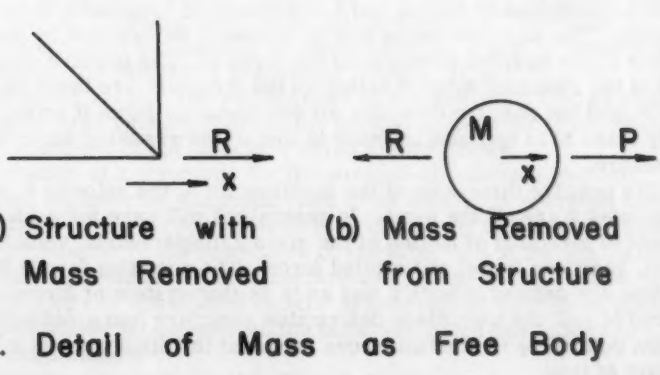

(a) Structure with Mass Removed

(b) Mass Removed from Structure

Fig. 2. Detail of Mass as Free Body

The sign convention and notation are chosen so as to make it apparent that the masses M modify or filter the forces P and transmit them to the structure in modified form as R. If the forces P are applied very slowly there is only a small acceleration and R is approximately equal to P. If the forces are applied quickly the difference between R and P can be very large. All the stresses in the structure are defined by the system of forces R. The structure can be analyzed statically for these forces. In general the forces R may continue to exist even after the forces P have dropped to zero. Similarly, R may be defined by the foundation displacements as well as by the deflections of the masses, even when no force P acts on the masses.

In general all of the quantities so far defined are functions both of position on the structure and of time. If we consider a time t_n and designate the values of all of the various parameters including displacements and forces at that time with a subscript n, such as R_n, our problem becomes that of defining the displacements x_{n+1} and forces R_{n+1} as well as the velocities v_{n+1} and accelerations a_{n+1} at a time t_{n+1}, which differs from t_n by the time interval h.

In the argument which follows we shall deal with a single mass in a single direction, but we might just as well deal with the whole set of masses and their possible displacements and designate the various directions with additional subscripts m such as in $R_{n,m}$. However in the discussion which follows we shall drop the second subscript for convenience, remembering that for each of the degrees of freedom for each mass we have a set of equations similar to the general set presented here. The derivation which immediately follows is described in terms of a situation where damping does not exist, for convenience. Later the procedure will be revised to include damping forces.

In general at any time, (consequently omit the subscript n), the acceleration is given by the relation:

$$a = (P - R)/M \tag{1}$$

It is assumed that at time t_n we know the values of the displacement and the velocity as well as the acceleration, but we know nothing about the situation at time t_{n+1}. Although there are methods of numerical integration which permit us to make estimates, at least for small time intervals, of the displacements and velocities at the later time knowing only the situation at the earlier time, these methods which do not take account of the change in resisting force during the time interval are not as accurate as the method described herein.

The method presented here was derived by the writer and first presented in Ref. 1. The relations which follow are given in terms of the acceleration at the end of the interval, a_{n+1}, although this is not in general known. A discussion of how the procedure can be handled in spite of this fact will be given subsequently. Two parameters, γ and β, are introduced to indicate how much of the acceleration at the end of the interval enters into the relations for velocity and displacement at the end of the interval. The relations which are adopted are given below:

$$v_{n+1} = v_n + (1 - \gamma)\, a_n h + \gamma\, a_{n+1} h \tag{2}$$

$$x_{n+1} = x_n + v_n h + (\tfrac{1}{2} - \beta)\, a_n h^2 + \beta\, a_{n+1} h^2 \tag{3}$$

It will be shown subsequently that unless the quantity γ is taken as 1/2, there is a spurious damping introduced, proportional to the quantity

$$\gamma - 1/2$$

It can be seen that if γ is taken as zero a negative damping results, which will involve a self-excited vibration arising solely from the numerical procedure. Similarly, if γ is greater than 1/2 a positive damping is introduced which will reduce the magnitude of the response even without real damping in the problem. Taking account of the fact that γ must equal 1/2, we can rewrite Eq. (2) as follows:

$$v_{n+1} = v_n + a_n h/2 + a_{n+1} h/2 \tag{4}$$

Application of the General Procedure

In general unless β is 0 we may proceed with our calculation as follows:

(1) Assume values of the acceleration of each mass at the end of the interval.

(2) Compute the velocity and the displacement of each mass at the end of the interval from Eqs. (4) and (3), respectively. (Unless damping is present it is not necessary to compute the velocity at the end of the interval until step (5) is completed.)

(3) For the computed displacements at the end of the interval compute the resisting forces R which are required to hold the structural framework in the deflected configuration.

(4) From Eq. (1) and the applied loads and resisting forces at the end of the interval recompute the acceleration at the end of the interval.

(5) Compare the derived acceleration with the assumed acceleration at the end of the interval. If these are the same the calculation is completed. If these are different, repeat the calculation with a different value of assumed acceleration. It will usually be best to use the derived value as the new acceleration for the end of the interval.

The rate of convergence of the process toward equality of the derived and assumed accelerations is a function of the time interval h. For a single-degree-of-freedom system having a circular frequency of vibration ω, the ratio of the error in derived acceleration to the error in assumed acceleration, (where the error is the difference between a value and the "correct" value), is given by the relation:

$$\frac{\text{error in derived acceleration}}{\text{error in assumed acceleration}} = \rho = -\beta \omega^2 h^2 \tag{5}$$

It is convenient to define the quantity ωh by the symbol θ according to Eq. (6):

$$\omega h = \theta \tag{6}$$

With this notation Eq. (5) can be rewritten as:

$$\rho = -\beta\theta^2 \tag{7}$$

Since the circular frequency ω is related to the period T by the relation

$$\omega = \frac{2\pi}{T} \tag{8}$$

Eq. (7) can be rewritten as follows:

$$\rho = -\beta\left(\frac{2\pi h}{T}\right)^2 \tag{9}$$

Now for convergence in a sequence of calculations the quantity ρ must be numerically less than 1. The critical value, for convergence, of the time interval h_c can then be computed from Eq. (9) by setting the right-hand side numerically equal to 1, with the result:

$$\frac{h}{T} = \frac{1}{2\pi}\sqrt{\frac{1}{\beta}} \tag{10}$$

Critical values of the convergence limit as a function of β are contained in Table 1.

For practical purposes the time interval would ordinarily be taken as smaller than that which corresponds to pure oscillation, or $\rho = -1$, in order to insure rapid enough convergence. If $\rho = -0.32$, the errors will be reduced to one per cent of their original value in four steps or four cycles of iteration. It would appear that, since for small values of β the convergence is most rapid, the lower values of β would be best to use. However other considerations affect the choice. The most important of these is the matter of stability which is discussed in the next section.

For a complex system, it can be shown that the rate of convergence is dependent upon the frequency or the period of the highest mode of the system. Consequently, the time interval used must be related to the shortest period of vibration, or the period in the highest mode of vibration, for the lumped mass system. Since stability also depends on a similar criterion, it appears that the greater the number of masses into which a system is broken down the shorter will be the permissible time interval for numerical calculation of the dynamic response of the system.

Stability and Errors in Numerical Computation

In order to study the stability of the numerical integration procedure, let us consider the special case of a simple system, a mass with one-degree-of-freedom without external force acting on it. For such a condition, and for some initial displacement and velocity, the motion of the system should be a pure oscillation, with a circular frequency of vibration as given by the relation

$$\omega^2 = \frac{K}{M} \tag{11}$$

in which K is the spring constant and M the mass. The relationship between the acceleration and the displacement is given by:

$$a = -\omega^2 x \tag{12}$$

With the above relations, and with the use of the symbol α^2 as defined by

$$\alpha^2 = \frac{\theta^2}{1 + \beta\,\theta^2} \tag{13}$$

we can derive a difference equation relating the values of three successive displacements of the system. The equation in general terms is:

$$x_{n+1} - (2 - \alpha^2)\,x_n + x_{n-1} + (\gamma - \tfrac{1}{2})\,\alpha^2\,(x_n - x_{n-1}) = 0 \tag{14}$$

From the general relations between finite differences and derivatives, it can be seen that the last term on the left of this equation corresponds to a factor times the velocity of the system, and consequently can be interpreted as a viscous damping term even though the system was defined as having

no damping. This spurious last term can be eliminated by the choice of $\gamma = 1/2$. In this case the general difference equation can be rewritten as:

$$x_{n+1} - (2 - \alpha^2)\, x_n + x_{n-1} = 0 \tag{15}$$

The general solution of the finite difference equation, Eq. (15), can be written in the case where the quantity $\alpha 2$ is less than 4. In this case, define a quantity ϕ by the relation:

$$\alpha = 2 \sin \varphi/2 \tag{16}$$

The solution of Eq. (15) can then be written in the form

$$x = A \cos \varphi\, t/h + B \sin \varphi\, t/h \tag{17}$$

This can also be stated in terms of a pseudo period T_s, and an initial displacement x_o and a parameter B which is of the same form as a velocity. The result is:

$$x = x_o \cos 2\pi t/T_s + B \sin 2\pi t/T_s \tag{18}$$

This may be compared with the exact solution, $\bar{x}$, which is given by Eq. (19):

$$\bar{x} = x_o \cos 2\pi t/T + \frac{v_o}{\omega} \sin 2\pi t/T \tag{19}$$

It can be seen that the approximate solution, Eq. (18), is similar to the exact solution and gives precisely the same response for an initial displacement, but gives a different period from that of the actual system. The value of the pseudo period T_s is given by the relation:

$$T_s = 2\pi h/\varphi \tag{20}$$

The relation between the pseudo period T_s and the true period T is:

$$T_s/T = \theta/\varphi \tag{21}$$

The following approximate formula may be used for a simpler definition of the relative value of the pseudo and the real period of vibration:

$$T_s/T = \sim 1 - (1 - 12\beta)\, \theta^2/24 - (17 - 120\beta + 720\beta^2)\, \theta^4/5760 - \ldots \tag{22}$$

The response of the system to an initial velocity is given by the second term in Eq. (18). The relationship between this response and the true response to an initial velocity, as shown by the second term in Eq. (19), is indicated in Eq. (23):

$$\frac{B}{v_o/\omega} = \left[1 + (\beta - \tfrac{1}{4})\, \theta^2\right]^{-1/2} = \sim 1 + \frac{1/4 - \beta}{2}\, \theta^2 + \ldots \tag{23}$$

If β is exactly equal to 1/4, the maximum velocity response is correct but if it is different from 1/4 there is an incorrect maximum velocity response.

Values of the errors in the period and of the errors in maximum response to an initial velocity are given in Tables 2a and b for several values of β and for a range in values of h/T. There is also given in Table 2c the rate of convergence for the corresponding tabular entries. For a system with a number of degrees of freedom, the limits are expressed in terms of the shortest period of the system.

When $\alpha 2 > 4$, the solution of Eq. (15) oscillates without bounds, and the calculation does not yield results even in remote agreement with the exact solution. The solution is said to be "unstable".

TABLE 1

CONVERGENCE AND STABILITY LIMITS

Item	Values of β				
	0	1/12	1/8	1/6	1/4
Convergence Limit, h/T	inf.	0.551	0.450	0.389	0.318
Stability Limit, h/T	0.318	0.389	0.450	0.551	inf.

The stability limit criterion, corresponding to a value of $\alpha^2 = 4$, can be expressed in terms of the time interval also. The relation between α and θ in Eq. (13) can be expressed as:

$$\theta^2 = \frac{\alpha^2}{1 - \beta \alpha^2} \tag{24}$$

from which the stability limit h_s can be written as:

$$\frac{2\pi h_s}{T} = \frac{2}{\sqrt{1 - 4\beta}} \tag{25}$$

which can be simplified to the form:

$$\frac{h_s}{T} = \frac{1/\pi}{\sqrt{1 - 4\beta}} \tag{26}$$

Values of the stability limit are shown in Table 1 as a function of β.

From Table 1, it can be seen that for values of β greater than 1/8, if the time interval is chosen for convergence the numerical procedure will always be stable. However, for values of β less than 1/8, convergence does not insure stability. Lack of stability gives no warning of difficulty, but introduces a spurious increasing oscillation into a system which may be in oscillation anyway. Therefore an inexperienced computer may not recognize the difficulty. Moreover, an instability in the higher modes only may not even be apparent to an experienced computer. Consequently it appears that unless other steps are taken to insure stability, one should limit the time interval by the stability criterion rather than by the convergence criterion.

Interpretation of Parameter β

A method very much similar to that described here for $\beta = 0$ has been discussed in Ref. 2. A method corresponding in many respects to that for $\beta = 1/12$ has been given in Ref. 3. However, the general treatment previously presented is different from that given here, particularly in the treatment of the starting of the motion. A method similar to that for $\beta = 1/4$ was first presented by S. Timoshenko in Ref. 4. However, he did not carry the procedure to the point of generalizing it for other than simple one-degree-of-freedom systems, nor did he develop the conditions on stability and convergence.

TABLE 2

EFFECTS OF LENGTH OF INTERVAL ON ERRORS DUE TO NUMERICAL PROCEDURE

h/T	Values of β				
	0	1/12	1/8	1/6	1/4
	(a) Relative Errors in Period				
0.05	-0.004	-0.0001	0.002	0.004	0.006
0.10	-0.017	-0.0003	0.008	0.017	0.033
0.20	-0.076	-0.006	0.028	0.059	0.121
0.25	-0.130	-0.015	0.038	0.087	0.179
0.318	-0.363	-0.045	0.047	0.129	0.273
0.389	*	-0.220	0.035	0.170	0.382
0.450	*	*	-0.100	0.195	0.480
	(b) Relative Errors in Maximum Response to an Initial Velocity				
0.05	0.012	0.008	0.006	0.004	0
0.10	0.052	0.034	0.025	0.017	0
0.20	0.209	0.166	0.116	0.073	0
0.25	0.614	0.306	0.202	0.122	0
0.318	inf.	0.732	0.414	0.225	0
0.389	*	inf.	1.000	0.414	0
0.450	*	*	inf.	0.732	0
	(c) Rate of Convergence				
0.05	0	0.008	0.012	0.016	0.025
0.10	0	0.033	0.049	0.066	0.099
0.20	0	0.132	0.197	0.263	0.395
0.25	0	0.206	0.308	0.411	0.617
0.318	0	0.333	0.500	0.667	1.000
0.389	*	0.500	0.750	1.000	1.500
0.450	*	*	1.000	1.333	2.000

* Values indicated are beyond limit for stability.

It is interesting to note the correspondence between β and the variation in acceleration during the time interval. Although a physical relationship is not possible for all values, for at least four values of β it is possible to define consistent variations of acceleration in the time interval. Three of these are shown in Fig. 3. It appears that a choice of $\beta = 1/6$ corresponds to a linear variation of acceleration in the time interval; a choice of $\beta = 1/4$ corresponds to a uniform value of acceleration during the time interval equal to the mean of the initial and final values of acceleration; and a value of $\beta = 1/8$ corresponds to a step function with a uniform value equal to the initial value for the first half of the time interval and a uniform value equal to the final value for the second half of the time interval.

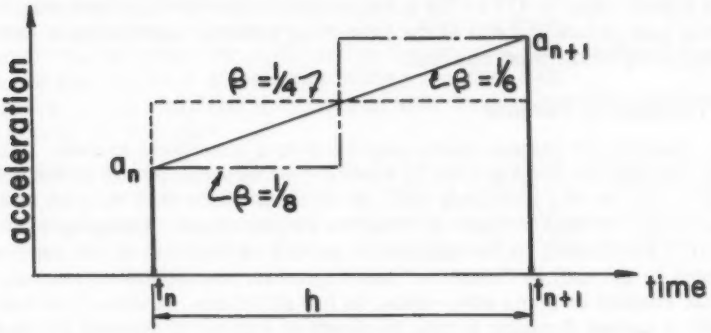

Fig. 3. Consistent Variations of Acceleration in a Time Interval

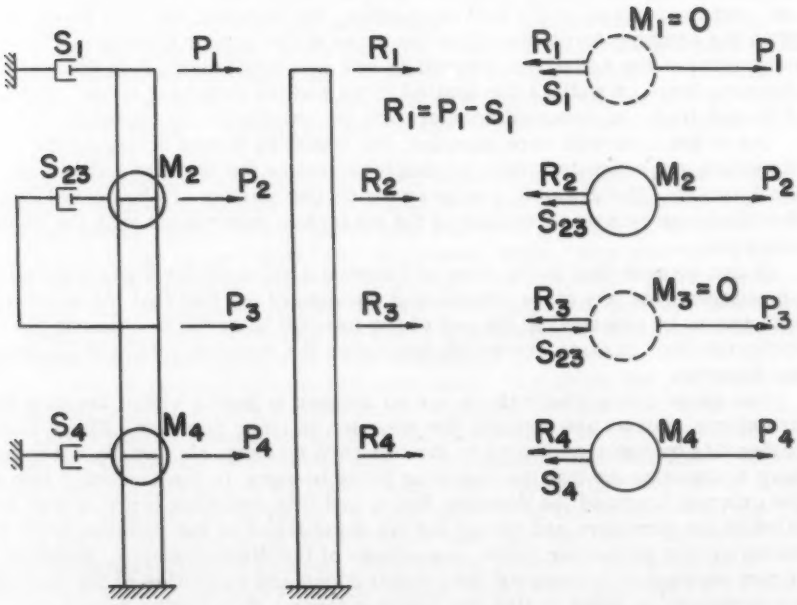

Fig. 4. Structure with Absolute and Relative Damping

It can also be shown that $\beta = 0$ corresponds to double pulses of acceleration at the beginning and end of the time interval with each double pulse consisting of a part equal to 1/2 of the acceleration times the time interval, one occurring just before the end of the preceding interval and the other just after the beginning of the next interval.

Treatment of Damping

Damping of various kinds may exist in a structural system. Damping forces may be proportional to velocity, or to some power of the velocity, or they may be of a frictional type, or in some cases they may be even proportional to displacement or relative displacement. Damping may be "absolute", and depend on the particular motion or velocity of the mass with respect to ground, or "relative" and depend on the motion or velocity of the mass with respect to some other point on the structure. A structure with several points having damping forces is shown in Fig. 4. If masses M_1 and M_3 are different from zero, then the damping forces can be applied to the masses, as indicated on the right-hand side of the figure, and the calculation is made in the following way:

After the acceleration at the end of the interval is assumed, the velocity at the end of the interval and the displacement are computed from Eqs. (4) and (3). The complete motion of the system is now defined at the end of the interval, and regardless of the kind of damping, the damping force is determinable. With the damping force placed on the mass in the proper direction, the acceleration at the end of the interval is now computed taking into account the damping force as well as the applied force and the resisting force. If this is different from the assumed acceleration the calculation is repeated.

As in the case with zero damping, the resisting forces acting on the structure are computed from the displacement of the structure at the end of the interval. The damping forces acting on the masses are computed from the displacements or velocities of the masses in accordance with the damping law used.

It can be seen that in the case of damping a value of $\beta = 0$ presents no real advantages over any other choice of β because of the fact that the acceleration still has to be assumed at the end of the interval in order to compute the velocity or other parameters which determine the damping forces at the end of the interval.

For those cases where there are no masses at points where damping forces or external forces are applied, the situation is more complex. Fig. 4 illustrates this by applying forces to the two zero masses, M_1 and M_3. It is necessary in these cases that the resisting force be equal to the algebraic sum of the external load and the damping force, and this resisting force is then applied to the structure and except for its dependence on the damping force remains at this particular value, regardless of the displacements. However, it is now necessary to compute the accelerations and velocities of the point on the structure in order to find the damping force. This can be done in the following way for the points where the mass is zero:

(1) Assume a value of acceleration of the mass point even though the mass is zero.
(2) Compute the velocity and displacement of the point and determine the damping force.

(3) Now apply the net resistance, corresponding to the difference between the applied force and the damping force, to the structure and determine the displacements of the structure at all points when the prescribed displacements are put in at the points where masses exist.
(4) Compute the acceleration at the end of the interval that is required to give the displacement determined in the preceding step.
(5) Compare the acceleration so computed with the one initially assumed and repeat if necessary.

This procedure is considerably more complex than that which is used when masses exist at all nodes. Consequently, it may be better to put in an actual small mass than to make the mass zero. However, if damping forces are not acting at points where there are zero masses, then it is relatively simple to handle the problem directly.

Recommended Time Interval and Choice of β

In any set of calculations in which an error in any one step makes all subsequent steps incorrect, it is desirable to have a self checking procedure. Consequently the procedure described herein works best where it is used with a converging system of approximations because under these conditions the calculations in any one time interval are repeated several times with slightly different values of the numbers involved. A close agreement between the results of successive calculations is in general a sufficient check on the accuracy of the numerical work when the work is done on a desk calculator. (Such a check may not be necessary on a high-speed computer.) It can be seen, therefore, that a value of $\beta = 0$, where there is no damping, is not necessarily a good choice because a separate check will be required in these cases to insure accuracy.

Studies of the effect of damping and of negative spring constants such as those corresponding to a decrease in load with increase in displacement, indicate that better results are obtained with values of β in the range from 1/6 to 1/4 than in the range below 1/8. In general, with a time interval of the order of 1/5 to 1/6 of the shortest natural period of vibration, the rate of convergence will be rapid enough for all practical purposes, and the errors will be small enough to be tolerable for every combination of damping or negative spring constant that appears to be practicable.

As a structure goes into the inelastic range, in general the periods of vibration all become longer and the shortest period becomes longer as well. For purely plastic resistance at the limit condition of an elasto-plastic structure, the period is infinitely long. Consequently the time interval can become considerably longer as plastic action develops in the structure. It is generally desirable to increase the time interval in accordance with the change in the structural rigidity as the structure becomes inelastic. However, it is not always convenient to compute the shortest period of vibration for a structure which goes partly into the plastic range. Consequently it is desirable to establish the conditions which govern the choice of time interval on some measurable behavior of the structure which is a natural function of the method of calculation. Since in general it is not practicable to consider modal behavior for structures which are not elastic, it is not desirable nor convenient to separate the individual modes of action of the structure.

With the use of a value of β greater than 1/8, the more convergence of the sequence of calculations is sufficient to insure stability and the rate of

convergence will be an adequate criterion for the time interval. Consequently, one can establish a rate of convergence based on the number of iterations which it is desirable to make in a time interval and then examine the rate of convergence of the actual calculations as the calculations progress. For example, if it is desired to have three significant figure accuracy in displacement and velocity, three significant figures in the acceleration are also desirable. A rate of convergence such that the error is less than one part in a thousand at the end of three cycles would imply a rate of convergence of 10 per cent or of 0.10. By reference to Table 1c it can be seen that a ratio of time interval to natural period of the order of 0.10 for $\beta = 1/4$ will insure this rate of convergence. Similarly, a time interval slightly longer will be adequate for $\beta = 1/6$. However, it appears that these time intervals will introduce errors of the order of 2 per cent to 3 per cent in the period. If this is not admissible, then a faster rate of convergence can be established to keep the error in the period down as well.

Let us say for example that a time interval consistent with a rate of convergence of 10 per cent is desirable and that three cycles of iteration will normally be considered convenient so as to bring the results to an error of less than one part in a thousand at the end of the third cycle. Then a fourth cycle will verify that this is in fact the case. Under these conditions, then, we can assume a time interval and run through the calculations several times. If the desired rate of convergence is not obtained, we have obviously assumed too long a time interval and we can shorten the length. Since the rate of convergence is generally a function of the square of the time interval, the next estimate can usually be decided on from the course of the preceding calculations. If the time interval is made smaller in accordance with the estimate of convergence, and if convergence is now in fact obtained with about three to four cycles of iteration, then this time interval can be used in subsequent steps. If however the time interval chosen leads to convergence in only two or three cycles, we have probably taken too short a time interval and in the next cycle in the calculations we may choose to use a longer time interval.

With this type of procedure, and with continual reexamination of the time interval in terms of the rate of convergence, one can take account of the change in the characteristics of the structure without loss in accuracy and without supplementary calculations. The procedure described above can readily be programmed for a high-speed digital computer. However, an upper limit on the time interval is usually desirable to avoid difficulty in terms of accounting appropriately for the variations in the applied loading.

Calculation of Resistance

For the general case of a framed structure with either flexural or axial resistance, and with deformation in all of the members, it is a relatively simple matter to perform the calculation for the resisting forces if the displacements are given. All that is required is to take the set of displacements at a given time instant, pull the joints of the structure into the corresponding configuration, compute the axial forces in the members from the changes in length between the nodes, and compute the moments in the members by a process which involves two stages as follows:

(1) Consider the joints locked against rotation and determine the fixed end moments in all of the members corresponding to the deformations.

(2) Relax the joints by permitting them to rotate. Either moment distribution or some other technique of calculation can be used to determine the final moments in all the members.

The shears and axial forces can now be computed in all the members, and one can compute the horizontal and vertical components of the forces on the pins which hold the structure in the displaced configuration. These forces, reversed in direction, are the resisting forces acting on the structure.

If the structure is not elastic, it is possible to make the calculation for any known load-deformation or axial-displacement deformation or curvature-moment relationship. The technique of the calculations is unchanged. However, for nonlinear behavior it is essential that one take account properly of the direction of loading in a member or element so as to be sure that the element is continuing to deform in the same direction with the appropriate reduced stiffness, and to determine when it is recovering or unloading with the appropriate increased stiffness. A test of the direction of relative deformation can readily be made to determine this.

In a structure such as shown in Fig. 5, where masses might be considered placed at all the joints of the structure, it is usually neither convenient nor desirable to consider the most general situation in which the masses can be displaced horizontally as well as vertically. The reason for this is that the period of vibration of the masses in the horizontal direction is very short compared with the period of vibration in the vertical direction. If one were to solve the problem with the general procedure, one would have to use an extremely short time interval which would make the calculation tedious.

In such cases it is usually desirable to consider a restricted type of deformation of the structure to reduce the number of degrees of freedom. This can be done by connecting the masses to the structure by means of vertical links as shown in Fig. 5, and specifying that only vertical forces can act on the masses which in turn are considered to move only vertically. The links are considered to remain vertical by making them long enough so that the horizontal motions of the truss joints do not introduce an angle into the link between the truss joint and the mass.

In the structure shown in Fig. 5 the number of degrees of freedom with a mass at each node would be 20. However for the system shown only 5 degrees of freedom are needed. Both the difficulty in the calculation and the number of repetitions of calculations for a given duration of motion will be greatly increased if the 20 degree-of-freedom structure is used. However, some difficulty in computing the resistance functions in Fig. 5 is encountered because it is not possible directly to determine the changes in length of all the members from only the vertical component of displacement of the lower chord of the truss.

In cases of this sort, it is possible to proceed in a slightly different fashion by determining either directly, or by inversion of the influence matrix for the structure, the set of forces required to produce the given set of vertical displacements. In the general case, one can summarize the calculations as follows:

(1) Compute the vertical displacements of each of the masses for individual unit values of vertical force at each of the masses in turn. The set of values obtained is designated as the influence matrix for deflection of the structure.

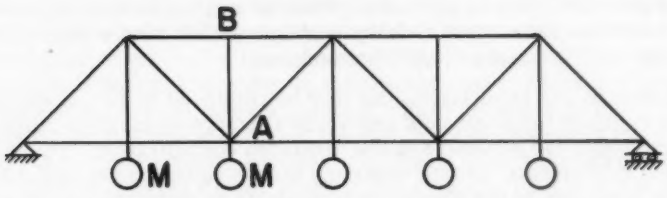

Fig. 5. Structure with Reduced Number of Degrees of Freedom

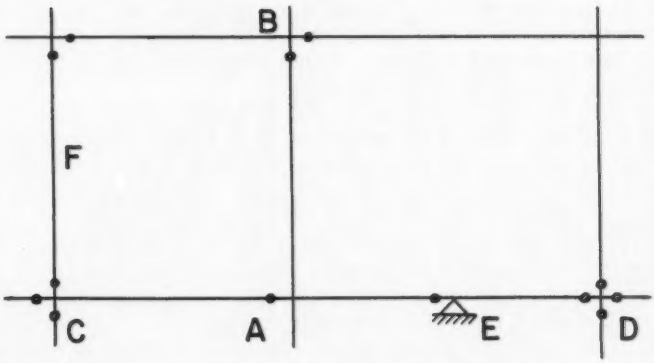

(a) Frame with Plastic Hinges

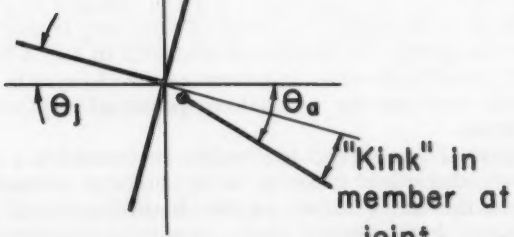

(b) Detail of Joint

Fig. 6. Elasto-Plastic Frame

(2) From these influence coefficients, compute the set of forces on the structure for given values of the displacements. The calculation involves solving a set of simultaneous equations for each set of values of displacement. This can be systematized by "inverting" the influence matrix to obtain the stiffness matrix for the structure, which represents the forces acting on each of the masses for a unit displacement of each of the masses in turn. If this inversion is performed once, the matrix of values can be applied to any set of displacements to determine the required resisting forces.

(3) The coefficients in the influence matrix will change when any elements in the structure become plastic. Consequently the calculation of the influence matrix and the inversion of the matrix to obtain the stiffness matrix must be performed for each change in stiffness that occurs during the history of the structure. It may be desirable to make the calculations by a "relaxation" procedure for more complex structures of this type. However, in principle the structure can always be analyzed to find the forces consistent with a given set of deformations.

It might be pointed out that for a beam of the same span as in Fig. 5, with a series of masses acting on it, it is not necessary to use the influence matrix and invert it to find the stiffness matrix. The structure can be analyzed directly by pulling the joints into the deflected configuration, locking them against rotation, and then distributing the fixed end moments corresponding to these deformations to find the shears in the members and the consequent forces acting on the masses. Although in such a case there would be theoretically 10 degrees of freedom, 5 of the degrees of freedom are associated with horizontal axial deformations in the beam, and these are not "coupled" with the vertical deformations because of the nature of the system. This observation is true only for a straight beam. In a later discussion, the procedure applicable to an arched beam will be described.

The structure in Fig. 5 is one of several special cases which require a slightly modified form of treatment. Another case concerns any structure with constraints on the deformation of some of the members. Such a structure might be a polygonal arch which is considered to deform only in flexure and which is not considered to have any axial deformation of the arched members. In this case also the number of degrees of freedom are reduced, but the treatment must be somewhat different from that for the truss because the number of constraints may reduce the number of degrees of freedom even below the number corresponding to a mass at each node prescribed to move in a particular direction. Further discussion of this topic is contained in the last chapter of this paper.

Both Figs. 4 and 5 show structures with zero masses at some of the nodes. A general procedure for such structures can be discussed. In general, one can handle the problem in the following way when damping forces are not present. The modification for damping is readily made as has been discussed previously.

(1) Assume values of acceleration only at the joints where masses exist and in the direction in which the masses can move.

(2) Compute the displacements of the masses, but not the displacements of the joints not having masses.

(3) Let the joints without masses be free to deflect but apply to these joints the external forces which are applied at these points. If these external

forces are zero, no restraints and no loads are applied at the massless nodes.

(4) We now have a system with prescribed deflections at some points only and with prescribed loads at other points. It may be pointed out that at some particular joint for example there may be a prescribed vertical displacement and a prescribed zero horizontal load, if we consider that only vertical displacement of the mass is to be considered at that point.

(5) We now require the calculation of the resisting forces at the masses in the direction of motion. In general this can be done by an influence coefficient procedure in which we apply unit forces at the masses which are displaced, one at a time, and compute the displacements at these masses. We use these influence coefficients to write a set of equations which in effect says that the product of each unknown reaction force at each mass multiplied by the influence coefficient for deflection at each of the masses, and summed for each of the masses individually, leads to a deflection at each mass equal to the prescribed deflection minus the deflection in that direction at that mass due to the prescribed forces acting at the nodes where no masses exist.

(6) The solution of this set of equations yields the desired results. We may now have to complete the calculation by determining the displacements at the massless nodes of the structure if these are required for any other purpose. In most instances they will not be needed and need not be determined. Where damping forces exist, however, we will need these displacements so that we can determine the velocities and accelerations at these points in order to check on the values of the damping forces dependent on these quantities.

Non-Elastic Behavior

General Comments

For trusses the problem of inelastic behavior of the members is a relatively simple and straightforward one. One need take into account only the change in deformation of the members in each time interval to determine whether the plastic action is continuing or the member is unloading elastically. Having knowledge of the load-deformation characteristics of the member, the required force in each member can be determined and the restraining forces or the resisting forces in the structure are directly determinable. Although the general concept for framed members is the same, there are some difficulties which require consideration.

Elasto-Plastic Frames

The method for dealing with elasto-plastic behavior in frames is described here. Consider a general framework consisting of members acting in flexure as shown in Fig. 6a. At some stage in the deformation, the moment at the ends of the members shown as black dots in the figure has reached the plastic limit moment. One or several of the members meeting at a joint may be loaded to the plastic limit moment.

It is general enough to consider members which are not loaded internally and in which the moments arise from a prescribed set of displacements of the joints. In a situation such as that shown at E in the figure we might have had

an interior load applied dynamically. Then we will in effect have a prescribed displacement of joint E which can be considered to be an external hinged support as shown. Consequently, our method of treatment is general and can deal with internal loads as well as loads applied at the joints.

At some time t_n the structure has been analyzed with the result that we have determined the plastic hinges which exist at that time and, as a consequence, we have determined the velocities, displacements, and resisting forces in the structure. We can also determine from the final configuration and moments in the structure at that time the rotations of the joints θ_j and the rotations at the plastic hinges θ_a. If we have analyzed the structure by moment distribution, the fixed end moments can be computed and distributed and from a comparison of the fixed end moments and final moments the rotations at each end of each member can be determined. The rotation of a joint is the same as the rotation of the ends of all members meeting at that joint which do not have plastic hinges. The "kink" or relative angle between a member having a plastic hinge at the joint and the angle of the joint is measured by the difference between θ_a and θ_j. The kink angle is of importance in determining whether the member is loading or unloading at that joint.

It is considerably simpler to deal with the structure in each interval by making calculations of the change in the structure. In other words, one works with the change in displacements during the interval as defining the fixed end moments at the end of the interval and the final moments so computed are the changes in moment to be added to the original moments in the various members. In this process one can deal with the elasto-plastic hinges as actual hinges if the structure is loading during the interval and the hinges will be removed if the structure is unloading during the interval.

Three situations require consideration:

(1) If the total moment, including the original moment plus the increment in moment during the interval, at the end of any member exceeds the plastic hinge moment, then a hinge must be placed in that member.
(2) If a hinge exists in a member and the increment in kink angle in the member at the joint at the end of the interval is in the same direction as the preceding total kink, then the hinge remains.
(3) If the kink angle in what was originally a plastic hinge should decrease, then the plastic hinge must be removed.

The structure is modified by adding, keeping, or removing the plastic hinges originally assumed for the calculation at the end of the interval, in accord with the above criteria, and the calculation repeated until the conditions obtained are consistent.

Only in unusual cases can there be plastic hinges in all members meeting at a joint. Such a case is shown at D in Fig. 6. In such an instance the joint rotation can be assumed to remain at its value at the time the last members at the joint become plastic. (It is clear that in such a joint at least two members must become plastic finally, and at least two members must simultaneously "unload" and have the hinges removed.)

The only other special case that needs consideration is that shown by the member F in which both ends develop plastic hinges. Such a member can be considered to have end rotations the same as those which existed prior to the development of the last hinge in the member.

In some cases it may be desirable to study the formation of plastic hinges in a structure as the loading on the structure is applied, more or less

"statically", or applied and released in various ways. This can be done very simply by specifying a relatively slow rate of application of the loading, corresponding to a maximum being reached in not less than twice the natural period of vibration in the fundamental mode. It is usually convenient to introduce damping so as to avoid oscillatory motion during or following the loading cycle. The masses can be taken arbitrarily small in such a calculation if we are not concerned with the dynamic response, so as to make the fundamental period relatively short.

Time-Dependent Boundary Conditions

In general if the boundaries or supports of a structure move with time no change is required in the method of calculation and the general procedures described herein are directly applicable. However, there are instances where it is desirable, or convenient, to deal with the motion of the elements of the structure relative to the base or foundation of the structure, rather than in absolute terms. Such situations arise commonly in earthquake motions. The method described herein is useful primarily in those cases where the foundation moves as a single unit and where motion of the foundation of the structure with all masses equal to zero would not introduce stresses in the structural framework.

Consider the structure shown in Fig. 7 where the base can move as a unit in the horizontal direction. Let the motion of the base be defined as a function of time by the quantity y. The motions of any of the masses in the structure are defined by x. Let us assume that the axial deformations of the members can be neglected and that we have only flexural deformations to consider. In such cases, we can lump the masses at each floor level at one point as shown. The more general case offers no difficulties, however.

If now we apply to the structure with masses on it a force F, in accordance with the relation

$$F = M \ddot{y} \tag{27}$$

then the structure and the foundation will move as a unit with no relative displacement between the two.

If now we apply to the structure considered supported on a fixed foundation a force $\bar{P}$, defined by the relation

$$\bar{P} = P - F \tag{28}$$

we have changed the problem from one in which there are external forces and a time-dependent boundary motion into one in which we have external forces and no boundary motion. The displacements for the modified forces $\bar{P}$ will be designated by u, where

$$u = \bar{x} - y \tag{29}$$

it can be seen, of course, that the total motions of the masses, x, are the sum of the relative motions u plus the foundation motions y, and the total loads applied are the external forces P. Consequently, the procedure is valid.

For more complex systems, one must modify this procedure by taking into account the displacements at each of the several points of support, and defining the quantity y for the motion of the masses as being the motion at that point on a massless structure consistent with the foundation motions. In the

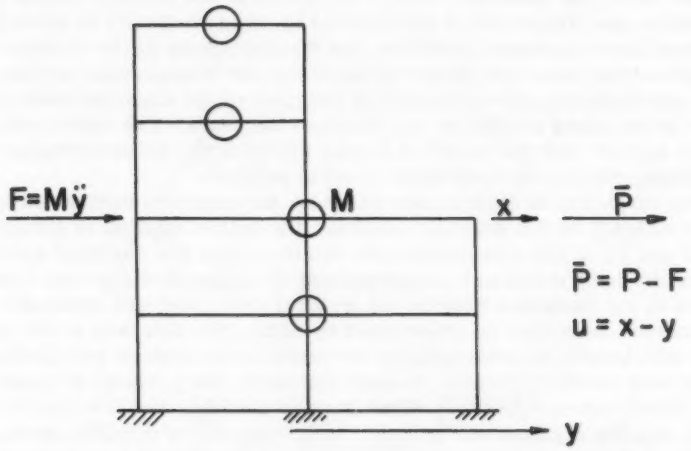

Fig. 7. Structure with Time-Dependent Boundary Conditions

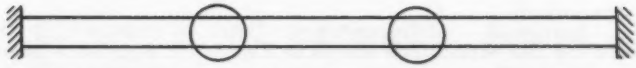

(a) Structure with Weak or Zero Coupling Between Sets of Modes

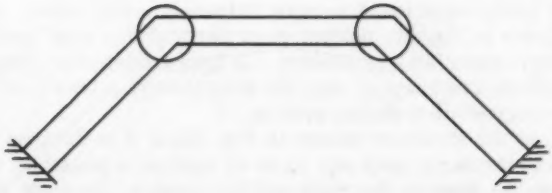

(b) Structure with All Modes Coupled

Fig. 8. Examples of Different Types of Coupling Between Modes

case of a beam, for example, simply supported at one end and hinged at the other where the hinged end is constrained to move vertically in accordance with some time-dependent condition, the displacements of the masses along the length of the beam are proportional to the end displacement and are equal to that end displacement multiplied by the ratio of the distance from the simple support to the mass divided by the length of the beam. The same method of analysis applies, and the modified forces will give the relative displacements of the beam, relative to boundaries fixed in position.

In this case, and in other cases where no stresses are introduced in the weightless beam by the boundary motions, the entire solution is straightforward and all of the stresses can be obtained from the modified system. However, in more complex cases where the boundary motions may introduce stresses in the massless system, the general principles are applicable but the total stresses must then be determined by adding the stresses in the massless system with boundary motions to the stresses in the system with fixed boundaries and with modified forces. In such instances, the problem of plastic behavior introduces complexities which may be unwieldy and it is not desirable to work with the replacement system. In all cases it is possible to work with the original system directly with the general methods that have been described.

Curved Frames and Arches

General Procedure

Consider the two structures shown in Fig. 8. In Fig. 8a, a beam is shown with two masses. These masses may move vertically with consequent flexure of the beam or horizontally with consequent axial deformation. There is no coupling between these sets of motions. There are two degrees of freedom in each set or type of motion and four degrees of freedom altogether. The vertical motions can be dealt with as if in a two-degree-of-freedom system and the axial motions can be dealt with also as in a two-degree-of-freedom system with neither being considered to have influence on the other. However, in the structure shown in Fig. 8b, neither pure vertical nor pure horizontal motion of each mass is possible. In general, all four modes of motion or all four degrees of freedom are coupled, and the structure requires treatment as if it were a four-degree-of-freedom system.

However, in the structure shown in Fig. 8b, if it is desired to avoid axial deformation of the bars, only one mode of motion is possible, with the mass to the left moving down to the right and the mass to the right moving up and to the left. The system has only one degree of freedom, and can be analyzed as such although the method of analysis requires some care in order to avoid introducing motions that are inadmissible.

Inextensible Members—Constraint Relations

Consider the structure shown in Fig. 9a. Here there are three interior masses and if the members are considered inextensible there will be two degrees of freedom. We arrive at this number by considering the total number of degrees of freedom of the system if the members were capable of deformation, namely 6, and subtracting from this number the number of constraint conditions or in this case the number of inextensible members, namely 4.

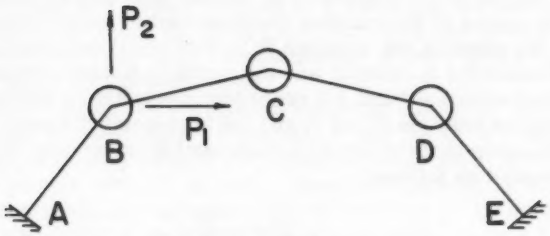

(a) Arch Considered

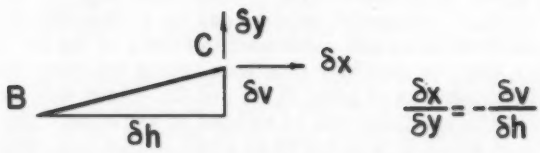

(b) Constraint Relation for Zero Extension of BC

Fig. 9. Extensible and Inextensible Arched Structures

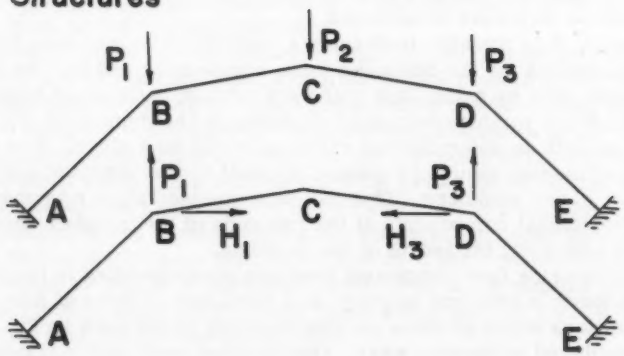

Fig. 10. Symmetrical Loading Producing No Displacement in an Inextensible Arch

For any one of these members, such as BC, the condition that the deformations at the joints correspond to no change in length of member BC can be expressed in terms of the relative displacement of joint C compared with joint B and the slope of the member BC. For small deformations, where δx and δy represent the horizontal and the vertical motion of point C with respect to point B, and where δV and δH represent respectively the vertical difference in elevation between C and B and the horizontal distance between C and B, the relationship that the relative deformation involve no change in length can be expressed as follows:

$$\frac{\delta x}{\delta y} = - \frac{\delta V}{\delta H} \tag{30}$$

This equation can be interpreted as meaning that the deformation is such that point C moves perpendicularly to member BC.

A similar constraint relation can be written for each of the bars. If the total deformations are expressed in terms of the increments in the deformation, one can find four relations among the three horizontal and three vertical displacements of point B, C, and D. These will be somewhat more complex but the relations can be written in any case. The number of independent relations which it is possible to write in this case will be equal to the number of constraint conditions, namely four. With four relations among six displacements, it appears that there are only two independent displacements remaining. These can be chosen as any two components of displacement, and the calculations carried through in the usual way, but with only two masses and two directions of motion considered. By the use of the constraint relationships, when the two deflections which are independent are assumed the remaining deflections can be readily computed, and the entire pattern of deformation of the structure established.

However, it is possible to develop a more direct procedure for determining the relationships for the resisting force components and for the displacements. This can be done by noting that there are certain patterns of loading on the structure which produce only axial stresses in the members. For these loading components no deformations of the arch can take place. It is obvious that one type of loading would correspond to axial forces directed along the length of any one of the members. This can be expressed also in terms of the vertical and horizontal components at the two ends of the member such that the resultant lies along the length of the member.

By considering four component loadings corresponding to loadings producing axial force in only one member at a time, one arrives at four independent load conditions which produce no displacement in the arch in Fig. 9. These can be combined in various ways. One obvious combination consists in a pattern of only vertical forces at the interior nodes. These of course would be resisted by vertical and horizontal reactions at the ends but these do not enter into the picture if the ends do not move. This pattern of loading is shown in the upper part of Fig. 10. A second pattern of loading in the lower part of Fig. 10 consists of the two sets of loadings which produce tension only in the outer members of the arch. If the structure is symmetrical, and if the loads B and D are made equal, then the loading pattern will be symmetrical. The loading pattern in the upper part of Fig. 10 will always be symmetrical for a symmetrical structure. These two loadings represent the two independent types of symmetrical loadings producing no displacement in the inextensible arch of Fig. 9. Of course any combination of these two loadings will also be a

symmetrical loading producing no displacement. Consequently, one can arrive at a loading consisting of a downward load at C and equal horizontal loads with no upward load at joints B and D. There are two other independent loadings which are anti-symmetrical. From combinations of the four loadings, various types of loading patterns can be derived.

The advantage of having the constraint conditions stated in this way is that now we can add any of these types of loadings to any set of resistances or of external loadings so as to preserve the number of degrees of freedom of the structure at the proper number, in this particular case two. In other words, after the two independent displacements are decided on such as the horizontal and vertical displacement at joint B in Fig. 9, and the corresponding displacements at C and at D are determined consistent with these, then both the external forces and the resistance can be modified by adding force patterns similar to those in Fig. 10, (plus the two anti-symmetrical loadings), so as to make the accelerations in the various directions of all of the masses consistent.

Consistency in the vertical displacements during the interval requires consistency in the vertical accelerations at the end of the interval. Since the displacements at the beginning of the interval have been made consistent, and since the velocities and accelerations at the beginning of the interval are consistent, we need only insure that the accelerations at the end of the interval are properly consistent. In order for these to be properly consistent, they must obey the same relationship that the displacements obey. In other words, we have the same relationships among the accelerations in the various directions at the joints or nodes as we have constraint relations corresponding to zero extension of the members. It is a simple matter to adjust the resisting forces by adding the proper components of loadings so as to make the net acceleration at all of the masses consistent.

As a by-product of the results shown in Fig. 10, one can apply the principle of virtual work to find relationships among the displacements at the various joints. For any pattern of loading which produces no displacement, the product of the loadings in the pattern times the displacements in any set of consistent displacements of the structure in the direction of the loadings in the pattern must be zero. This follows from the principle of virtual work directly. In the case of an arch the vertices of which lie in a parabola, as in Fig. 9, the loadings at the three vertices, as shown in the upper part of Fig. 10, will be equal. This implies that the sum of the vertical deflections at B, C, and D, taken as positive downward, must be zero. A similar relationship can be arrived at from the loadings in the lower part of Fig. 10 or from each of the load conditions considered.

Reduction in Number of Effective Degrees of Freedom

The operations above suggest a modification for the approximate dynamic analysis of an arch which is inextensible. Consider the arch shown in Fig. 11 which is the same as in Fig. 9 except that the masses are carried by vertical links, which remain vertical, in the same manner as in the truss in Fig. 5. Here now we constrain the masses to move only in the vertical direction. There are then only three degrees of freedom for the structure. If the structure were extensible, we have reduced the number of degrees of freedom from 6 to 3, but we have lost the horizontal motion of the masses. If we know that these are unimportant or feel that they might be, or if we wish to permit

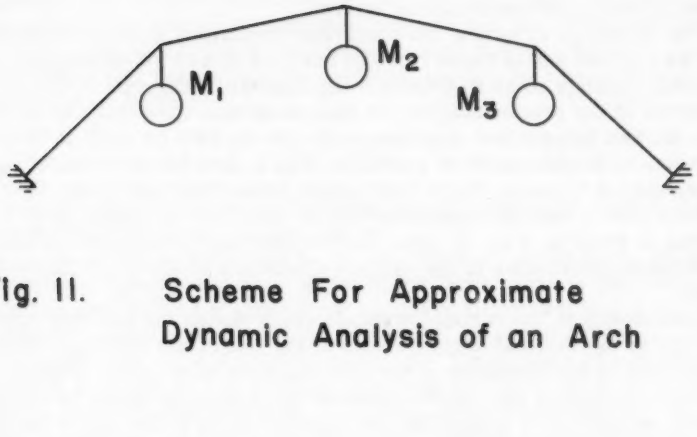

Fig. 11. Scheme For Approximate Dynamic Analysis of an Arch

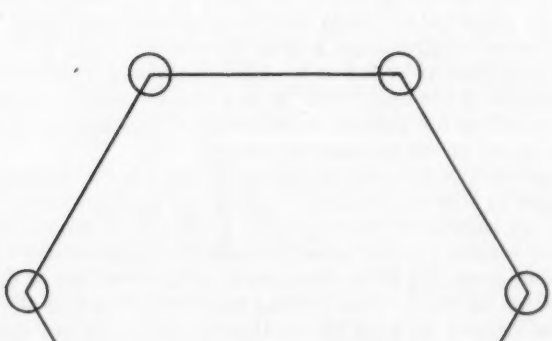

Fig. 12. Hexagonal Ring

this approximation in order to find a quicker solution to the problem, as we might in the case of a very flat arch, we can work with this problem in the same fashion that we solved the problem in Fig. 5 earlier. We need now find only the influence matrix and the corresponding stiffness matrix in order to find the solution.

If, however, the arch is inextensible, there are really only two degrees of freedom of the structure and we have a system which apparently has three. However, by use of the fact that for the arch shown a set of loadings consisting of equal vertical loads at each of the three joints will produce no deformation, we arrive at the condition that the sum of the three vertical displacements must be zero. Then we could use this as a constraint condition which will permit us to work with only two independent vertical displacements. We can define the third vertical displacement in terms of the other two, and arrive at a consistent set of forces by adding to any set that we compute at the two independent joints a proper combination of three equal vertical loads so as to make the vertical accelerations at the three points consistent. Consistency in the vertical accelerations means consistency in the increments in deflections, which means that the vertical accelerations must also obey the rule that the sum of the vertical accelerations at points 1, 2, and 3 as shown in Fig. 11 must be zero.

It can be seen that in general for an arch with N nodes, the number of degrees of freedom for an extensible arch will be 2N, and for an inextensible arch, N-1. The number of degrees of freedom for vertical motion at the nodes will also be N-1.

Extensible and Inextensible Rings

If the ends of the arch are free to move, additional degrees of freedom are introduced. These represent no real difficulty and can be considered either for the extensible or inextensible case in a relatively simple manner. However, more complexities are introduced in the case of a complete ring.

Consider, for example, the hexagonal ring in Fig. 12. There are six masses at the nodes of the ring. For other shapes or number of sides, the relationships can readily be determined. In this particular case, it is clear that the number of degrees of freedom for an extensible ring is 12. However three of these are the rigid body motions for an object in a plane and produce no internal stresses. In the general extensible case of deformation, with two degrees of freedom for each mass, one would compute ordinarily 12 displacements, one in each of the two directions at each of the 6 masses. The statically required forces needed for consistent accelerations will automatically be achieved, and the system can be treated as if it had in fact 12 degrees of freedom.

In the case of the inextensible ring, there are in the case of the hexagon six constraint relations corresponding to the six bars. This means that there are essentially only 3 degrees of freedom for the system rather than 9 for the inextensible case. Here again the 3 rigid body motions correspond to no stress in the system. However the system can be treated as if it had in fact six degrees of freedom since the rigid body motions will automatically be achieved. The six constraint relations must be used to insure consistent values of acceleration and displacement.

Miscellaneous Problems

Space Frames and Space Structures

Space frameworks or space structures of a more complex character than those generally described herein can be handled by the same general principles. For a structure in space, there are in general 3 degrees of freedom for each mass at a node, and consequently 3 components of external force and resisting force which must be considered. This introduces complication only in the order of magnitude of the calculations which are involved.

Buckling

For structures in which axial loading produces secondary effects because of the deflections of the parts of the structure, thereby increasing the moments and the deflections for a given loading, the calculations are more complex. In general, the resisting forces for a given amount of prescribed deflection are reduced, in about the same ratio that the deflections for a given loading are increased when buckling loads are present. This reduction in resisting force means generally a greater acceleration and a consequent greater dynamic displacement in a structure in which buckling tendencies exist. These tendencies can be taken into account but the methods for doing so become relatively unwieldy. One can compute the resisting forces on the assumption that the buckling tendencies are negligible, and then for these resisting forces determine the relative deflections corresponding to the secondary effects of the forces produced by the deflection of the structure. Then by reducing the resisting forces in a more or less arbitrary manner, one can arrive at a set of resistances which would account for the prescribed deflections. Although this method is not entirely satisfactory, it does give a means of taking into account approximately the buckling tendencies for complex structures. For simple structures, the problems can sometimes be handled directly. The real difficulty in the case of buckling problems is that buckling is a nonlinear effect and the methods of calculation used to handle the calculations in each interval in the process depend on linearity, within that interval at least.

REFERENCES

1. N. M. Newmark, "Computation of Dynamic Structural Response in the Range Approaching Failure," Proceedings of the Symposium on Earthquake and Blast Effects on Structures, Los Angeles, 1952, Published by Earthquake Engineering Research Institute.

2. S. Levy and W. D. Kroll, "Errors Introduced by Step-by-Step Integration of Dynamic Response," National Bureau of Standards Report, February 1951.

3. L. Fox and E. T. Goodwin, "Some New Methods for the Numerical Integration of Ordinary Differential Equations," Proc. Camb. Philos. Soc., Vol. 45, pp. 373-388, 1949.

4. S. Timoshenko, "Vibration Problems in Engineering," D. Van Nostrand Co., New York, first edition, 1928, pp. 79-81. (and in later editions, see for example 4th edition, 1954, pp. 143-145.)

Journal of the
ENGINEERING MECHANICS DIVISION
Proceedings of the American Society of Civil Engineers

ULTIMATE STRENGTH CRITERIA FOR REINFORCED CONCRETE

Ladislav B. Kriz[1]

SYNOPSIS

Criteria for ultimate strength of structural members are derived by determining analytically the value of extreme compression edge strain which results in a maximum value of moment or load. The following rectangular members are considered: (a) homogeneous beams, (b) reinforced concrete beams, and (c) eccentrically loaded reinforced concrete columns. In all three cases, ultimate strength so derived is in agreement with tests, and is a function of only the stress at the extreme compression edge and properties of the cross-section involved.

INTRODUCTION

Ultimate strength of structural members is commonly determined on the basis of the assumptions that plane sections remain plane during bending and that stress is a function of strain only. Within the range of linear stress-strain relationship the stress distribution throughout a member is determined from the equations of equilibrium of forces and of moments together with the requirement of linear distribution of strains. If the stress-strain relationship is non-linear, simplifying assumptions, such as the parabolic, trapezoidal or rectangular stress distribution, are commonly introduced, or else the ultimate strength design equations are derived empirically from test data.

By another approach, the problem of ultimate strength may be studied analytically by finding the maximum value of certain load functions expressed in terms of the internal resisting forces of the loaded member. This can be done without defining mathematically the stress-strain relationship of the inelastic material. In this manner, criteria for ultimate strength may be derived which

Note: Discussion open until December 1, 1959. To extend the closing date one month, a written request must be filed with the Executive Secretary, ASCE. Paper 2095 is part of the copyrighted Journal of the Engineering Mechanics Division, Proceedings of the American Society of Civil Engineers, Vol. 85, No. EM 3, July, 1959.

1. Asst. Development Engr., Structural Development Section, Research and Development Div., Portland Cement Assn., Chicago, Ill.

are independent of the quantitative definition of the stress-strain relationship of the material.

Considerable difficulty, due to complexities of the mathematics involved, may be encountered in maximizing the load function in the case of members with an irregular cross-section or of non-homogeneous members such as reinforced concrete. However, for homogeneous rectangular beams, and for reinforced concrete rectangular members governed by tension, this procedure leads to relationships suitable for use in design without simplification.

Notation

The notation of the American Concrete Institute Building Code (ACI 318-56) is used wherever applicable.

A_s = area of tensile reinforcement

A_s' = area of compressive reinforcement

b = width of a section measured parallel to the neutral axis

C = resultant of compressive stresses

c = distance from extreme compressive fiber to neutral axis

d = distance from extreme compressive fiber to centroid of tensile reinforcement

d' = distance from extreme compressive fiber to centroid of compressive reinforcement

e = eccentricity of axial load measured from the centroid of tensile reinforcement

f = stress given by $f = F(\epsilon)$

f_c' = 28-day cylinder strength of concrete

f_s = stress in tensile reinforcement

f_s' = stress in compressive reinforcement

f_y = yield point of tensile reinforcement

f_y' = yield point of compressive reinforcement

f_u = stress in extreme compressive fiber at ultimate strength, given by $f_u = F(\epsilon_u)$

h = total depth of a rectangular cross section

k_2 = ratio of distance between extreme compressive fiber and resultant of compressive stresses to distance between extreme fiber and neutral axis

M_u = ultimate (maximum) resisting moment

p = A_s/bd

p' = A_s'/bd

P_u = ultimate axial load

S_p = plastic modulus

y = distance from neutral axis

ϵ = strain

ϵ_c = strain in extreme compressive fiber

$\epsilon_{c'}$ = strain in extreme tensile fiber

ϵ_u = strain in extreme compressive fiber at ultimate strength

Fundamental Relationships

Pure bending of an inelastic material is considered, for which the stress, f, is a function of the strain, ϵ, given by $f = F(\epsilon)$. It is assumed that stress is a function of strain only, and that the stress function is the same for tension and compression, i.e. $F(-\epsilon) = -F(\epsilon)$. It is further assumed that plane sections remain plane during bending.

If a member with a symmetrical cross section such as that shown in Fig. 1 is subjected to pure bending in the plane of symmetry, the two equations of equilibrium and the equation expressing compatibility of strains are:

$$\int_A f\,dA = \int_{c'}^{c} F(\epsilon)b\,dy = 0 \tag{1}$$

$$\int_A f y\,dA = \int_{c'}^{c} F(\epsilon)yb\,dy = M \tag{2}$$

$$\epsilon = \epsilon_c\, y/c \tag{3}$$

The variable width, b, may be expressed as a function of the distance from the neutral axis, $b = B(y)$. Substituting into Eqs. (1) and (2), and transforming variables by Eq. (3), $y = c\epsilon/\epsilon_c$ and $dy = (c/\epsilon_c)d\epsilon$, we obtain:

$$\frac{c}{\epsilon_c}\int_{\epsilon_{c'}}^{\epsilon_c} F(\epsilon)\,B(c\epsilon/\epsilon_c)\,d\epsilon = 0 \tag{1a}$$

$$\frac{c^2}{\epsilon_c^2}\int_{\epsilon_{c'}}^{\epsilon_c} F(\epsilon)B(c\epsilon/\epsilon_c)\,\epsilon\,d\epsilon = M \tag{2a}$$

The bending moment M is thus expressed as a function of one independent variable, ϵ_c.

If the material (such as concrete in flexural compression) exhibits a stress-strain relationship of the type shown by Fig. 2 characterized by a descending branch, it is apparent that as the external moment M is increased, with a corresponding increase in ϵ_c, the compressive and tensile forces cannot increase indefinitely, but, in the absence of a prior failure, will reach certain maximum values and thereafter decrease. Also, within the non-linear portion of the f versus ϵ diagram an increase in ϵ_c must move the centroids of the resisting forces closer to the neutral axis which results in a shortening

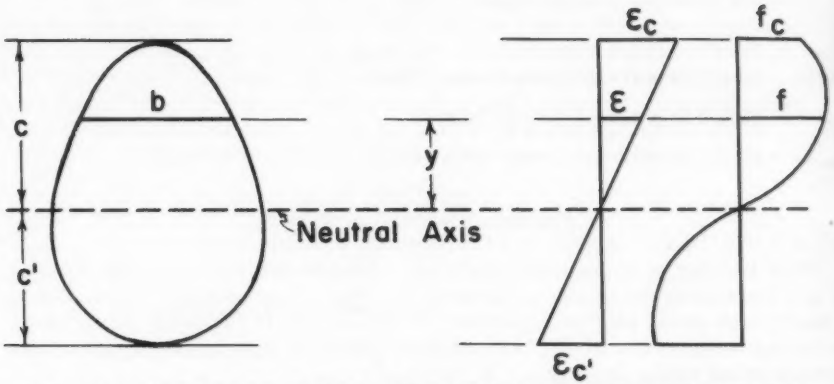

Fig. 1 - STRAIN AND STRESS DISTRIBUTION IN SYMMETRICAL BENDING

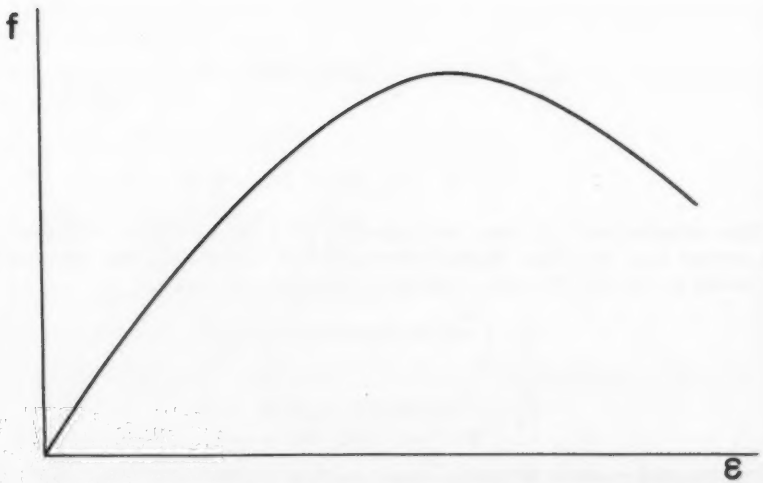

Fig. 2 - GENERAL STRESS-STRAIN RELATIONSHIP

of the internal moment arm. It is evident, then, that as M increases a condition may be reached beyond which a further increase of ϵ_c will cause a decrease of the internal resisting moment. At this point the member has developed its ultimate flexural strength, M_u, as is shown in Fig. 3. An analytical study of these maximum conditions discloses certain relationships which appear to be in agreement with experimental data and which confirm certain design procedures which have been arrived at earlier by more or less empirical methods.

The ultimate strength corresponds to a value of $\epsilon_c = \epsilon_u$ for which

$$\frac{dM}{d\epsilon_c} = 0 \tag{4}$$

The maximum moment is then a function of the strain ϵ_u, obtained by substituting $\epsilon_c = \epsilon_u$ into Eqs. (1a) and (2a).

The discussion which follows applies only to materials which satisfy the above limitations imposed by the special nature of the stress-strain relationship.

Rectangular Cross Section

In a beam of rectangular cross section, the width b = B(y) is a constant. If the bending moment acts in the plane of symmetry of the cross section, $c = c' = h/2$. Eq. (2a) can then be written as:

$$M = 2b\frac{c^2}{\epsilon_c^2}\int_0^{\epsilon_c} F(\epsilon)\,\epsilon\,d\epsilon \tag{2c}$$

Differentiating with respect to ϵ_c, and equating to zero, we obtain:

$$\frac{dM}{d\epsilon_c} = 2b\frac{c^2}{\epsilon_c^2}\epsilon_c F(\epsilon_c) - 4b\frac{c^2}{\epsilon_c^3}\int_0^{\epsilon_c} F(\epsilon)\,\epsilon\,d\epsilon = 0 \tag{5}$$

The value of the strain ϵ_c satisfying this maximum criterion is designated $_u$, the strain at ultimate strength. Multiplying Eq. (5) by ϵ_c and substituting $\epsilon_c = \epsilon_u$ and $F(\epsilon_u) = f_u$, leads to:

$$2bc^2 f_u - 4b\frac{c^2}{\epsilon_u^2}\int_0^{\epsilon_u} F(\epsilon)\,\epsilon\,d\epsilon = 0 \tag{5a}$$

By comparison with Eq. (2c) it is seen that the second term of Eq. (5a) is equal to twice the ultimate moment M_u, so that:

$$M_u = bc^2 f_u \tag{6}$$

In the theory of plastic design the term bc^2 is known as the plastic modulus, S_p, of a rectangular cross section. Eq. (6) may then be written as:

$$M_u = f_u S_p \tag{6a}$$

The stress f_u at the extreme edge depends only on the stress function $f = F(\epsilon)$ when the cross section is rectangular. It is given by Eq. (5a), which yields, for the condition at maximum moment:

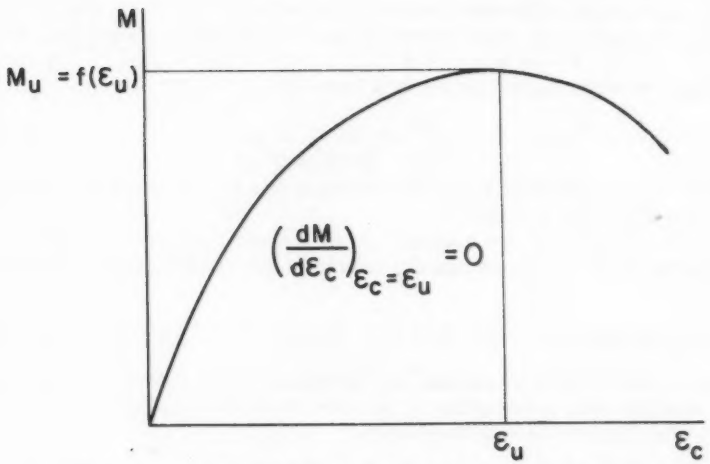

Fig. 3-ULTIMATE MOMENT BEFORE FAILURE

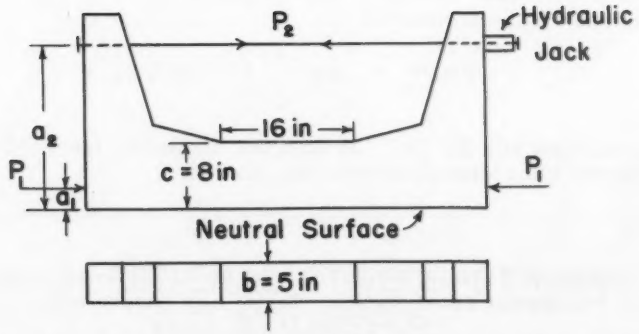

Fig. 4-PCA ECCENTRIC LOAD SPECIMEN

$$\int_0^{\epsilon_u} F(\epsilon)\,\epsilon\,d\epsilon = \tfrac{1}{2} f_u\,\epsilon_u^2 \tag{7}$$

This equation indicates that at maximum moment, the moment with respect to the stress axis of the area under the stress-strain diagram between the given limits is equal to the moment about the stress axis of a rectangle with f_u and ϵ_u as its sides.

Hence, for a material with an identical stress-strain relationship in tension and compression of the type shown in Fig. 2, the ultimate moment for symmetrical bending of a beam with a rectangular cross section may be determined by assuming a rectangular stress distribution with a stress equal to the actual stress at the extreme edge of the cross section. This relationship is true as long as the maximum moment satisfies Eq. (4), as is shown in Fig. 3.

Dividing Eq. (7) by the stress integral, we obtain:

$$\frac{\int_0^{\epsilon_u} F(\epsilon)\,\epsilon\,d\epsilon}{\int_0^{\epsilon_u} F(\epsilon)\,d\epsilon} = \frac{f_u\,\epsilon_u^2}{2\int_0^{\epsilon_u} F(\epsilon)\,d\epsilon} \tag{7a}$$

The left-hand side of Eq. (7a) is the moment divided by the area of the stress-strain diagram, and is thus equal to the distance from the stress axis to the centroid of the area under the diagram between the given limits. Designating this distance, in accordance with common beam notation, as $(1 - k_2)\epsilon_u$, we obtain:

$$\int_0^{\epsilon_u} F(\epsilon)\,d\epsilon = \frac{f_u\,\epsilon_u}{2(1-k_2)} \tag{8}$$

The average stress as given by Eq. (8) for the maximum moment is

$$f_{ave} = \frac{1}{\epsilon_u}\int_0^{\epsilon_u} F(\epsilon)\,d\epsilon = \frac{f_u}{2(1-k_2)} \tag{9}$$

which is equal to f_u only when $k_2 = 1/2$. Hence, the rectangular stress block from which the ultimate moment may be determined is equivalent to the actual stress block only insofar as it gives an identical value for the bending moment. It cannot be used to compute exact values of the total compressive and tensile forces acting on the cross section, since the stress at the extreme edge is not necessarily equal to the average stress on the cross section.

The total compressive and tensile forces acting on the cross section of the beam are given by the function:

$$C = T = b\frac{c}{\epsilon_c}\int_0^{\epsilon_c} F(\epsilon)\,d\epsilon$$

derived from Eq. (1a). This function reaches its maximum when

$$\frac{dC}{d\epsilon_c} = \frac{dT}{d\epsilon_c} = bc\,\frac{\epsilon_c F(\epsilon_c) - \int_0^{\epsilon_c} F(\epsilon)\,d\epsilon}{\epsilon_c^2} = 0 \tag{10}$$

Multiplying Eq. (10) by ϵ_c^2/bc and substituting ϵ_u' for ϵ_c yields for maximum values of C and T,

$$F(\epsilon'_u) = f'_u = \frac{1}{\epsilon'_u} \int_0^{\epsilon'_u} F(\epsilon) d\epsilon = f'_{ave} \quad (11)$$

Hence, at the maximum value of the internal resisting forces in a member of the type under discussion, the average stress between the neutral axis and the extreme fiber is equal to the stress at the extreme fiber. As indicated by Eq. (9) this condition corresponds to the maximum moment only if $k_2 = 1/2$. If $k_2 < 1/2$ at the ultimate strength, then f_u will be greater than f_{ave}, and the maximum moment will be reached before C and T reach their maximum values.

Eccentric Loading of Plain Concrete

The stress-strain relationship of concrete in flexure, used later in the analysis of reinforced concrete members, was determined at the PCA laboratories by a special testing technique developed specifically for that purpose.(1) A plain concrete specimen of rectangular cross section, Fig. 4, was loaded by two eccentric loads, the major thrust P_1 being applied by a testing machine. The minor thrust P_2 provided by a hydraulic jack was varied independently in such a manner that the neutral axis was maintained at one face of the specimen. The two loads and the strains in the extreme fibers of the specimen were measured continuously throughout the loading range to failure, so that the average compressive force on the cross-sectional area, as well as the position of the resultant of the compressive forces, could be correlated with the corresponding strain in the extreme compressive fibers. The stress-strain relationship was then derived by mathematical analysis.

The conditions in the specimen described above can be compared to those of the compression zone of a rectangular beam of twice the depth of the specimen under consideration, made of a hypothetical material which has a stress-strain relationship in both compression and tension identical to the stress-strain relationship of the concrete in flexural compression, as is shown in Fig. 5.

It then follows that the moment of the compressive forces in the specimen about the neutral axis is equal to one half the moment in the hypothetical beam, if the curvature of both is the same. Accordingly, the maximum moment by Eq. (6) is:

$$M_u = \tfrac{1}{2} b c^2 f_u \quad (12)$$

From the test data of the twenty specimens tested at the PCA laboratories, and the stress-strain relationships derived from them, the values of the maximum moments and corresponding stresses in the extreme compressive fibers were obtained. Substituting these stress values into Eq. (12), the theoretical values of the maximum moments were calculated. The results, presented in Table I, appear to confirm both the validity of Eq. (12) and the accuracy of the stress-strain relationships reported in reference (1).

Reinforced Concrete Members

Tension Failure of Rectangular Beams

In a rectangular reinforced concrete beam, Fig. 6, in which the stress in the tensile and compressive reinforcement is equal to the yield stress, the two equations of equilibrium are

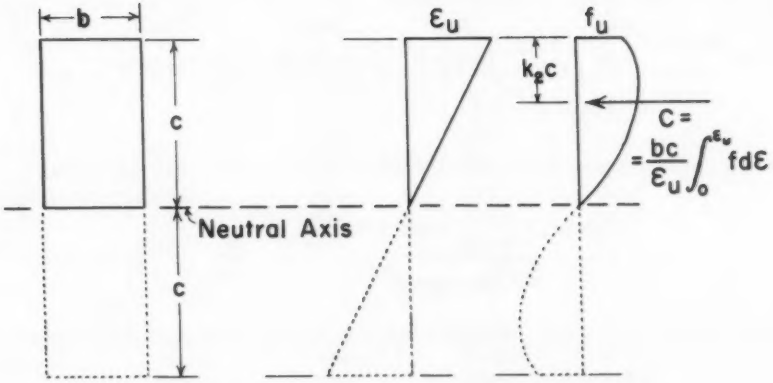

Fig. 5 - CONDITIONS AT ULTIMATE LOAD IN PCA ECCENTRIC LOAD SPECIMEN

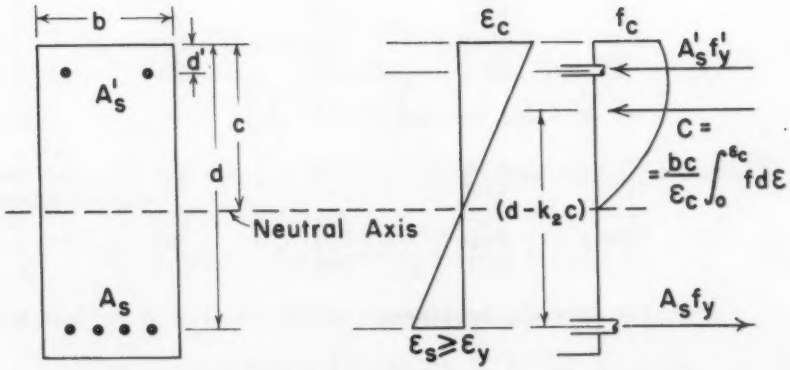

Fig. 6 - CONDITIONS IN R.C. BEAM AFTER YIELDING OF REINFORCEMENT

TABLE I

ULTIMATE MOMENT IN PCA ECCENTRIC LOAD SPECIMEN

Age at test, days	f'_c psi	f_u psi	M_{test} in-kips	M_{calc} in-kips	$\frac{M_{test}}{M_{calc}}$
7	775	871	142	139	1.02
	1670	1544	262	247	1.06
	2950	2772	438	443	0.99
	5350	4067	663	651	1.02
	5715	4472	757	716	1.06
	Av. 7 - day specimens				1.03
14	1420	1448	227	232	0.98
	2870	2668	433	427	1.01
	4595	4245	677	679	1.00
	6070	5145	771	823	0.94
	6480	5337	871	854	1.02
	Av. 14 - day specimens				0.99
28	1650	1810	274	290	0.94
	3050	3336	505	534	0.95
	5170	4414	729	706	1.03
	6720	5442	872	871	1.00
	7540	6190	989	990	1.00
	Av. 28 - day specimens				0.98
90	2175	2084	334	334	1.00
	3710	3264	544	522	1.04
	5470	4558	729	729	1.00
	6480	5409	824	865	0.95
	7610	5977	988	956	1.03
	Av. 90 - day specimens				1.00
	Av. all specimens				1.00

$$A_s f_y = \frac{bc}{\epsilon_c} \int_0^{\epsilon_c} F(\epsilon)d\epsilon + A'_s f'_y \tag{13}$$

$$M = (A_s f_y - A'_s f'_y)(d - k_2 c) + A'_s f'_y (d - d') \tag{14}$$

The moment arm of the resultant of the concrete compressive forces with respect to the centroid of the tensile reinforcement is determined to be:

$$d - k_2 c = d - \frac{1}{b}(A_s f_y - A'_s f'_y) \frac{\epsilon_c \int_0^{\epsilon_c} F(\epsilon)d\epsilon - \int_0^{\epsilon_c} F(\epsilon)\epsilon d\epsilon}{\left[\int_0^{\epsilon_c} F(\epsilon)d\epsilon\right]^2} \tag{15}$$

Substituting Eq. (15) into Eq. (14), differentiating with respect to ϵ_c, and equating to zero, yields

$$\frac{dM}{d\epsilon_c} = \frac{d}{d\epsilon_c} \frac{\epsilon_c \int_0^{\epsilon_c} F(\epsilon)d\epsilon - \int_0^{\epsilon_c} F(\epsilon)\epsilon d\epsilon}{\left[\int_0^{\epsilon_c} F(\epsilon)d\epsilon\right]^2} = 0$$

Performing the above operation and substituting ϵ_u for ϵ_c and f_u for $F(\epsilon_u)$, we obtain:

$$2\epsilon_u f_u - \int_0^{\epsilon_u} F(\epsilon)d\epsilon - 2 f_u \frac{\int_0^{\epsilon_u} F(\epsilon)\epsilon d\epsilon}{\int_0^{\epsilon_u} F(\epsilon)d\epsilon} = 0 \tag{16}$$

Dividing Eq. (16) by $2 f_u \int_0^{\epsilon_u} F(\epsilon)d\epsilon$, yields

$$\frac{\epsilon_u \int_0^{\epsilon_u} F(\epsilon)d\epsilon - \int_0^{\epsilon_u} F(\epsilon)\epsilon d\epsilon}{\left[\int_0^{\epsilon_u} F(\epsilon)d\epsilon\right]^2} = \frac{1}{2 f_u} \tag{17}$$

Substituting Eq. (17) into Eqs. (14) and (15), the equation for the maximum moment becomes:

$$M_u = (A_s f_y - A'_s f'_y)\left(d - \frac{A_s f_y - A'_s f'_y}{2b f_u}\right) + A'_s f'_y (d - d')$$

Assuming that $f_y = f'_y$, and letting $A_s = pbd$ and $A'_s = p'bd$, we obtain

$$M_u = (A_s - A'_s) f_y d \left[1 - (p - p')\frac{f_y}{2 f_u}\right] + A'_s f_y (d - d') \tag{18}$$

The stress f_u in the extreme concrete fiber at ultimate strength is a function of the stress-strain relationship of concrete in flexure only, when the beam cross section is rectangular and when the beam is governed by tension. The stress f_u can be determined from Eq. (17), which may be rewritten in the form

$$\int_0^{\epsilon_u} F(\epsilon)\,d\epsilon = 2k_2\epsilon_u f_u \qquad (19)$$

Hence, when the maximum moment is reached in a rectangular reinforced concrete beam governed by tension under symmetrical bending, the concrete stress distribution in the compression zone is such that the total compressive force is equal to that obtained from an equivalent rectangular stress block in which: (a) the stress is equal to the actual stress in the extreme compressive fibers, and (b) the depth is equal to twice the distance from the extreme compressive fibers to the centroid of the concrete compressive forces. Thus, the equivalent rectangular stress block gives, in this case, both the correct value of the total compressive force, and of its moment.

For design purposes, it is then sufficient to establish the value of the stress f_u as a function of concrete strength f'_c. This can be done by solving Eq. (18) when test values of beam properties, concrete strength, and ultimate moment are known, in which case it is not necessary to know the entire concrete stress-strain relationship in flexure.

From Eq. (19), the stress f_u and the corresponding strain ϵ_u can be determined when the stress-strain relationship of concrete is known from experiments. Using the stress-strain relationship obtained by Hognestad, Hanson and McHenry,(1) a relationship between f_u and f'_c was determined for concrete at age 28 days. The function obtained is represented by the curve shown in Fig. 7, and may be approximated very closely by the equation

$$f_u = 5\, f_c'^{\,0.8} \qquad (20)$$

in which f_u and f'_c are in psi.

However, since the ultimate beam moment given by Eq. (18) is not sensitive to the value of f_u, such refinement is hardly justifiable in design. A straight-line relationship between f_u and f'_c, which is on the safe side, leads to:

$$f_u = 0.85 f'_c \qquad (21)$$

The strain ϵ_u at ultimate moment was found to be independent of concrete strength and is approximately 0.0025.

Substituting Eq. (21) into Eq. (18) yields

$$M_u = (A_s - A'_s) f_y d \left[1 - 0.59(p - p')\frac{f_y}{f'_c}\right] + A'_s f_y (d - d') \qquad (22)$$

which is identical to, and therefore confirms, Eq. (A3) of the 1956 ACI Building Code.

Letting $A'_s = 0$, and substituting $A_s = pbd$ and $q = pf_y/f'_c$, Eq. (22) yields Eq. (A1) of the Code.

Tension Failure of Eccentrically Loaded Short Columns

A short column is defined herein as a column of such proportions, and with an axial load applied at such eccentricity, that the eccentricity may be considered constant throughout the loading range.

If such a column of rectangular cross section, shown in Fig. 8, is loaded in the plane of symmetry by a load P applied at a distance e from the tensile reinforcement, then the equations of equilibrium are

$$P = C + A_s' f_s' - A_s f_s \tag{23}$$

$$P = \frac{C}{e}(d - k_2 c) + A_s' f_s' \frac{d - d'}{e} \tag{24}$$

Assuming that both tensile and compressive reinforcement yield before failure, $f_S = f_y$ and $f_S' = f_y'$. The two equations of equilibrium then become

$$P = C + A_s' f_y' - A_s f_y \tag{23a}$$

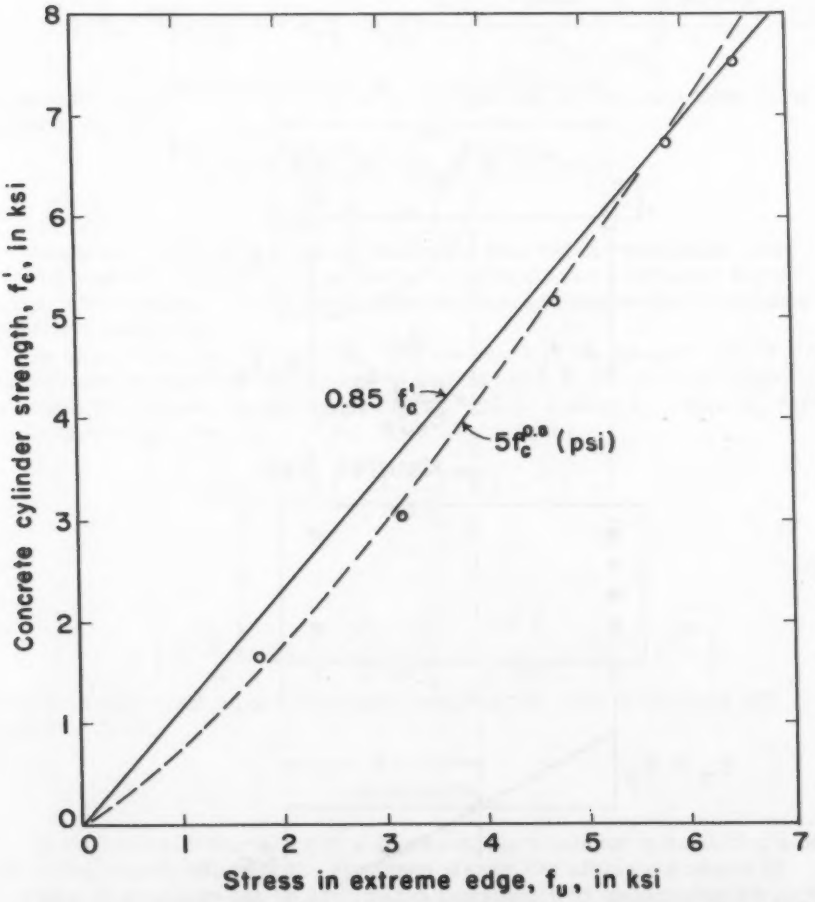

Fig. 7-STRESS IN EXTREME EDGE AT ULTIMATE STRENGTH OF R.C. MEMBERS GOVERNED BY TENSION

$$P = \frac{C}{e}(d - k_2 c) + A_s' f_y' \frac{d - d'}{e} \tag{24a}$$

Differentiating both Eq. (23a) and (24a) with respect to ϵ_c, and equating to zero we obtain:

$$\frac{dP}{d\epsilon_c} = \frac{dC}{d\epsilon_c} = 0 \tag{25}$$

$$\frac{dP}{d\epsilon_c} = \frac{d - k_2 c}{e} \cdot \frac{dC}{d\epsilon_c} + \frac{C}{e} \cdot \frac{d}{d\epsilon_c}(d - k_2 c) = 0 \tag{26}$$

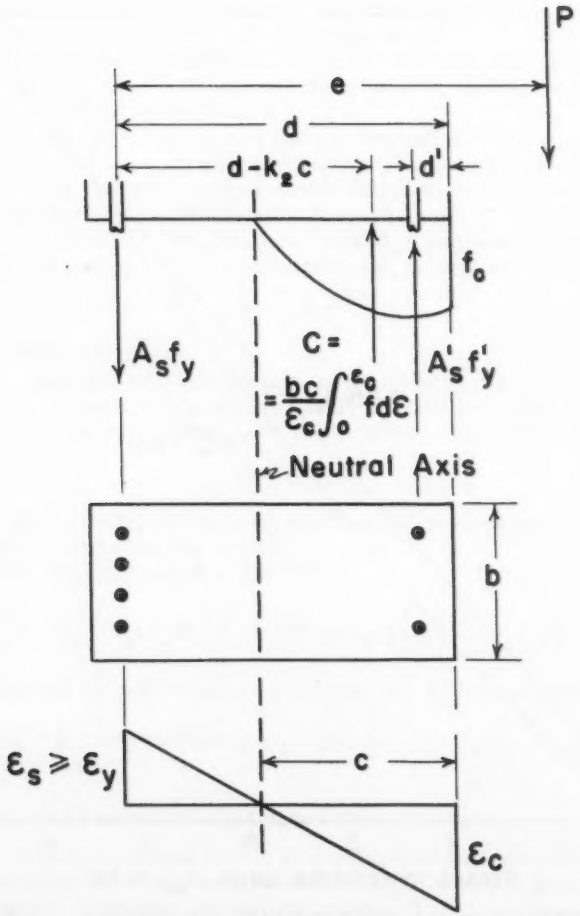

Fig. 8 - CONDITIONS IN ECCENTRICALLY LOADED R.C. COLUMN

Substituting Eq. (25) into Eq. (26) and multiplying by e/C yields

$$\frac{d}{d\epsilon_c}(d - k_2 c) = 0 \tag{27}$$

The moment arm of the resultant of the concrete compressive forces with respect to tensile reinforcement is given by

$$d - k_2 c = d - c + \frac{c\int_0^{\epsilon_c} F(\epsilon)\epsilon\, d\epsilon}{\epsilon_c \int_0^{\epsilon_c} F(\epsilon) d\epsilon} \tag{28}$$

Solving Eq. (23a) for c and substituting into Eq. (28) we obtain:

$$d - k_2 c = d - \frac{1}{b}(P + A_s f_y - A_s' f_y') \frac{\epsilon_c \int_0^{\epsilon_c} F(\epsilon) d\epsilon - \int_0^{\epsilon_c} F(\epsilon)\epsilon\, d\epsilon}{\left[\int_0^{\epsilon_c} F(\epsilon) d\epsilon\right]^2} \tag{29}$$

Differentiating Eq. (29) with respect to ϵ_c, equating to zero, and simplifying leads to Eq. (17);

$$\frac{\epsilon_u \int_0^{\epsilon_u} F(\epsilon) d\epsilon - \int_0^{\epsilon_u} F(\epsilon)\epsilon\, d\epsilon}{\left[\int_0^{\epsilon_u} F(\epsilon)\, d\epsilon\right]^2} = \frac{1}{2 f_u} \tag{17}$$

Hence the criterion derived for maximum moment in rectangular reinforced concrete beams failing in tension applies also as a criterion for the maximum eccentric load on rectangular reinforced concrete short columns governed by tension.

By substituting Eq. (17) into Eq. (29) the length of the moment arm $(d - k_2 c)$ at ultimate strength is determined. With this value of $(d - k_2 c)$ the ultimate strength P_u is then obtained by solving Eq. (24a). Letting $A_s = pbd$, $A_s' = p'bd$, and expressing f_u by means of Eq. (21), this leads to:

$$P_u = 0.85 f_c' bd \left\{ \frac{p' f_y' - p f_y}{0.85 f_c'} + \left(1 - \frac{e}{d}\right) + \right. \tag{30}$$

$$\left. + \left[\left(1 - \frac{e}{d}\right)^2 + 2\left(\frac{e}{d} \cdot \frac{p f_y - p' f_y'}{0.85 f_c'} + \frac{p' f_y'}{0.85 f_c'} \cdot \frac{d - d'}{d} \right) \right]^{1/2} \right\}$$

which is equivalent to, and therefore confirms, Eq. (A9) of the 1956 ACI Building Code.

SUMMARY

In the case of materials with a stress-strain relationship exhibiting a descending branch following the maximum stress, the ultimate strength of structural members can be determined analytically by maximizing the applicable strength function. In this manner, criteria for ultimate strength are obtained.

(1) The maximum resisting moment of rectangular homogeneous beams in pure flexure is given by the product of the plastic modulus of the section

and the stress in the extreme fibers at ultimate strength. If the stress-strain relationship of the material is known, the stress f_u in the extreme fibers at ultimate strength may be found, since the moment with respect to the stress axis of the area under the stress-strain curve at ultimate strength must be equal to the moment of a rectangle with the ultimate strain ϵ_u and $f_u = F(\epsilon_u)$ as its sides.

(2) The ultimate strength of rectangular reinforced concrete members governed by tension is a function of the properties of the cross section of the member, the yield strength of the reinforcement, and the concrete stress distribution as represented solely by the stress in the extreme compressive fibers at ultimate strength. This function is expressed by Eq. (22) for beams in pure bending, and by Eq. (30) for eccentrically loaded short columns. The concrete stress in the extreme fibers at ultimate strength is such that the area under the corresponding stress-strain curve is equal to the area of a rectangle with $f_u = F(\epsilon_u)$ and $2k_2\epsilon_u$ as its sides.

(3) The relationship between stress in the extreme compressive fibers at ultimate strength, f_u, and the 28-day concrete cylinder strength was found to be approximated with sufficient accuracy by $f_u = 0.85f'_c$, corresponding to a strain of 0.0025. The analytical criteria presented herein then lead to design equations identical to those given by the 1956 ACI Building Code for ultimate strength, governed by tension, of members of rectangular cross section. Hence, the study presented reflects a theoretical substantiation of Eqs. (A3) and (A9) of the ACI Building Code, which equations were previously derived on an empirical basis.

ACKNOWLEDGMENT

The paper presented herein was submitted by the author to the Graduate School of Northwestern University as a project report in partial fulfillment of the requirements for a Master of Science Degree in Civil Engineering.

Dr. S. L. Lee, Associate Professor of Civil Engineering, of Northwestern University; Dr. E. Hognestad, Mr. D. McHenry and Dr. C. W. Yu, Manager, Structural Development Section, Director of Development, and Development Engineer, respectively, of Portland Cement Association; and Dr. I. M. Viest, Bridge Research Engineer, of the AASHO Road Test Project, have contributed by reviewing the manuscript and by helpful suggestions.

REFERENCES

1. Hognestad, E., Hanson, N. W., McHenry, D., "Concrete Stress Distribution in Ultimate Strength Design," ACI Journal, December 1955, Proc. Vol. 52, pp. 455-479.

2. "Building Code Requirements for Reinforced Concrete" (ACI 318-56), ACI Journal, May 1956, Proc. Vol. 52, pp. 913-986.

Journal of the
ENGINEERING MECHANICS DIVISION
Proceedings of the American Society of Civil Engineers

SHRINKAGE, SWELLING AND CREEP IN CEMENT

A. Hrennikoff,[1] F. ASCE

INTRODUCTION

The study of shrinkage and swelling of hardened cement described in this paper has been prompted by an earlier study of creep.(1) It has been observed that both phenomena are associated with the presence of water, and that they both manifest themselves in linear and volumetric changes. This suggests a common origin for the two phenomena related to water. The shrinkage study has led to the enunciation of the active water theory, which is described in this paper in detail. The theory attributes the phenomena considered to the stress condition in the film of water surrounding cement grains when cement is moist. The theory agrees well with several aspects of cement behaviour in the course of shrinkage and swelling. It also provides a convincing explanation for creep.

Shrinkage - Swelling Studies

It has long been known that cement shrinks on drying and swells on wetting. A detailed study of the circumstances surrounding a cycling variation of water content in cement provides some clues on the role of moisture in cement permitting to link the phenomenon of shrinkage and swelling to creep.

The experimental study of shrinkage and swelling involved preparation of prismatic specimens of cement approximately 3/4" x 3/4" x 4" in size, of different water cement ratios and cement grain sizes. These specimens were subjected to cycles of drying and wetting with water and other liquids. The principal items of information obtained from the experiments were the values of weight and length taken periodically in the test.

The weights were taken at first by an ordinary balance to 0.01 gm., and later by a self indicating Mettler balance to the same precision. The length

Note: Discussion open until December 1, 1959. To extend the closing date one month, a written request must be filed with the Executive Secretary, ASCE. Paper 2096 is part of the copyrighted Journal of the Engineering Mechanics Division, Proceedings of the American Society of Civil Engineers, Vol. 85, No. EM 3, July, 1959.

1. Prof. of Civ. Eng., Univ. of British Columbia, Vancouver, Canada.

was measured directly by a home made apparatus, shown in the photograph, Fig. 1, involving a frame and a dial gauge, sensitive to 0.0001". Although somewhat crude, the method of the length measurement was found adequate. A surprising degree of consistency was observed in successive measurements of length, although the individual readings could not be relied on closer than to 0.0002" or 0.0003". The errors were caused mostly by the relative roughness of the ends of the specimens and by the difficulty of bringing the measuring points of the apparatus exactly on the targets.

For interpretation of the results, the readings of the increments or decrements of the weight and of the length were plotted on the graph paper as the abscissae and the ordinates respectively. The increments were plotted in the positive directions of the axes, i.e. to the right and up, and the decrements in the negative directions.

Each graph refers to one specimen only, and it represents its several cycles of wetting and drying. The loss and gain of weight is looked upon as the decrement and increment of the internal volume of voids occupied by the liquid. When the liquid is water its specific gravity is assumed unity, although it may not always be so, and the losses and gains in weight are plotted as the variations of the internal volume of water in cu. cms.

Other liquids: kerosene, lubricating oil SAE.10 and methyl alcohol were also used. The changes in weight incurred by these liquids were converted into volumes, prior to plotting them on the graph, by division by their specific gravities.

Several types of cement specimens were studied: ordinary cement, fine cement, coarse cement, of water-cement ratios corresponding to plastic and more liquid consistencies. Several specimens of each type were used, and were subjected to different manners of drying and wetting. Some specimens were hardened in the moist closet under spray, others in the atmosphere of steam in the boiler, under conditions similar to the ones prescribed by ASTM for the standard soundness test.

Figs. 2 to 7 represent a set of typical graphs of this kind, the proportion of ingredients by weight being 0.003 : 0.24 : 1 of pozzolith (a dispersing agent), water and ordinary portland cement, Type 1, manufactured by British Columbia Cement Company. The specimens were kept for one day in moist closet, removed from the forms and then kept for two days (about 6 hours each day) in the atmosphere of steam. This was followed by drying them in the oven at 120° F. and 130° F. When in a week or 10 days the weight was substantially stabilized the specimens were transferred to the oven with the temperature of 200° F., and kept there until the weight stopped to decrease. This followed by wetting in several different ways.

The weights and lengths of the prisms were taken at appropriate time intervals, more frequently when they were changing fast, and the ages of prisms in days at the time of measurement were recorded on the graphs. When drying in the oven the length measurements were naturally taken after cooling the specimens to the room temperature.

Here are some of the significant features of the graphs:

Hardening in Atmosphere of Steam produces some minor swelling and some increase in weight. The latter is caused by hydration, resulting in decrease of the absolute volume of products of cement hydration, followed by a tendency to form voids and by the suction of the moisture from the outside. This phenomenon, not particularly important in connection with the present studies, was also observed by others and described by the term "self dessication".(2)

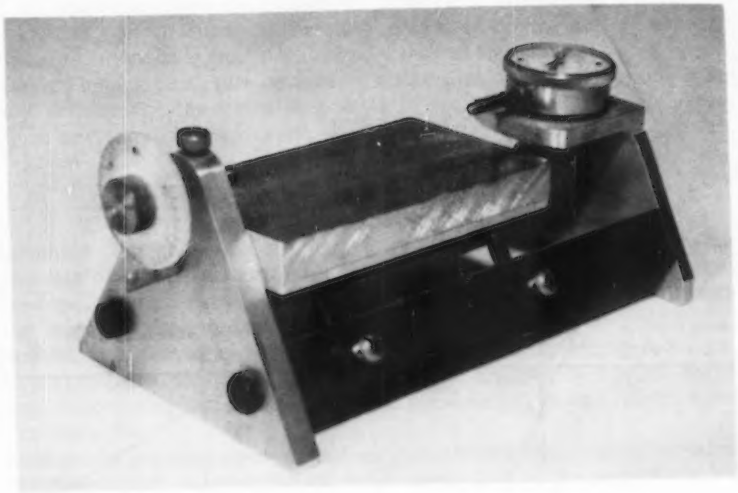

Fig. 1(a)

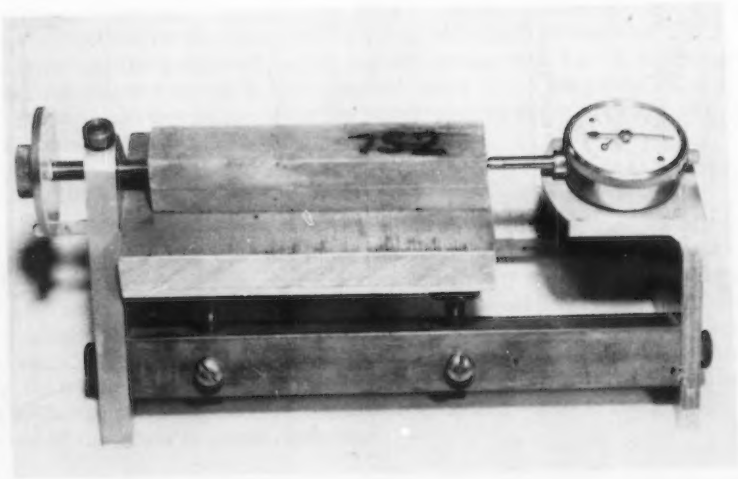

Fig. 1(b)

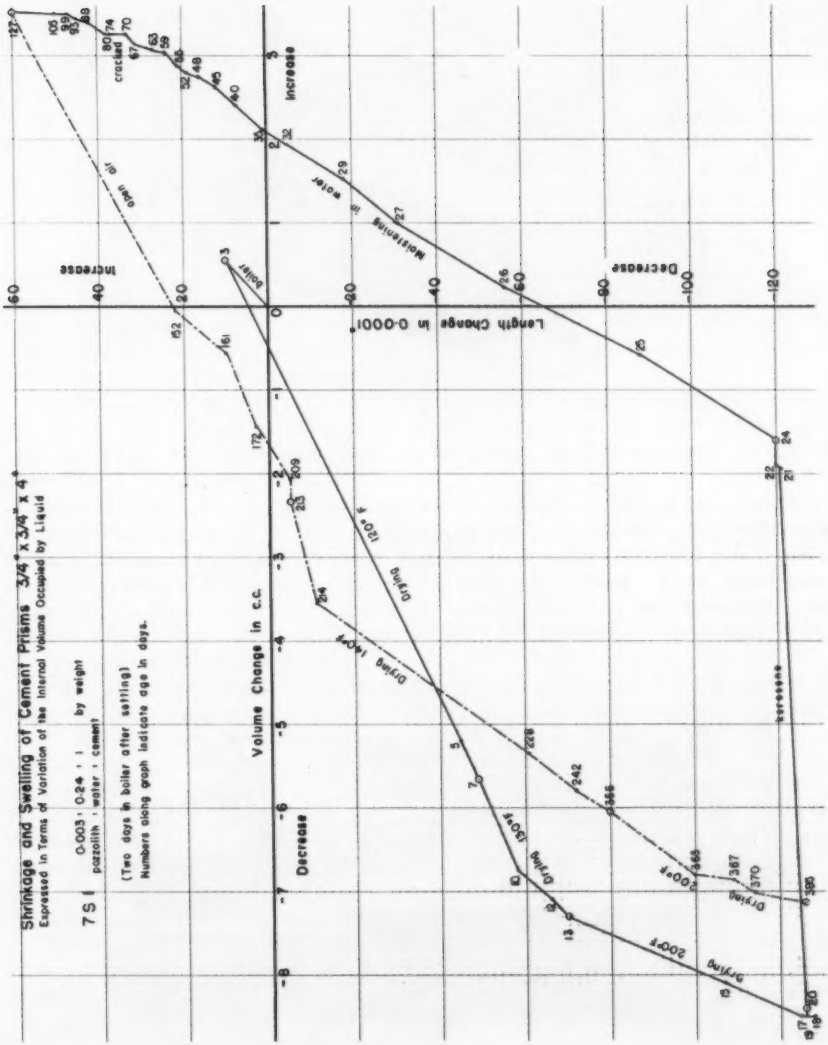
Shrinkage and Swelling of Cement Prisms 3/4" x 3/4" x 4"
Expressed in Terms of Variation of the Internal Volume Occupied by Liquid
7 S 1 0·003 : 0·24 : 1 by weight
pozzolith : water : cement
(Two days in boiler after setting)
Numbers along graph indicate age in days.
Length Change in 0·0001"
Volume Change in c.c.
Increase
Decrease
Increase
Decrease
Drying 120°F
Drying 140°F
Drying 200°F
Drying 300°F
Drying 400°F
Boiler
Wetting in water
Oven dry
cracked

Fig. 2

Drying. In spite of minor inaccuracies of measurement the drying curves of all six specimens are very similar. The most significant characteristic of the curves is their flatness at the early stages of drying and steepness at later stages, indicating that the loss of water at the end of drying results in greater shrinkage per gram or c.c. of water lost, than at the early stage. Expressed differently, the water lost early in drying is comparatively "inactive" as far as shrinkage is concerned, while the water lost later is "active".

Structure of Hardened Cement

Hardened cement consists mostly of gel,[3] a hard porous sponge like mass, whose cells or individual units are too small to be seen under an ordinary microscope. Gel contains some 20-25% of voids filled mostly with water, if cement has been kept moist.

Hardened cement also contains some unhydrated material—remains of larger cement grains, and some bubbles of air trapped in cement during its making. The air bubbles contain no gel, because gel is capable of forming only in water.[3]

Since gel is amorphous it should be visualized as consisting of the elements of hydrated cement surrounded by water according to the scheme of Fig. 8 and not in the form of a solid mass containing intercommunicating internal cavities according to Fig. 9. This follows from the fact that gel is deposited in water and in view of being amorphous, its elements do not merge into one another but remain distinct, and consequently separated from each other by a layer of water, however thin it may be.

The arrangement of Fig. 9 could be true when applied to a single crystal. The voids then would be the imperfections in the crystal brought about by some disturbing influences. This however does not apply to cement. Some observations with electron microscope[4] corroborate the structure of Fig. 8.

Considering the graphs of drying in conjunction with Fig. 8, it appears that the inactive water belongs to the enlarged parts of the gel voids, because these parts would dry first, while the water coming from the regions of grain to grain contacts belongs to the active kind.

Wetting with Water

After drying, the specimen 7 S 3 (Fig. 4) was wetted by immersing in water. By the next day the specimen had absorbed nearly the full weight of water lost earlier in drying, but had recovered only a small part of its shrunk length. The curve of the first day of wetting is accordingly flat. Continued immersion resulted in a slow gain in weight, accompanied by a substantial swelling. Thus the water absorbed early in the course of wetting was inactive, while the water absorbed later—active. It appears then that the swelling is largely due to the saturation of the less accessible voids in the gel, i.e. the regions of the grain to grain contacts.

Wetting in Moist Atmosphere

The specimen 7 S 5 (Fig. 6) was left after drying in the open air. This resulted in absorption of moisture. The wetting of the specimen has been slow and accordingly, the curve of wetting in air is quite different from the curve of wetting in the water. It follows closely the curve of drying remaining

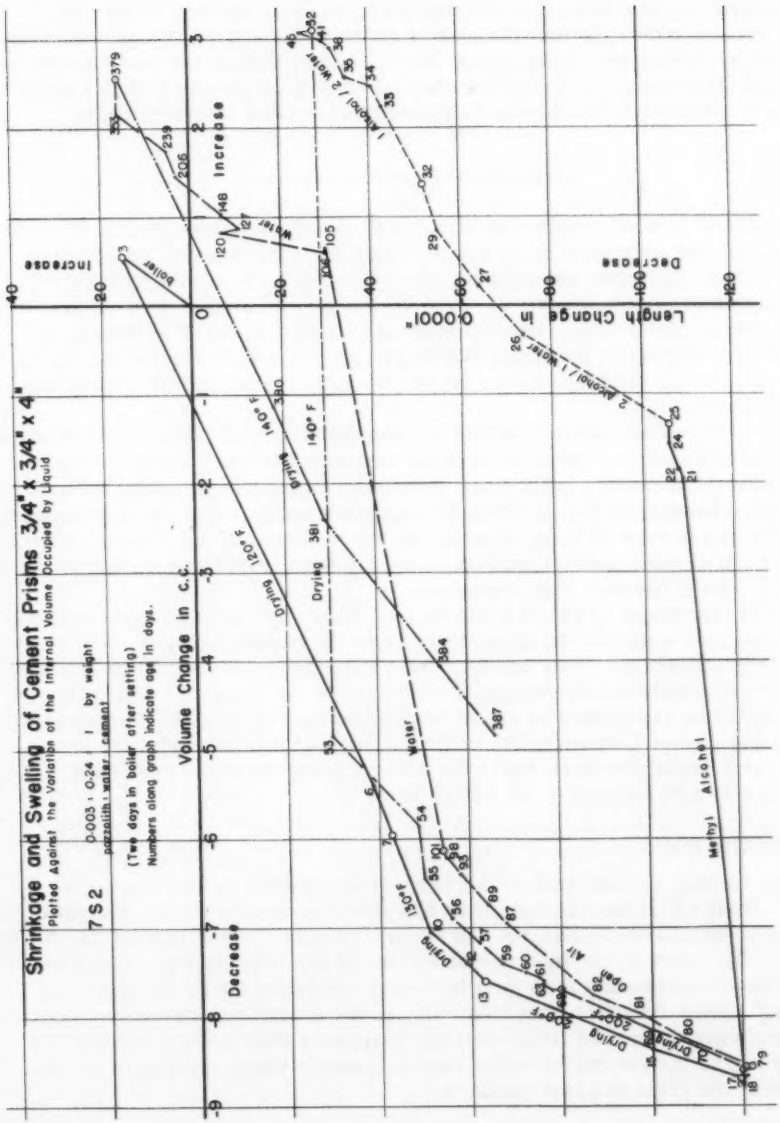
Shrinkage and Swelling of Cement Prisms 3/4" x 3/4" x 4"
Plotted Against the Variation of the Internal Volume Occupied by Liquid
7 S 2 0.003 : 0.24 : 1 by weight
pozzolith: water: cement
(Two days in boiler after setting)
Numbers along graph indicate age in days.
Volume Change in c.c.
Length Change in 0.0001"
Increase
Decrease
Boiler
Water
Drying 120° F
Drying 140° F
Drying 150° F
Drying 200° F
Drying 250° F
Drying 380° F
Drying 381
Drying 384
Drying 387
Drying 80° F
Drying 90° F
Drying 100° F
Drying 105° F
Drying 120° F
Drying 140° F
1 Alcohol / 2 Water
2 Alcohol / 1 Water
Methyl Alcohol
Open Air

Fig. 3

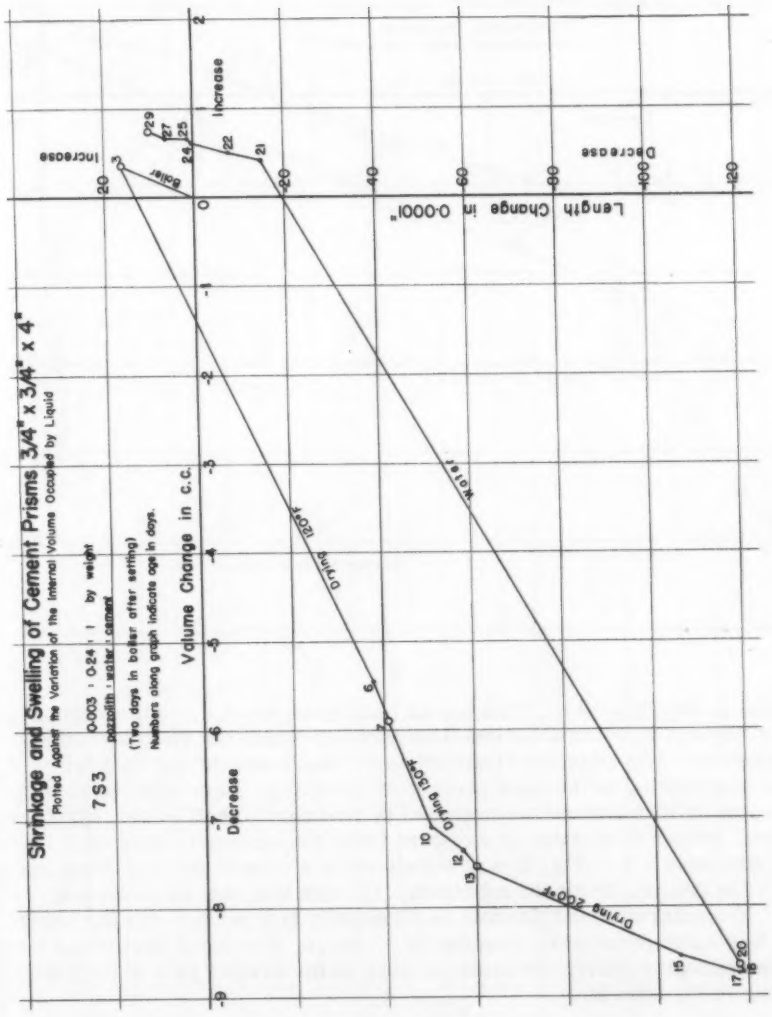
Shrinkage and Swelling of Cement Prisms 3/4" x 3/4" x 4"
Plotted Against the Variation of the Internal Volume Occupied by Liquid
7 S 3 0.003 : 0.24 : 1 : 1 by weight
pozzolith : water : cement
(Two days in boiler after setting)
Numbers along graph indicate age in days.
Volume Change in c.c.
Length Change in 0.0001"
Increase
Decrease
Boiler
Drying 120°F
Drying 130°F
Drying 200°F

Fig. 3

Fig. 4

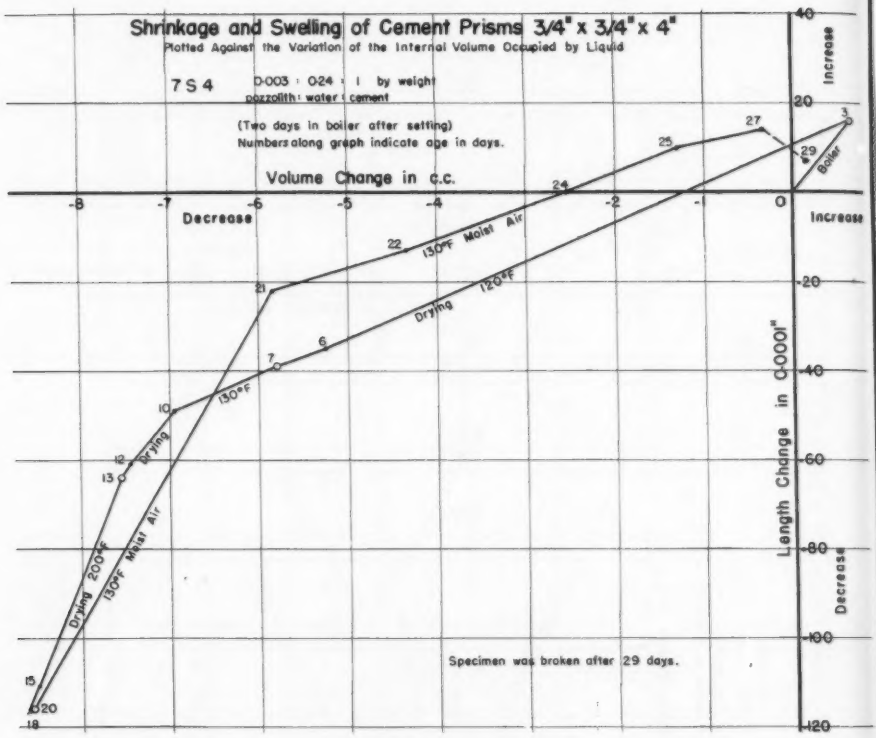

Fig. 5

somewhat to the right of it. This means that, apart from a small amount of inactive water, the water absorbed first was active and the water absorbed later—less so. The moisture absorbed early thus found its way into the regions contributing to the most pronounced swelling. After absorption of a certain amount of moisture accompanied by recovery of half of the length lost on drying, further absorption of moisture from the air nearly stopped.

The specimen 7 S 4 (Fig. 5) was moistened in a closed can containing some water at the bottom, below the specimen. The can was kept in an oven at 140° F. The saturation in this case was naturally fast because the hot water vapour was more penetrating than the cool vapour. The early part of the curve of wetting occupies nearly the same location as the earlier part of the curve of wetting in the open air.

Wetting with Inert Liquids

Specimens 7 S 1 and 7 S 6 were placed after drying in kerosene (Fig. 2) and light lubricating oil SAE 10 (Fig. 7). These liquids are known to be inert, i.e. they normally do not affect the strength and other mechanical properties of cement to any appreciable extent.(5) Accordingly their lines of saturation on the graphs are almost completely horizontal, i.e. these liquids cause no swelling of cement, although the internal volumes occupied by them are comparable to the volumes vacated by water on drying.

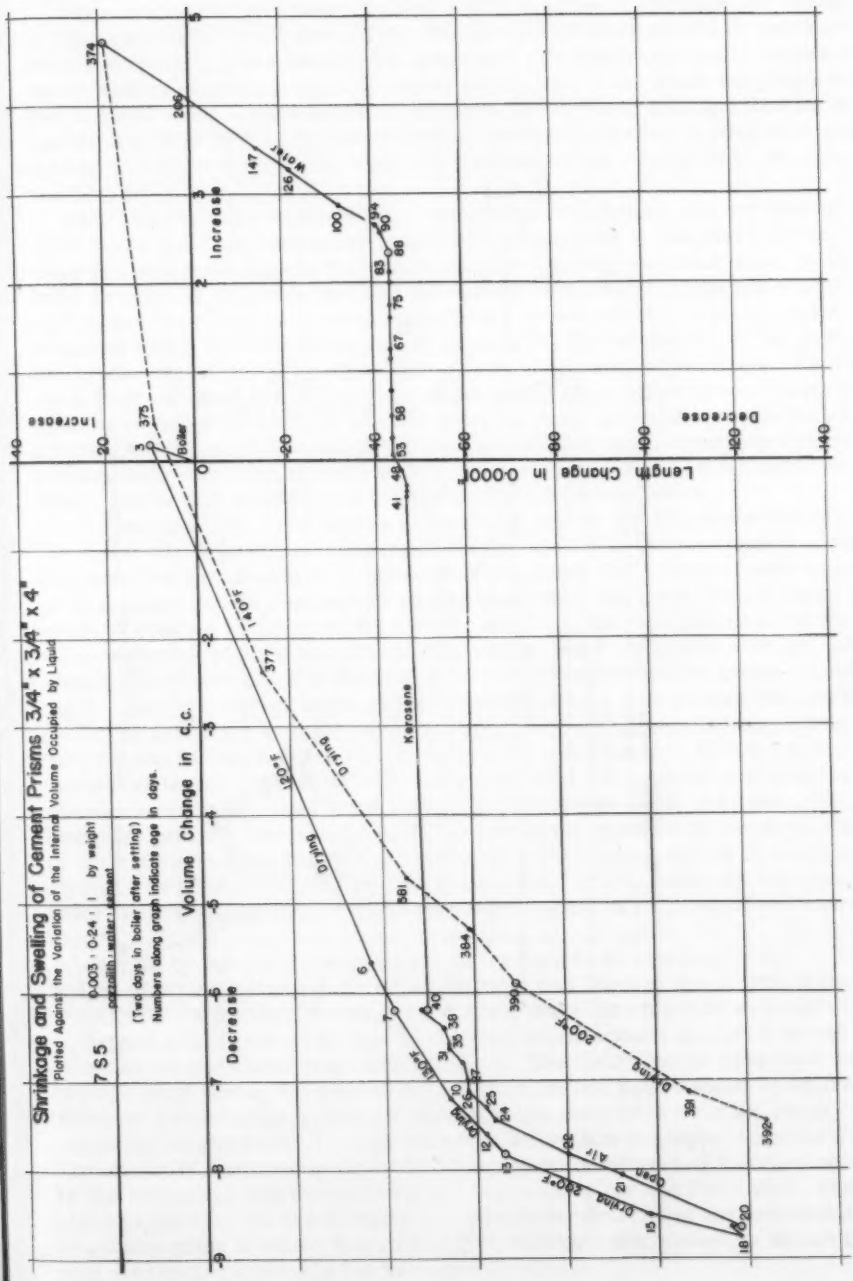
Shrinkage and Swelling of Cement Prisms 3/4" x 3/4" x 4"
Plotted Against the Variation of the Internal Volume Occupied by Liquid
7 S 5 0.003 : 0.24 : 1 by weight
portland : water : cement
(Two days in boiler after setting)
Numbers along graph indicate age in days.
Volume Change in c.c.
Length Change in 0.0001"
Increase
Decrease
Boiler
Water
Kerosene
Drying
Air
Open
140°F
120°F
200°F
374
375
377
561
384
399
398
392
147
126
100
194
90
88
83
75
67
58
53
41
48
40
39
38
35
32
31
25
24
23
12
15
22
21
20
18
6
1

Fig. 6

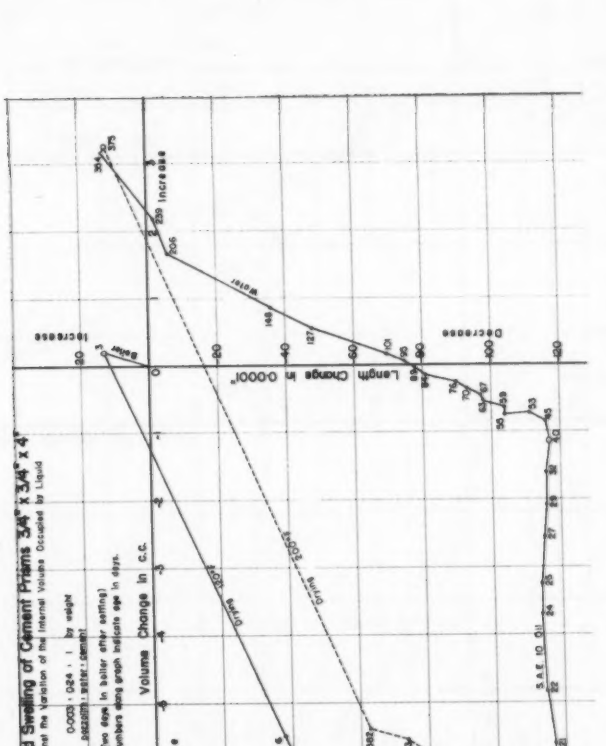
Shrinkage and Swelling of Cement Prisms 3/4" x 3/4" x 4"
Plotted Against the Variation of the Internal Volume Occupied by Liquid
Volume Change in c.c.
Increase
Decrease
Length Change in 0.0001"
Water
Glycerine
SAE 10 Oil
Numbers along graph indicate age in days.

Fig. 7

After saturation with these liquids, which required a considerable period of time especially in the case of oil, the specimens were placed in water and here a surprising phenomenon was observed: the specimens began to absorb water without displacement of kerosene or oil, and at the same time they began to swell along a comparatively straight line more or less parallel to the line of drying at 200° F. In due time the specimens swelled beyond their original length before drying, and absorbed a greater total volume of liquid than was lost on drying.

This experiment with successive saturation of hardened cement first with inert liquid and then with water is the most significant in the whole series of tests and it gives a clue to the nature of active water. How can water penetrate cement, if all pores in it are filled with kerosene, a liquid nonmiscible with water, and especially when no kerosene is forced out? An explanation suggests itself, that the water enters the cement not by the way of its voids but by the way of creeping along the surface of the cement elements. On the surface of the specimens there are some spots, from which the kerosene has been removed or to which it has not adhered, such as the sharp corners on the grains. Once placed in contact with some cement grains, the water creeps around them coming in contact with more grains where the latter touch each other, and in this manner penetrating inside the cement mass.

Virtual equality of the moduli of elasticity and of the Poisson's ratios in the moist and dry cement specimens, demonstrated in the previous studies,(1) suggests that the presence of water does not soften the grains of cement gel or change the grains themselves in any other way. On first thought these facts seem to conflict with the phenomenon of swelling, but the hypothesis of the water creeping along the grains and spreading them apart like a wedge, while jumping from one grain to another, provides a plausible explanation. According to this view, active water is the water forming a film around the cement grains or adsorbed by their surface. This water is not an ordinary liquid water because liquid water cannot spread the grains apart; strong intermolecular forces transform this water from liquid into solid—a plastic or viscous solid rather than a rigid solid, since a rigid solid could not creep along the grains. The water that fills the central parts of the voids in Fig. 8 is not active because it is too far removed from cement grains to be attracted strongly by them. For this reason replacement of this water by kerosene or other inert liquid makes no difference with regard to swelling of the cement mass.

Judging by the increase in weight in the course of swelling in Fig. 2, the weight of active water equals approximately one third of the weight of the total chemically uncombined water. Other tests make this fraction even smaller.

Separation of cement grains by the film water occurs against a strong intergranular attraction holding them together. The active water then must be under a very strong compression. For this reason active water is entirely different from capillary water which is in the state of tension or, more correctly, in the state of compression smaller than atmospheric pressure.(6) Consequently, regions occupied by active water similarly to the ones occupied by the cement grains themselves, are unavailable for capillary flow. Only the parts of the void spaces filled by inactive water determine the permeability of cement mass to water flow, while full, although diminished by shrinkage, void spaces are available for kerosene flow.

The conclusion that the volumetric changes in cement are caused by water present in a state other than capillary, conflicts with the general opinion which

holds that the capillary action of water is the cause of swelling and shrinkage.(3) There is however some other evidence tending to refute the latter view and to minimize in general the capillary effects produced by water in cement.

The writer experimented with placement of small drops of water and kerosene on the surface of hardened cement. The surface had been prepared by drying a specimen, cutting it and polishing roughly the surface of the cut. This surface was held in a horizontal position and viewed through a microscope pointed horizontally. The kerosene drop was observed to spread quickly over the surface. On the other hand the water drop retained for some time a roughly hemispherical shape showing no tendency either to expand over a wider area or to contract to a smaller area. At the same time the water in the drop percolated into the cement and spread slowly underneath the surface. As the drop decreased in volume the inclination of its sides remained the same but its skin formed wrinkles, being apparently supported by a crystalline framework precipitated from the solution. When the drop finally collapsed it left some crystalline residue behind.

The point which has a considerable importance in appraising the role of capillary forces in moist cement is the magnitude of the angle of contact of the water surface with the cement surface, which was found to be 80° - 90°. This compares with the angle of 15° - 20° formed by the water in similar circumstances with the glass surface. In the textbooks the latter angle is usually assumed zero.(7) The contact angle of the liquid has a direct relation to the height of its capillary rise in small bore tubes and to the negative water pressure formed underneath the surface meniscus. If in a fine glass tube the capillary rise is high, in a tube of the same diameter but made of cement it is smaller by a coefficient equal to the cosine of the contact angle.(8) Should the water in the fine passages between the elements of cement gel meet the cement at the same 80° - 90° angle as at the outside cement surface, the capillary phenomena associated with the presence of water inside cement would be insignificant. On the other hand the kerosene, forming a zero angle with the cement surface, should produce a substantial capillary rise in cement even though the surface tension of kerosene is only half as great as that of water.(9)

Experiments were made with the rise of kerosene and water in dry cement prisms whose bottom ends were immersed 1/16" into these liquids. The rise of kerosene was the faster of the two and it could have been caused by the capillary forces only; it produced no contraction or expansion of the prism. The water rise, however, although slower and smaller than that of the kerosene, was accompanied by a substantial swelling. The kerosene rise proves that swelling of cement is not caused by capillary forces, while swelling concurrent with the water rise suggests that such rise is brought about at least in part by a cause other than capillary. This cause, accounting also for the swelling, is the adsorbed water.

The presence of film water in cement was demonstrated by several other investigators,(3) without however attributing to it the mechanical action brought up in this paper.

Before proceeding further with presentation of other significant features of volume - shrinkage graphs, it is desirable to speculate on the nature and causes of the phenomena discussed.

Active Water Hypothesis

Cement grains like other elements or particles composing solid bodies are held together by intergranular attraction. The law of attraction is not known but it must be of the type

$$A = \frac{a}{d^n} \qquad (1)$$

Where a is a constant coefficient, d - the distance between the particles and n a sufficiently large positive number. The law of attraction of this type makes the force decrease rapidly as the distance increases.

In addition to the attraction there must also be a force of repulsion R, because once the particles come in contact they are quickly stopped in their mutual approach. Each particle is then in equilibrium under the forces A and R (Fig. 10).

The expression for the force R may be assumed similar to Eq. (1) except that the exponent n in the denominator is even greater for R than for A, since the force of repulsion appears to be virtually non-existant beyond a certain very close range.

Presenting the force-distance relations graphically in Fig. 11, the curve of the force of repulsion R appears much steeper than the curve of A. At the same time the graph of R must become nearly horizontal at its bottom end, because all repulsion disappears abruptly when the particles lose contact. The distance d_o at which the particles find their equilibrium is determined by intersection of the lines A and R.

Suppose now that the particles are pushed against each other, by equal external forces F, shown dotted in Fig. 10. The total force tending to bring the particles together is now (A+F), while the force resisting an unduly close approach of the particles is still R. If the ordinates of the line A are increased by the force F, the new distance of equilibrium d_1 (Fig. 11) is found by the intersection of the lines (A+F) and R, the distance (d_o-d_1) being the amount of the deformation at the point of contact. Similarly, if the force F is tension, the position of equilibrium is determined by the intersection of the lines (A-F) and R. If the tension force F_u is so great that the line $(A-F_u)$ touches the line R near its bottom end, tension failure ensues, the force F_u being the ultimate tensile strength for one pair of particles.

This general qualitative scheme of mechanical action of dry hardened cement under stress can scarcely be doubted. Now the water will be introduced into the picture.

In Fig. 12(a), AB represents the surface of a cement grain in contact with water, pictured plane for simplicity. It is assumed that the water is strongly attracted by cement in accordance with an inverse power law of the type of Eq. (1). The variation of this force with the distance t from the cement surface is pictured in Fig. 12(b). This force f, expressed in units of force per unit volume of liquid is very great near the surface AB and is virtually zero at some distance t_o. It is only within the thickness t_o that the liquid is active.

Attraction of water to cement creates pressure p in the former. Its intensity can be easily determined from equilibrium of a prism of water C D L E in Fig. 12(a). This prism of cross-section dA extends from t to the limit of active water t_o.

Evidently,

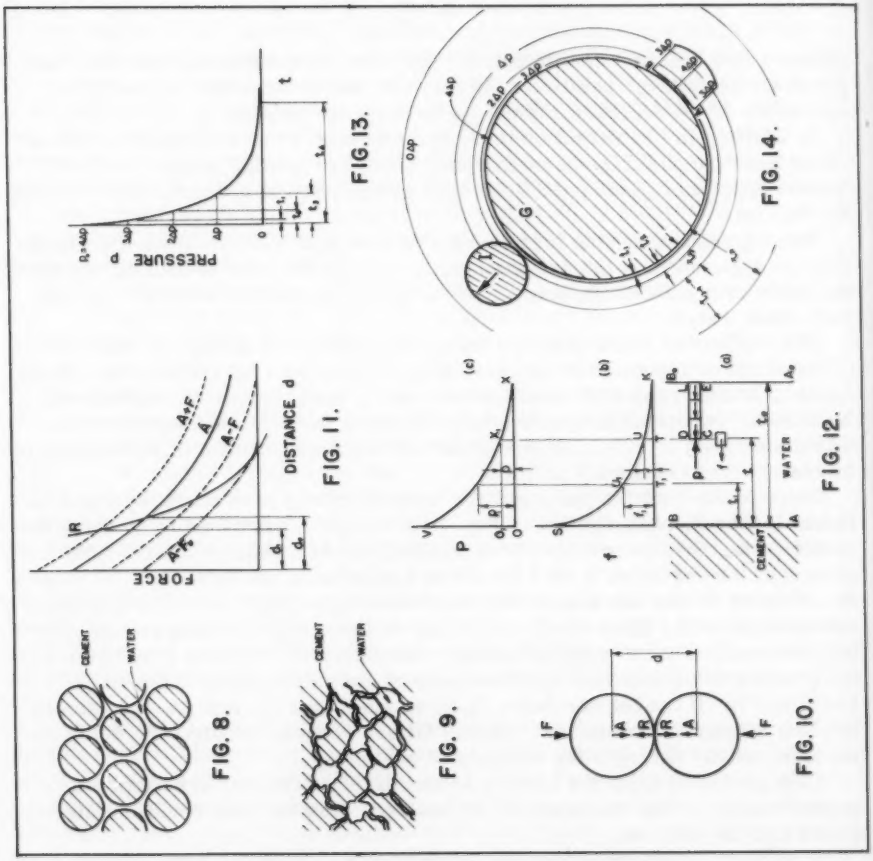
PRESSURE p
t
FIG. 13.
FIG. 14.
DISTANCE d
FORCE
FIG. 11.
FIG. 12.
CEMENT
WATER
FIG. 8.
FIG. 9.
FIG. 10.

$$p\,dA = \int_t^{t_o} f\,dA\,dt \quad \text{and} \quad p = \int_t^{t_o} f\,dt \tag{2}$$

In order to be mathematically exact the upper limit of the integral should be infinity.

The variation of p in accordance with Eq. (2) is shown in Fig. 12(c). The curve of p resembles the curve of f in its general shape.

It is evident from the expression (2) that the pressure ordinates represent the areas under the curve of the force of attraction. Thus the pressure p at the distance t equals the area KTU and the pressure p_1 - the area K T_1 U_1.

It has been assumed so far that there is an unlimited amount of water available in contact with cement, in other words the thickness of the water layer is not less than t_o. Suppose now that this thickness of water is $t < t_o$. This does not change the graph of f, although its effective part is now only U U_1S, but the pressure graph changes. At the distance t the pressure now is zero and at the distance t_1 it becomes

$$(p_1 - p) = \int_{t_1}^{t} f\,dt \tag{3}$$

In bther words the pressure ordinates in Fig. 12(c) are now measured from the axis O_1X_1 instead of OX.

What has been said about the attraction of water to cement grain with a plane surface is believed to apply without a change to a curved cement surface provided that the radius of curvature of the grains is much greater than the thickness of layers of adsorbed water. If however the curvature of the grain is comparable to the thickness of the film, the situation is probably different.

Once water comes in contact with cement and forms a film, it creeps along, and an isolated grain becomes surrounded by a film of water of uniform thickness. The cause of lateral spreading of the film around the grain is the need for lateral confinement. Thus, the water prism C D L E considered above in Fig. 12(a), being under a strong pressure in horizontal direction, is not in equilibrium unless it is restrained laterally i.e. in up and down direction, by similar neighbouring prisms under pressure. In the absence of such confinement the water must spread out.

When in equilibrium the film water still possesses the basic property of liquid of having its pressure at a point equal in all directions and normal to the plane of action. Film water differs however from ordinary water in that respect that a period of time, and even a long period, is required for adjustment of its shape to a change in conditions. This is indicated by the slowness of swelling of dry cement prisms on immersion in water, particularly after saturation with inert liquid. In this respect film water behaves as a plastic solid. This change in the properties of water should be attributed to strong forces of attraction bringing about some regularity in the arrangement of the molecules.

Let the curve in Fig. 13 represent the diagram of variation of water pressure in the film around the cement grain, similar to Fig. 12(c). The pressure p_o next to the surface of the grain may be relatively high. Divide p_o into a number of equal parts Δp. Four such parts are shown in Fig. 13. The abscissae of the points with the ordinates $4\Delta p$, $3\Delta p$, etc., are $t_o = 0$, t_1, t_2 etc.

Imagine now an isolated spherical grain of cement G surrounded by ample amount of water (Fig. 14). The pressure in the film water of the grain may be

described by spherical surfaces of equal pressure $p_o = 4\Delta p$, $3\Delta p$, etc. These surfaces appear in Fig. 14 as circular isobars. The isobar number zero with pressure $4\Delta p$, is the surface of the grain, the next isobar number one has the pressure $3\Delta p$, and the distance t_1 from the grain. The distances between the two successive isobars increase outward. The distance t_{3-4} between the isobars $p = \Delta p$ and $p = 0$ is relatively large. If the amount of water around the grain is limited to the thickness t_2 for example, the isobars number 3 and 4 disappear, while all others remain in exactly the same positions, although their pressures decrease by $2\Delta p$, i.e. the surface of the grain becomes the isobar $2\Delta p$, the isobar #1 becomes Δp, and the isobar #2 becomes zero.

If a plane, such as AB (Fig. 14) is passed through the film water the pressure in this plane is normal to it, and the variation of its intensity is as shown on the drawing.

Suppose that an inert body I is brought into the vicinity of the grain G (Fig. 14). The isobars outside the region I including the space between I and G remain completely unchanged. The reason for this condition is that although the thickness of the water film between G and I is reduced, the water on the sides of I crowds in and maintains the same pressure between I and G as elsewhere at the corresponding distances from the grain surface.

If two cement grains surrounded by skins of film water are brought in close proximity within the range of their intergranular attraction, they approach each other and find a position of equilibrium by distorting the films at the point of their near contact. The system of isobars in that vicinity is completely modified, and the water pressure in the film transmits not only the attraction between the cement and water but also the attraction between cement and cement.

In interaction of dry grains of cement discussed earlier the force of repulsion of the grains R (Fig. 11) is one of the two principal factors. As to the moist grains, considered now, the repulsion force is not believed to be of primary significance. If the grains are smooth the water film is likely to prevent their touching each other, which is the prerequisite for bringing the force R into action. Should the grain surface be jagged it is possible that some solid to solid contact may take place at the protuberances, while the major parts of the film remain unpierced, however the action of R under these conditions is probably of secondary importance, and may now be ignored.

Two sets of isobars may be considered when two cement grains are brought in close proximity: the isobars corresponding to the independent action of the grains, and the isobars produced by the combination of attractions of both grains.

It has been demonstrated that the isobars of an isolated spherical grain are concentric circles, and so they remain when one grain is brought close to another, as has been shown in Fig. 14 by reference to the body I.

The two sets of isobars may also be combined into one by direct addition of pressures brought about by the attractions of the two grains. That this procedure is correct becomes clear from the following two considerations: first, that the forces of attraction of any element of water by the two grains are entirely independent of each other, and second, that the pressures produced at any particular point by each set of forces are equal on all planes, as well as normal to them.

How this combination of isobars can be carried out is shown in Fig. 15. Here three circular isobars are shown surrounding each cement grain. They correspond to pressures Δp, 2 (Δp) and $3(\Delta p)$. The isobars $4(\Delta p)$ coincide

with the surfaces of the grains. Parts of the isobars $0.1(\Delta p)$ are also shown. The combined pressures can be easily determined at the points of intersection of the isobars of the two families. Thus, at the intersection of the isobars $2(\Delta p)$ and Δp the pressure is $3(\Delta p)$ etc. On the straight line between the centres of the grains the pressure varies between approximately $6(\Delta p)$ next to the grains and perhaps $5.5(\Delta p)$ half way between the grains. The combined isobars, easily sketched from these points, are shown by solid lines.

Although the combined isobars present a clear picture of the pressure distribution in the film water, the individual circular isobars of Fig. 14 are more convenient for the purpose of calculation in problems involving swelling and shrinkage of cement, and for this reason they will be used in preference to the combined isobars.

The Shrinkage - Swelling Problem

The basic problem in shrinkage is finding how far apart the cement grains would move when seeking their position of equilibrium in conditions of a variable thickness of water film or a variable moisture content. When the water film is thin the grains are relatively close together. As the thickness of the film increases the grains move away from each other. The amount of water equal to or greater than necessary to form the maximum effective film thickness, corresponds to the greatest separation of the grains.

The exact numerical solution of this problem at present is impossible due to the lack of knowledge of the exact laws of attraction between cement and water, and cement and cement, but a detailed outline of the method follows clearly from the theory presented.

Suppose that two equal cement grains (Fig. 16) surrounded by water are brought into their relative position of equilibrium lying within the field of action of their mutual attractions A. Consider the forces acting on the lower grain G_1. They are the attraction force A developed by the other grain G_2 and the pressure of the surrounding water film. The latter is produced by two causes:

a) The attraction of water by cement of this particular grain.
b) The attraction of water by cement of the other grain.

The two pressures caused by these two attractions can be either combined as was explained above with reference to Fig. 15, or considered separately, which is more expedient in this case.

The water pressure on G_1 corresponding to the attraction (a) is self balanced (Fig. 16b), i.e. it produces a zero resultant on the grain G_1. Then the water pressure on the grain G_1 caused by the grain G_2 is the only one which remains to be considered, and it is balanced by the intergranular attraction A. This pressure corresponds to the isobars of the grain G_2 at the surface of the grain G_1 (Fig. 16a) and it is depicted in Fig. 16(c) as the line cbabc. The intensity of this pressure is the greatest at the point a, and the least on the sides, i.e. at the points c. The surface of the bottom half of the grain G_1 is so far removed from the grain G_2 that the pressure on it is always virtually zero.

The water pressure acts on the grain in the direction normal to its surface, as indicated by arrows in Fig. 16(c), but, as in similar conditions in elementary hydrostatics, the horizontal components of pressure are mutually balanced,

and the vertical components add up to a resultant which may be found by summing up or integrating the pressure intensities over the horizontal diametral area of the grain. This resultant is represented by the volume of the body of revolution under the surface described by the pressure line in Fig. 16(c). As pointed out above, this pressure produced repulsion, is equal to the force of attraction A.

If the moisture content of cement is decreased, the films around the grains become thinner and the ordinates of the pressure line on the grain G_1 (Fig. 16c) becomes smaller, so that the resultant repulsion becomes represented by a smaller volume, such as the one under the pressure line bab. Since this force is less than the attraction A, the grains must come closer together. This raises both the attraction A and the pressure repulsion, the latter faster than the former. In this manner the equilibrium is re-established with the grains brought closer together.

The opposite effect occurs with the introduction of more water in a comparatively dry cement. This thickens the active films, causing an increase in their pressure, which brings about greater repulsive forces and some displacement of the grains away from each other. The effective intergranular attractions extend apparently for greater distances than the pressure produced repulsions and so the active water cannot cause a complete separation of grains or the slaking of cement.

Film Decrease - Shrinkage Ratio

As was pointed out earlier, the volume - shrinkage graphs (Fig. 2 - Fig. 7) are very steep on the dry end, indicating that at the conclusion of drying a small loss of moisture corresponds to a relatively large linear shrinkage. However even at this stage, if the loss of moisture is translated into a decrease of thickness of the active film, this decrease still exceeds the distance by which the grains of cement approach each other. Stated differently, if in the process of drying the active films around the grains should become thinner say by 10^{-6} inches, the grains would approach each other in the course of shrinkage not by $2(10^{-6})$ inches but several times less.

How great is this disparity between the decrease in the film thickness and the amount of shrinkage, may be estimated from the shrinkage graphs. Visualize cement (Fig. 17) to consist of spheres of equal diameter R covered by films of thickness t, small in relation to R. At the points of contact of the spheres the films are considerably thinner than elsewhere. However, in view of the smallness of the thickness t the part of the surface area of the grain covered by the film of reduced thickness may be considered negligible compared to the total surface area.

Take the volume of cement prism as 37 cc. and the volume of uncombined water in it removed by drying at 200° F., as 9 cc., which figures are typical of all specimens in the shrinkage graphs, Fig. 2 to Fig. 7. Then the absolute volume of dry cement grains may be taken as $V_c = 37-9 = 28$ cc. Actually some uncombined water undoubtedly still remains in cement when it is dried at 200° F., but this water will be considered as a part of the dry volume 28 cc.

If prior to this drying the specimen still contains the volume of water V_w, all of which is active water, the thickness of the film t of this water may be estimated by the following relation:

$$\frac{V_c + V_w}{V_c} = \frac{4/3\pi(R+t)^3}{4/3\pi R^3}$$

from which, ignoring terms with higher poweres of t

$$t = \frac{R}{3}\frac{V_w}{V_c} \qquad (4)$$

Strictly speaking R in this expression represents the radius of cement grains including the thickness of the water film unexpelled by drying at 200° F., but in view of the negligible thickness of the latter, R may be taken as the radius of the grain itself.

Apply this formula to the specimen with the graph of Fig. 6 whose drying part appears more regular than similar parts in the other graphs. Drying of this specimen at 200° F. may be assumed complete at 18 days. The volumes of moisture still present in it at 15, 13 and 7 days respectively are 0.25, 0.91 and 2.55 cc. Then the film thicknesses by Eq. (4) at different ages are:

$$t_{15} = \frac{R}{3}\frac{0.25}{28} = 0.003\ R$$

$$t_{13} = 0.011\ R$$

$$t_{7} = 0.030\ R$$

The decrease in the film thicknesses in different time intervals are as follows:

7 to 13 days - 0.019 R

13 to 15 days - 0.008 R

15 to 18 days - 0.003 R

The corresponding magnitudes of shrinkage in the same time intervals are found from the graph as $24(10^{-4})$, $32(10^{-4})$ and $20(10^{-4})$ inches on 4" length or 0.0006, 0.0008 and 0.0005 inches per inch respectively.

Had the specimen shrunk for the full amounts of the decreases in the thickness of the film the corresponding shrinkage strains would have been 0.019, 0.008 and 0.003 inches per inch. Thus, the thickness of the film decreases much faster than the amount by which the specimen shrinks. For this particular specimen the film decrease—shrinkage ratios for different time intervals are as follows:

7 to 13 days - $\frac{0.019}{0.0006} = 31.7$, here the film water is comparatively inactive and the Eq. (4) perhaps does not apply.

13 to 15 days - $\frac{0.008}{0.0008} = 10$

15 to 18 days - $\frac{0.003}{0.0005} = 6$

It may be observed that the steeper the shrinkage graph the smaller is the film decrease - shrinkage ratio.

There is considerable variation between different specimens with regard to the terminal slopes of the shrinkage lines, partly from errors of

FIG. 17.

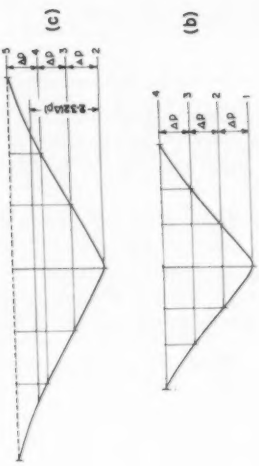

FIG. 18.

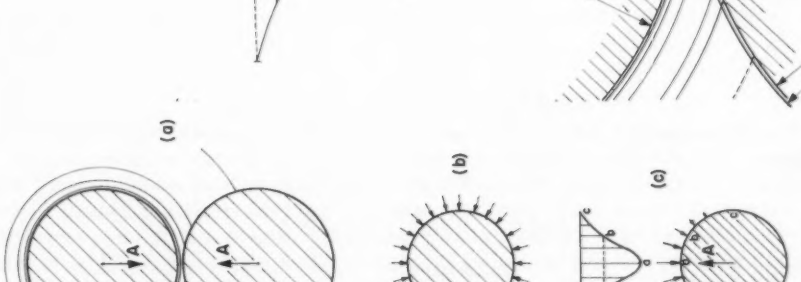

FIG. 16.

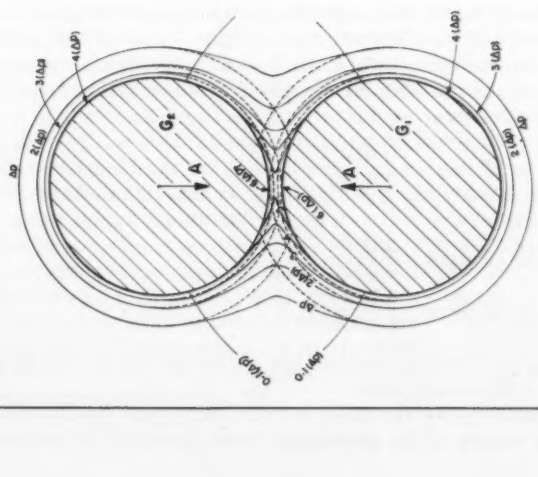

FIG. 15.

observation, and partly from causes to be pointed out later. In some specimens the terminal film decrease - shrinkage ratio is less than 6.

If it were possible to demonstrate on the basis of the active water theory that the film decrease - shrinkage ratio should necessarily be of the order observed in the tests, or at least much greater than one, that would be an additional evidence in favour of the theory. As the matters stand now, the fully conclusive proof of this proposition is at present out of the question, for lack of the necessary quantitative parameters, but the plausibility of it is easily demonstrable by choosing suitable data.

Fig. 18a shows two cement grains of radii R surrounded by films of water of equal thickness on both grains, although only the film belonging to the grain G_2 is shown. This film is described by the spherical surfaces 1, 2, 3, 4 and 5 which have equal pressure intervals between them. Thus, if the water film covering the grains extends to the surface 4, the pressures on the surfaces 4, 3, 2 and 1 are 0, Δp, 2 (Δp) and $3(\Delta p)$ respectively. The film thicknesses measured from cement to the surfaces 1, 2, 3, 4 and 5 are assumed arbitrarily $t_1 = 0.01$ R, $t_2 = 0.025$ R, $t_3 = 0.55$ R, $t_4 = 0.125$ R and $t_5 = 0.30$ R respectively. These values are probably too great in relation to the radius, but smaller thicknesses would be too small to handle in a graphical demonstration.

Suppose that the water film on both grains extends to the surface 4 and that the position of equilibrium of the grains covered by this amount of water is such that the grain G_1 touches the surface 1 of the grain G_2. This is the position 1 of the grain G_1 in Fig. 18(a). As has been explained above, the force of mutual repulsion of the grains, caused by the pressure created in the film water, can be found by constructing the diagram of pressure in the film water of the grain G_2 at the surface of the grain G_1. This diagram is presented in Fig. 18(b). It is constructed by observing the points of intersection of the surface of the grain G_1 with the isobars 4, 3, 2 and 1 of the grain G_2 and by measuring the distances of these points of intersection from the vertical axis of the grains.

The force of repulsion between the grains is equal to the volume of the body of revolution, whose axial cross-section is represented by the pressure diagram.

By the theorem of Pappus, assuming the shape of the generating figure as a triangle and scaling its base, the force of repulsion P is found thus:

$$P = \tfrac{1}{2}(3)(\Delta p)(0.345\ R)\ 2\pi\ (1/3)(0.345)\ R = 0.3738\ (\Delta p)\ R^2$$

Since the relative position of the grains considered here is assumed to be the position of equilibrium, the force of attraction A of the grains in this position is equal to the same value.

Assume now that after adsorption of a greater amount of water the grains move away from each other, so that the surface of the grain G_1 touches the sphere 2 of the grain G_2. The question is, how thick a water film is required for the equilibrium. Assuming tentatively that the necessary film extends all the way to sphere 5, the water repulsion then corresponds to the pressure diagram shown in Fig. 18(c) and extending vertically from the isobar 5 to the isobar 2. It is evident however by inspection that this repulsion is too great since it exceeds the one corresponding to Fig. 18(b), while actually it should be smaller than it, because the force of attraction between the grains at a greater distance apart must be smaller. Therefore the increase in the thickness of the film around the grains should not be so great.

Revising the earlier assumption, assume the outer boundary of the film when the grain G_1 is in position 2, to be at the sphere a. This corresponds to an increment in the film thickness $\Delta t_4 = 0.0375$ R with the radius of the sphere a being 1.1625 R. This leads to revision of the pressure diagram in Fig. 18(c), or rather of its base line, which should now be located at the level $0.32(\Delta p)$ from the pressure level 4, as determined by scaling of the distance KL in Fig. 18(a) and fitting it into the diagram, Fig. 18(c).

The new force of repulsion is found:

$$P^1 = \tfrac{1}{2}(2.32)(\Delta p)(0.38)\, R(2\pi)\, 1/3(0.38)\, R = 0.35(\Delta p)\, R^2$$

The expression for P^1 is smaller than the earlier expression for P corresponding to a drier state of cement in which the grains were located closer together. Therefore in the absence of a more precise knowledge of the action of forces involved, the thickness of the moisture films corresponding to the second position of equilibrium of the grains, may well be correct, and so it will be assumed.

Between the two relative positions of the grains considered here, the centres of the two adjacent grains have moved apart through the distance

$$t_2 - t_1 = 0.025\ R - 0.01\ R = 0.015\ R.$$

At the same time the film thicknesses on both grains increased by the amount 0.0375R each. The corresponding film decrease - shrinkage ratio is then $\frac{2(0.0375)R}{0.015\ R} = 5$. This value of the ratio is comparable to the actual amounts observed in the specimens near the end of the drying stage. This analysis may be considered as an indirect evidence in favour of the proposed shrinkage theory.

Other Influences Involved in Shrinkage - Swelling

The discussion of the shrinkage theory in this paper has been limited to a state of static equilibrium. Actually, however, the conditions are never static, since the cement is always either losing or gaining moisture. The water film on the drying side of cement grain is thinner than on the other side and in attempt to gain the equilibrium the water creeps or flows slowly along the surface from the moist side to the dry side. The outer parts of the drying specimen are always in a more advanced stage of drying and shrinkage than the inner parts, and so the values of the weight and length of the specimen at all but the extreme moist and the extreme dry stages represent the mean values of a wide range of conditions. This is another reason why the actual values of the film decrease - shrinkage ratio computed earlier should be regarded only as approximations.

Formation and dissolution of films is the major but not the only cause of shrinkage and swelling. Hydration is also a cause. Whether the nature of this phenomenon is purely chemical, or perhaps, partly physical, as the author thinks, hydration is never completed, and its progress is accompanied by linear and volumetric changes. No discussion of this important subject will be attempted here.

Another factor worthy of notice in connection with shrinkage and swelling is cracking. Some fine cracks are formed at various stages on nearly all specimens, especially the ones subject to a particularly high degree of shrinkage

and swelling. In this manner the author lost nearly all specimens made of cement finer than #325 mesh. Cracking is caused not by shrinkage and swelling proper, but by the non-uniformity of shrinkage and swelling, particularly the latter. Thus, if a dried prism is plunged in water it is likely to crack because it swells strongly at the surface while the centre still remains dry and therefore does not swell. The tension stresses thus set up in the interior region may be greater than the ultimate strength and so the material cracks. On the other hand, leaving a dry specimen in the open air causes a slower and more uniform absorption of moisture and swelling. A later immersion in water completes the saturation. The two-stepped procedure of this type is less severe as far as the integrity of the specimen is concerned than the early placement in water.

The most damaging operation from the viewpoint of cracking is the immersion in water after the specimen is saturated with an inert liquid like kerosene or oil. This is probably due to a particularly sharp division between the swollen and unswollen parts of the specimen, since the adsorption of moisture takes place through the mechanism of the water film advancing slowly along the surface of cement grains. On the other hand, when a dry specimen, devoid of inert liquid, is placed in water the transition between the swollen and the unswollen regions is probably less abrupt. It is believed that cracking of prismatic cement specimens of the type used in these studies cannot be completely avoided, although it can be reduced by proper precautions. Mortar specimens do not seem to crack on drying and possibly not on wetting.

Cracking of course is very damaging to the cement strength particularly the tension and the bending strengths. As to its effect on the volume - shrinkage graphs it appears to be small. There are usually no more than one or two cracks on any face of the prism, and the crack on one face is almost never matched by a crack on another face at the same section. Complete drying usually closes the crack and makes it inconspicuous. The thickest crack observed was about 0.0007" but usually the cracks are smaller—0.0002" or 0.0003". Compared to the total change in length of a 4" specimen in the course of drying or wetting, equal at least to 0.01" and usually 0.02" or more, the effect of cracking on the shape of the volume - shrinkage graphs seems small. This is corroborated by a close similarity of the shrinkage and swelling curves of similar specimens subjected to similar conditions. One would think that appreciable variations in the shape of the graphs would be observed, had the effect of cracking, which by its nature is a random phenomenon, been substantial.

Creep

The shrinkage studies were undertaken in consequence to the earlier studies of creep in cement, and their results have a direct bearing on creep. As explained earlier, the moist cement grains are surrounded by films of adsorbed water. The films are depressed at the point to point contacts of grains in response to their intergranular attractions, delicately balanced against the repulsions produced by the film pressure. With water films in between, the cement grains do not bear on each other directly. The film water, being under a strong attraction of cement, is not a liquid but a plastic solid.

With this picture in mind it is easy to see what happens when a moist cement is subjected to compression. On application of the load, cement grains

and water films deform as solid elastic bodies. The films directly between the grains are so thin in relation to grains that they have practically no effect on the elastic deformation. This explains the equality of the moduli of elasticity and Poisson's ratios for moist and dry cements during the rise or fall of load.(1) The compression load increases the force tending to bring the grains closer together in the direction of the load. Before the application of the load this force is A, - the grain to grain attraction. After the application of the load this force is A + G, the latter term being the effect of the applied load. The force of repulsion of the grains, caused by the film pressure, is still A, and consequently it is too small to balance the opposing force, A + C. In order to re-establish the equilibrium the water in the film flows slowly as a plastic solid bring the grains closer together, while raising the attraction force to a greater value A_1 and the repulsion to a still greater value $A_1 + C$. This slow adjustment of cement films is the creep.

While the creep phenomenon thus agrees well in general with the shrinkage theory, some details of it still require further study for their explanation.

CONCLUSION

All preceeding discussion is based on observations of shrinkage and swelling of cement prisms 3/4" x 3/4" x 4" subjected to various conditions of drying and wetting, and described by means of graphs whose abscissae represent the internal volumes emptied or filled by the liquid, and the ordinates—the corresponding changes in length of prisms. The shapes of these graphs, and especially the behaviour of prisms after placing them first in inert liquid and later in water, suggest the explanation for the volumetric changes in the form of the active water theory, according to which the water films are responsible for shrinkage, swelling and creep in cement. A detailed discussion of mechanical action of film water in the light of the theory is given. The theory is confirmed by the experimental evidence related to the behaviour of the drops of water and kerosene on the cement surface and the rise of these liquids in dry cement. Partial additional corroboration is also provided by the plausibility of explanation of the quantitative relation between the amount of shrinkage and the loss of water.

The volume - shrinkage graphs contain a wealth of information still largely unutilized and even undigested. They represent the outward manifestations of the physical and mechanical properties of cement and of the inner behaviour of this material under a variety of conditions. A change in the fineness and kind of cement, water - cement ratio, conditions of hydration and drying, age, saturation with various inert liquids and other factors are immediately reflected in the shape of the curves, giving information to the experimenter from which to deduce the basic nature of the material and the laws governing it.

Some peculiarities of the volume - shrinkage graphs still remain mysteries requiring further study, others have been explained but their discussion is postponed till a later opportunity.

ACKNOWLEDGEMENT

The experimental work described here has been conducted in the Materials Testing Laboratory, Department of Civil Engineering, the University of British Columbia. The work has been given generous financial assistance by

the Department of Building Research, The National Research Council of Canada. The author wishes to express his deep appreciation for this assistance to the President of the National Research Council, Dr. E. W. R. Steacie, to the Director of Building Research, Dr. R. F. Legget, and to the Assistant Director of Building Research, Dr. N. B. Hutcheon.

The author also wishes to thank Mr. J. F. Muir, Head, Department of Civil Engineering, The University of British Columbia for his cooperation in making available to the author the laboratory and shop facilities of the Department.

REFERENCES

1. Incremental Compression Test for Cement Research, by A. Hrennikoff, M. ASCE. Journal of the Engineering Mechanics Division, ASCE, April 1958.
2. Hydraulic Pressure in Concrete by T. C. Powers, paper No. 742, volume 81, Proceedings ASCE, July 1955.
3. Studies of the physical properties of Hardened Portland Cement Paste by T. C. Powers and T. L. Brownyard, Bulletin 22, Research Laboratories of the Portland Cement Association.
4. Chemistry of Portland Cement by R. H. Bogue, 2nd edition, Reinhold Publishing Corp. 1955, p. 627.
5. Concrete Information #ST4, Portland Cement Association.
6. Discussion by A. Hrennikoff: "Hydraulic Pressure in Concrete" by T. C. Powers, paper No. 742, volume 81, Proceedings ASCE, July 1955.
7. Elementary Mechanics of Fluids by Hunter Rouse, Wiley & Sons, 1946, p. 319.
8. Fundamentals of Hydro- and Aeromechanics by Prandtl & Tietjens, McGraw-Hill, 1934, p. 65.
9. Elementary Mechanics of Fluids by Hunter Rouse, Wiley & Sons, 1946, p. 361.

Journal of the
ENGINEERING MECHANICS DIVISION
Proceedings of the American Society of Civil Engineers

CONTENTS

DISCUSSION

Note: Paper 2099 is part of the copyrighted Journal of the Engineering Mechanics Division, Proceedings of the American Society of Civil Engineers, Vol. 85, EM 3, July, 1959.

ECCENTRICALLY LOADED, HINGED STEEL COLUMNS[a]

Discussion by Theodore R. Higgins
Closure by Richard E. Mason, Gordon P. Fisher, and George Winter

THEODORE R. HIGGINS,[1] F. ASCE.—The test data presented by the authors add further evidence that remarkably accurate predictions of column behavior are feasible when—and only when—all of the factors influencing this behavior have been accurately estimated, and provided the member is braced so as to eliminate premature lateral-torsional buckling. Of greater interest, perhaps, than the new data are the authors' conclusions, drawn largely from these and earlier observations.

Unless carefully read, the statement that the simple, widely used interaction formula of Type I is unconservative can lead to misunderstanding. Obviously, the type of formula can yield unconservative or grossly overconservative results, depending upon the values chosen for P' and M'. The AISC Specification for the Design, Fabrication and Erection of Structural Steel for Buildings is one of the several widely used design codes containing the type; so far as the writer is aware, the authors' equation (I) is not currently in use anywhere.

In Table 6 the data presented in Table 3 have been revised in terms of the AISC interaction formula, and also in terms of the same formula modified by injecting the factor $(1 - P/P_E)$. The following observations, derived from Table 6, should be compared with those given in Table 5.

Type of Observation	Range of Observations	Arithmetic Mean	Standard Deviation	Coefficient of Variation
Interaction Type I	0.926 to 1.193	1.057	0.0707	6.68%
Interaction Type II	1.117 to 1.384	1.236	0.0632	5.12%

To eliminate yield point as a factor in computing values for F_a corresponding to the slenderness ratios used in the tests, the following expressions were substituted for the usual AISC formula, which is based upon a yield stress of 33,000 psi:

a. Proc. Paper 1792, October, 1958, by Richard E. Mason, Gordon P. Fisher and George Winter.

1. Director of Eng. and Research, American Inst. of Steel Construction, New York, N. Y.

When σ_{ys} = 42,500 psi, F_a = $22{,}000 - 0.830\left[\frac{L}{r}\right]^2$

When σ_{ys} = 44,500 psi, F_a = $23{,}000 - 0.900\left[\frac{L}{r}\right]^2$

When σ_{ys} = 39,000 psi, F_a = $20{,}000 - 0.695\left[\frac{L}{r}\right]^2$

TABLE 6

INTERACTION FORMULAS - AISC WORKING STRESS RECOMMENDATIONS

Specimen t x b (in.)	L/r	$\frac{ec}{r^2}$	(1) $\frac{f_a}{F_a}$	(2) $\frac{f_b}{F_b}$	Type I Sum of (1)+(2)	(3) $\frac{f_b}{F_b(1-P/P_E)}$	Type II Sum of (1)+(3)
1/4 x 3	49	0.25	0.936	0.184	1.120	0.245	1.181
1/4 x 3	69	0.25	0.936	0.166	1.102	0.298	1.234
1/4 x 3	108	0.25	0.941	0.113	1.054	0.435	1.376
1/4 x 3	49	0.75	0.688	0.405	1.093	0.495	1.183
1/4 x 3	69	0.75	0.662	0.352	1.014	0.512	1.174
1/4 x 3	108	0.75	0.715	0.260	0.975	0.594	1.309
1/4 x 3	49	1.50	0.506	0.600	1.106	0.692	1.198
1/4 x 3	69	1.50	0.497	0.530	1.027	0.693	1.190
1/4 x 3	108	1.50	0.539	0.393	0.932	0.684	1.223
1/4 x 4	36	0.25	0.988	0.205	1.193	0.242	1.230
1/4 x 4	66	0.25	0.945	0.171	1.116	0.302	1.247
1/4 x 4	110.5	0.25	0.917	0.105	1.022	0.405	1.322
1/4 x 4	36	0.75	0.711	0.442	1.153	0.497	1.208
1/4 x 4	66	0.75	0.660	0.360	1.020	0.516	1.176
1/4 x 4	110.5	0.75	0.688	0.238	0.926	0.537	1.225
1/4 x 4	36	1.50	0.485	0.607	1.092	0.657	1.142
1/4 x 4	66	1.50	0.468	0.510	0.978	0.649	1.117
1/4 x 4	110.5	1.215	0.605	0.339	0.944	0.665	1.270
1/2 x 3	53	0.25	0.973	0.185	1.158	0.254	1.227
1/2 x 3	74	0.25	0.955	0.162	1.117	0.303	1.258
1/2 x 3	117	0.25	0.956	0.105	1.061	0.428	1.384
1/2 x 3	53	1.50	0.532	0.605	1.137	0.710	1.242
1/2 x 3	74	1.50	0.513	0.524	1.037	0.699	1.212
1/2 x 3	117	1.50	0.595	0.393	0.988	0.742	1.337

Values given in column (1) in Table 6 were obtained by dividing the test value for Pult listed in Table 2 by 1.65 A.F_a. As used in Table 3, M' is the plastic hinge moment. To convert the values for M/M' given in Table 3 to those comparable with the f_b/F_b term in the AISC interaction formula it is only necessary to multiply them by the ratio of plastic bending modulus to section modulus.

It is seen that, taken in context with the rest of the code of which it is currently a part, the simple interaction formula predicts the test results reported by the authors with about the same accuracy as do the secant formula, the Bijlaard method, and the authors' equation (II). On the other hand, when the AISC working stress provisions are placed in the Type II formula errors ranging from 12 to 38 percent on the wasteful side are indicated by the same

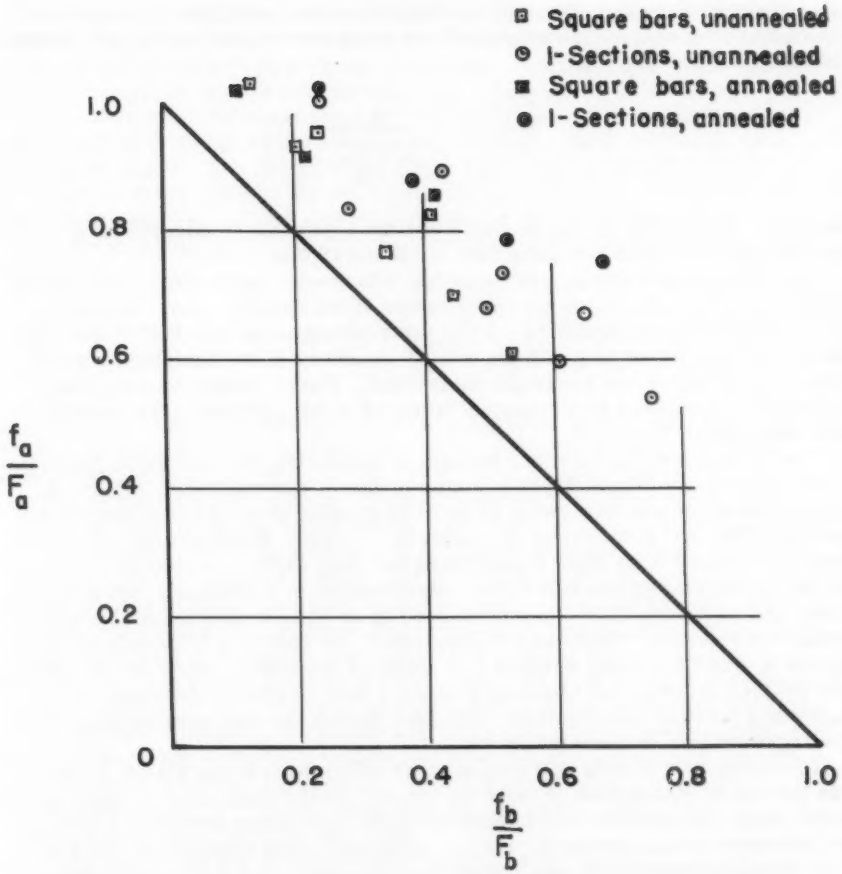

Figure 9

End-restrained Eccentric Columns

data. Using the same simple interaction formula, it is seen, in Fig. 9, that predictions by the AISC method are all on the conservative side of the test results presented in Fig. 7 for the 22 end-restrained columns whose plastic bending modulus was equal to 1.5 times their section modulus. Based upon the data presented, there would appear to be little to recommend the injection of the $1/(1 - P/P_E)$ factor into the AISC Specification, unless at the same time the more liberal stress functions proposed by the authors are also adopted.

It is interesting to note that a Type II interaction formula was suggested nearly sixty years ago(2) and included in at least one well-known design

specification[3] prior to the earliest adoption of the AISC Specification. As applied to compression members subject to combined axial and direct stress, this formula was given as

$$S = \frac{P}{A} + \frac{M.c}{I - \frac{P.L^2}{10E}}$$

where S, the working stress in compression, applicable to both the axial and the bending term, was not permitted to exceed 16,000 - 70L/r.

That this earlier design provision fell into disuse can be explained by the unwarranted complexity of the denominator of the bending term. The precision implicit in the factor $(1 - P/P_E)$ was incongruous with that of the working stress provisions and with the overall accuracy of the analysis by which values for M and P are generally determined. Hence, resort to a simpler expression, protected by a generous factor of safety, proved more popular with designers.

The development of functions capable of predicting the strength of laterally and torsionally braced beam-columns of known end-restraint, subject to direct load alone and to bending alone, with greater accuracy than heretofore, has again focused attention on the factor $(1 - P/P_E)$. However, specification provisions based upon these refinements will only place an added burden on the designer, without commensurate improvement in the balance between safety and economy, unless complemented by an equally precise evaluation of actual end restraint. When so complemented, the resulting improvement in accuracy would certainly warrant a re-study of necessary safety factor. Despite the lack of precision in existing rules, a vast number of columns, designed and erected in compliance with them during the past quarter of a century, have proven remarkably safe.

It is of interest to note that only through recognition of the plastic rather than the elastic properties of their specimens, as the criteria of flexural behavior, were the authors able to achieve close correlation between computed and observed column strength. By the extension of this observation the use of an allowable bending stress, higher than that permitted for axial tension, can also be justified, providing the resulting deformations are kept under control.

REFERENCES

2. The Theory and Practice of Modern Framed Structures, Seventh Edition (1901) by J. B. Johnson, C. W. Bryan and F. E. Turneaure - John Wiley & Sons.

3. The Design of Steel Mill Buildings, Fourth Edition (1921) by Milo S. Ketchum - McGraw Hill Book Co.

RICHARD E. MASON,[1] GORDON P. FISHER,[2] F. ASCE AND GEORGE WINTER,[3] F. ASCE.—It was the purpose of the writers to present test data on eccentric columns of a practically important type not hitherto investigated, and to compare these data with various theoretical methods of strength prediction. They have refrained from discussing the possible applications of these findings to any particular design codes, since this is not the purpose of a research report. Mr. Higgins' remarks, which deal precisely with the implications of these tests in regard to the AISC Specification, are most welcome as an indication of the practical relevance of this investigation.

Mr. Higgins attempts to demonstrate that the AISC interaction formula of Type I, i.e.

$$\frac{f_a}{F_a} + \frac{f_b}{F_b} = 1$$

gives safe results of satisfactory accuracy and that, on the other hand, the Type II formula is overly conservative when applied to these tests. This demonstration is achieved, however, by utilizing a safety factor of 1.65 in connection with the AISC column formula, whereas the actual safety factor for this formula is easily demonstrated to be not 1.65 but 2.0 (within a range of a few percent depending on L/r). It is now established, and so stated by the AISC, that for beams the safety factor in that specification is 1.85 (see Plastic Design in Steel, Am. Inst. of Steel Construction, 1959, p. 2). The Specification conforms with general practice in maintaining a slightly higher safety factor (2.0) for compression members than for flexural members and the framers of this specification would be the first to object if it were implied that the reverse is true. As will be shown below, if the correct safety factor of 2.0 is used in connection with the AISC column formula, then the AISC interaction formula, utilized in exactly the same manner as was done by Mr. Higgins, gives unconservative results when applied to the present tests. In fact this is so for 20 of the 24 eccentric column tests, with deviations on the unconservative side ranging up to 20%.

It is evident that for an interaction formula to be consistent, the terms P' and M' cannot be arbitrarily "chosen" as implied by the discussor, but must represent, to the best of available knowledge, the calculated strength of the particular member when loaded as a concentric column on the one hand (P'), and as a flexural member on the other (M'). For the hinged specimens at hand it is well established that M' must be the plastic moment of the section, and P' either the Euler value for long columns or the Engesser-Shanley value for short columns, the latter accounting for the influence of residual stresses (see Column Research Council: "The Basic Column Formula," Techn. Memo. No. 1, 1952). These values have been so used by the writers, and Mr. Higgins' transformation of the f_b/F_b term in the AISC formula correctly incorporates M' into his evaluation.

However, by using $P' = 1.65 \cdot A \cdot F_a$ as the denominator of the first term, Mr. Higgins maintains that the actual strength of a concentric, hinged, column

1. Asst. Prof., Dept. of Structural Engineering., Cornell Univ., Ithaca, N. Y.
2. Associate Prof., Dept. of Structural Eng., Cornell Univ., Ithaca, N. Y.
3. Prof. and Head, Dept. of Structural Eng., Cornell Univ., Ithaca, N. Y.

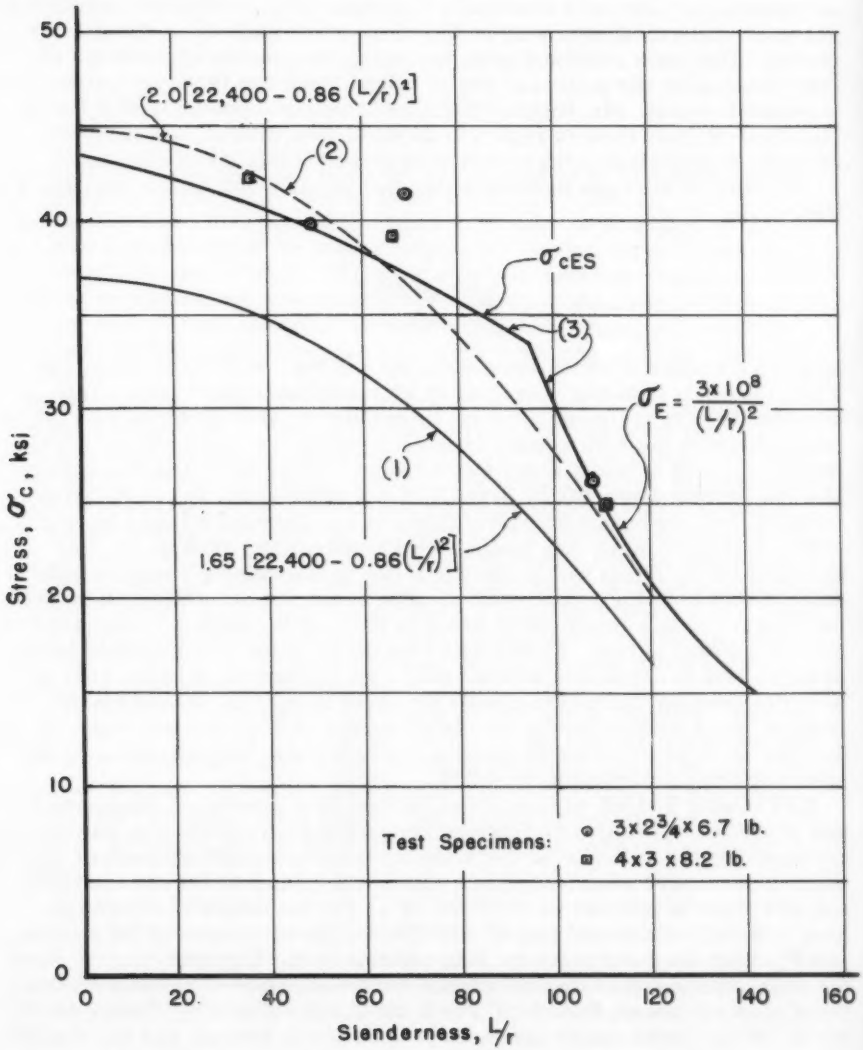

Figure 10 Concentric Columns

is satisfactorily predicted by multiplying the AISC value by 1.65. It is easily demonstrated that this is not so. A very short concentric column ($L/r \rightarrow 0$) evidently fails by simple yielding. Since the specified minimum yield point for ASTM A-7 steel is 33 ksi and the AISC column stress for $L/r = 0$ is 17 ksi, the latter must be multiplied by $33/16 = 1.94$ (rather than 1.65) to result in the correct strength. On the other hand for a long concentric column, say $L/r = 120$, the Euler stress is 20.56 ksi and the AISC allowable stress 10.02 ksi so that the latter must be multiplied by $20.56/10.02 = 2.05$ (rather than 1.65) to result in the correct strength. This, is an abbreviated way, demonstrates that, with minor deviations, the load factor implied in the AISC formula is 2.0.

The correctness of this fact is demonstrated further by evaluating the six concentric columns tests reported in Table 4 of the paper. For these two types of specimens the actual yield points were within 5% of each other, so that it is justified to take the average yield point, 43.5 ksi, for all six tests. For this yield point the AISC formula, modified exactly as was done by Mr. Higgins, becomes

$$F_a = 22{,}400 - 0.86\,(L/r)^2$$

This expression is bracketted, as it must be, by his formulas for the two pertinent steels with 42.5 and 44.5 ksi, respectively. Figure 10 shows the results of the six concentric tests of Table 4. Curve (1) of Fig. 10 shows the above AISC formula as used by Mr. Higgins, i.e. multiplied by 1.65. It is seen that this strength prediction is completely at variance with the tests and underestimates the real column capacities by a wide margin. Therefore, it cannot be used for P' in the interaction formula. On the other hand, curve (2) of Fig. 10 shows that same AISC formula multiplied by the correct load factor 2.0. It is seen that this curve agrees reasonably well with the concentric test results even though it implies considerably larger residual stresses than were present in the specimens. Also shown is curve (3) for σ_{cES} and σ_E as used by the writers for determining P'. It is seen to be in satisfactory agreement with these concentric tests although it is evident that this curve, likewise, is based on larger residual stresses than were actually present. This was noted in the paper and accounts for the deviation of σ_{cES} on the low side in the range of moderate L/r-ratios.

Having thus established, by theory and by comparison with tests, that the load factor applicable to the AISC column formula is 2.0 rather than 1.65, the writers have recalculated Mr. Higgins' Table 6 on this basis. The results are shown in Table 7, which was obtained from Table 6 by multiplying the f_a/F_a values by 1.65/2.0. It is seen, as mentioned before, that the AISC interaction formula of Type I overestimates the strength of all but four of the 24 test columns, by margins up to 20%. On the other hand, the Type II formula is conservative in all cases, in many instances by a considerable margin which is due to the excessively low proportional limit implied in the Higgins-AISC formula (when applied to these tests).

Evaluating Table 7 in the same manner as the discussor did with Table 6, the following distribution characteristics are obtained:

Type of Observation	Range of Observations	Arithmetic Mean	Standard Deviation	Coefficient of Variation
Interaction Type I	0.806 to 1.020	0.929	0.0655	7.06%
Interaction Type II	1.017 to 1.233	1.109	0.0589	5.31%

which confirm the above conclusions.

The same corrections of Mr. Higgins' evaluation should be applied to his Fig. 9, concerning the tests of the end-restrained columns given on Figs. 7 and 8 of the paper. There seems to be no point in carrying out these identical corrections for this set of tests, since their result is evidently of the same nature as just demonstrated for the hinged columns.

While the writers believe to have shown that Mr. Higgins' re-evaluation of their tests is distorted by an oversight in regard to the true safety factor of the relevant AISC formula, they appreciate Mr. Higgins' attention to these tests and the thoughtfulness expended on analyzing their implications on practical column design.

Typographical errors in original paper:

Page 8 Coefficient of second term of expression for σ_{cES} should be 5,000 (instead of 50,000).

Page 9 first line, inequality should read

$$(L/r)_c > L/r > (L/r)_c - 30$$

Page 10 line 14 from bottom. Expression in denominator of second term should be $(1 - P/P_E)$ (instead of $(1 + P/P_E)$).

TABLE 7

MR. HIGGINS' TABLE 6 CORRECTED FOR AISC COLUMN FACTOR OF SAFETY = 2.0 *

Specimen t x b (in.)	L/r	$\frac{ec}{r^2}$	(1) fa/Fa	(2) fb/Fb	Type I Sum of (1)+(2)	(3) $\frac{fb}{F_b(1-P/P_E)}$	Type II Sum of (1)+(3)
1/4 x 3	49	0.25	0.772	0.184	0.956	0.245	1.017
1/4 x 3	69	0.25	0.772	0.166	0.938	0.298	1.070
1/4 x 3	108	0.25	0.776	0.113	0.889	0.435	1.211
1/4 x 3	49	0.75	0.568	0.405	0.973	0.495	1.063
1/4 x 3	69	0.75	0.546	0.352	0.898	0.512	1.058
1/4 x 3	108	0.75	0.590	0.260	0.850	0.594	1.184
1/4 x 3	49	1.50	0.417	0.600	1.017	0.692	1.109
1/4 x 3	69	1.50	0.410	0.530	0.940	0.693	1.103
1/4 x 3	108	1.50	0.445	0.393	0.838	0.684	1.129
1/4 x 4	36	0.25	0.815	0.205	1.020	0.242	1.057
1/4 x 4	66	0.25	0.780	0.171	0.951	0.302	1.082
1/4 x 4	110.5	0.25	0.757	0.105	0.862	0.405	1.162
1/4 x 4	36	0.75	0.587	0.442	1.029	0.497	1.084
1/4 x 4	66	0.75	0.545	0.360	0.905	0.516	1.061
1/4 x 4	110.5	0.75	0.568	0.238	0.806	0.537	1.105
1/4 x 4	36	1.50	0.400	0.607	1.007	0.657	1.057
1/4 x 4	66	1.50	0.386	0.510	0.896	0.649	1.035
1/4 x 4	110.5	1.215	0.499	0.339	0.838	0.665	1.164
1/2 x 3	53	0.25	0.803	0.185	0.988	0.254	1.057
1/2 x 3	74	0.25	0.788	0.162	0.950	0.303	1.091
1/2 x 3	117	0.25	0.789	0.105	0.894	0.428	1.217
1/2 x 3	53	1.50	0.439	0.605	1.044	0.710	1.149
1/2 x 3	74	1.50	0.423	0.524	0.947	0.699	1.122
1/2 x 3	117	1.50	0.491	0.393	0.884	0.742	1.233

* F. S. = 2.0 = Average of 1.94 (at $L/r = 0$) and 2.05 (at $L/r = 120$)

SIMPLIFICATION OF DIMENSIONAL ANALYSIS[a]

Discussion by Enzo Oscar Macagno

ENZO OSCAR MACAGNO,[1] AFF. ASCE.—The authors' paper is a contribution to simplified ways of obtaining dimensionless variables, and includes some wise remarks about dimensional analysis.

For a long time and in many publications the rule mentioned by the authors in Step 2 has been given. The writer wishes to point out that although the rule works in most of the cases, it is not correct and fails sometimes. For instance, if we are asked to find an expression for the velocity c of propagation of elastic waves which is assumed to depend upon the specific mass ρ and the bulk modulus of elasticity E of a fluid, the matrix will be

	c	ρ	E
F	0	1	1
L	1	-4	-2
T	-1	2	0

According to Step 2 there will be no dimensionless group because the number of variables is equal to the number of dimensions. In fact, we know the answer is given by $c/\sqrt{E/\rho}$ as the dimensionless group. The correct rule is based on r being the rank of the matrix, instead of the number of dimensions involved.

REFERENCE

G. Birkhoff - "Hydrodynamics," Princeton University Press, 1950, p. 82.

a. Proc. Paper 1898, January, 1959, by Charles C. Bowman and Vaughn E. Hansen.

1. Research Eng., Iowa Institute of Hydraulic Research, Iowa City, Iowa.

EM 3

JULY 1959 — 27 NO. EM 3
VOLUME 85 PART 2

Your attention is invited

NEWS OF THE ENGINEERING MECHANICS DIVISION OF ASCE

JOURNAL OF THE ENGINEERING MECHANICS DIVISION
PROCEEDINGS OF THE AMERICAN SOCIETY OF CIVIL ENGINEERS

DIVISION ACTIVITIES

ENGINEERING MECHANICS DIVISION

Proceedings of the American Society of Civil Engineers

NEWS

July, 1959

EMD PROGRAMS AT WASHINGTON, D. C. CONVENTION

Professor E. Popov has announced the program for three half day sessions at the October 19-23, 1959, ASCE Annual Convention sponsored exclusively by the Engineering Mechanics Division as well as six half day sessions co-sponsored with the Structural Division. The papers for these sessions are listed below.

Monday Morning—October 19—Column Research Symposium
D. C. Drucker, N. J. Hoff, G. S. Vincent, presiding

(1) "Column Research Council", B. G. Johnston, Univ. of Michigan.
(2) "Basic Column Strength", L. S. Beedle and L. Tall, Lehigh Univ.
(3) "Effective Length of Framed Columns", T. C. Kavanagh, New York City.

Monday Afternoon—October 19—Column Research Symposium
R. Archibald, presiding

(4) "Lateral Buckling of Beams", J. W. Clark and H. N. Hill, Aluminum Co. of America.
(5) "Postbuckling Strength and Effective Width of Plates in End Compression", J. R. Jombock and J. W. Clark, Aluminum Co. of America.
(6) "Buckling Problems in Plate Girders", K. Basler and B. Thurlimann, Lehigh Univ.

Tuesday Morning—October 20—Column Research Symposium
G. Winter, presiding

(7) "Effect of Residual Stress on Eccentrically Loaded Columns", R. Ketter, Univ. of Buffalo.
(8) "General Instability of Low Framed Buildings", J. E. Goldberg, Purdue Univ.
(9) "Beam-Columns", W. J. Austin, Univ. of Illinois.

Note: No. 1959-27 is part of the copyrighted Journal of the Engineering Mechanics Division, Proceedings of the American Society of Civil Engineers, Vol. 85, EM 3, July, 1959.

Tuesday Afternoon—October 20—Column Research Symposium
T. R. Higgins, presiding

(10) "The Effect of Floor System Participation on Top Chord Stresses of Single Span Pony Truss Bridges", R. M. Barnoff, Harrisburg, Pa.
(11) "Design of Pony Trusses", E. C. Holt, Rice Institute.
(12) "A Digest of Design Criteria for Metal Compression Members", B. G. Johnston, Univ. of Michigan.

(Monday and Tuesday sessions co-sponsored with Structural Division.)

Wednesday Afternoon—October 21—Fluid Dynamics—Mechanics of Stratified Flow. W. D. Baines, presiding

(1) Introductory Remarks, D. R. F. Harleman, M.I.T.
(2) "Stratified Flow Into a Line Sink for a Linear Density Gradient", W. R. Debler, Univ. of Michigan.
(3) "Irrotational Motion of Two Fluid Strata Towards a Line Sink", G. Huber, McMaster Univ., Ontario.
(4) "Internal Waves in a Stratified Fluid—A General Review", G. H. Keulegan, National Bureau of Standards.

Thursday Morning—October 22—Lightweight Construction in Metals
R. D. Dewell and D. H. Pletta, presiding

(1) "Welded Aluminum Bridges for Military Traffic", F. J. Tamanini and W. Keyes, Fort Belvoir, Va.
(2) "Tests of a Composite Aluminum and Concrete Highway Bridge", S. J. Errera and H. Mindlin, Lehigh Univ.
(3) "Design of Welded Aluminum Structures", H. N. Hill, J. W. Clark, and R. J. Brungraber, Aluminum Co. of America.
(4) "Strength of Welded Aluminum Columns", R. J. Brungraber and J. W. Clark, Aluminum Co. of America.

Thursday Afternoon—October 22—Lightweight Construction in Metals
E. F. Masur, presiding

(5) "Light Gage, Cold-Formed Steel Construction", G. Winter, Cornell Univ.
(6) "Stability of Thin-Gage Metal Structures", G. Gerard, New York Univ.
(7) "Postbuckling Behavior of Rectangular Plates", M. Stein, NASA, Langley Field, Va.
(8) "Large Deflection Vibration of Plates", G. Herrmann, Columbia Univ.

(Thursday sessions co-sponsored with Structural Division.)

Friday Morning—October 23—Structural Dynamics
R. J. Hansen, presiding

(1) "Dynamic Elastoplastic Response of Rigid Frames", F. L. DiMaggio, Columbia Univ.
(2) "Dynamic Effect of a Moving Load on a Rigid Frame", R. C. DeHart, Southwest Research Institute.
(3) "Effect of End Fixity on the Vibration of Rods", D. Burgreen, Nuclear Development Corp. of America.

Friday Afternoon—October 23—Analysis of Highly Redundant Structures by Experimental and Analogue Techniques. J. S. Archer, presiding

(1) "Electronic Models for Structural Vibrations with Elastic-Plastic Couplings", H. M. Paynter, American Center for Analogue Computing.
(2) "Aircraft Structural Analysis with the Electric Analogue Computer", W. J. Brignac and R. G. Schwendler, Convair, Fort Worth.
(3) "Arch Dam Analysis with the Electric Analogue Computer", R. H. MacNeal, Pasadena, Calif.
(4) "Elastic Model Design of the B-58 Airplane Structure", J. W. Wells and H. B. England, Convair, Fort Worth.

EMD PROGRAM AT ASCE—ASME WEST COAST CONFERENCE ON APPLIED MECHANICS

Four papers at this conference (Stanford, California, September 9-11) are sponsored by the Engineering Mechanics Division of ASCE. The complete program will be arranged from these papers (see final selection below) together with several papers sponsored by the Applied Mechanics Division of ASME.

(1) "Limit Analysis of Simply Supported Circular Shell Roofs", M. N. Fialkow, U. S. Army, New York.
(2) "Large Deflection of Elasto-Plastic Plates Under Uniform Pressure", Thein Wah, Southwest Research Institute.
(3) "On the Asymmetrical Bending of Conical Shells", B. Wilson, Univ. of Kansas.
(4) "Bending of Plates on a Viscoelastic Foundation", K. S. Pister, Univ. of California, Berkeley, and M. L. Williams, California Institute of Technology.

INTERNATIONAL SYMPOSIUM ON FLUID MECHANICS IN THE IONOSPHERE

Professor R. E. Fadum calls the divisions attention to the above symposium being held at Cornell University, July 8-15, 1959. Its aim is to bring together international experts in the fields of Fluid Mechanics and Ionospheric Physics with the intent of gaining a more complete and satisfactory understanding of the dynamical processes occurring in the ionosphere. Emphasis will be placed upon the phenomenon of turbulence and its effects.

The meeting is being sponsored by the International Scientific Radio Union together with the International Union of Theoretical and Applied Mechanics, the International Union of Geodesy and Geophysics, and the International Astronomical Union; and with support from UNESCO and the U. S. National Science Foundation.

The major part of the Symposium will be the sessions on Monday, Tuesday, and Wednesday, July 13-15. July 8-10 will be devoted to semi-formal presentations for the purpose of exchanging existing knowledge between the fields of Fluid Mechanics and Ionospheric Physics.

The organizing secretary for this meeting is R. Bolgiano, Jr., School of Electrical Engineering, Cornell University.

COLUMN PAPERS AVAILABLE

Column Research Council of the Engineering Foundation has released the following list of publications currently available from the Secretary of Column Research Council. Requests may be addressed to: Secretary, Column Research Council, 319 West Engineering, University of Michigan, Ann Arbor, Michigan.

"The Basic Column Formula"—Technical Memorandum No. 1

"Buckling of Columns", Mirko Ros

"Design Charts for Elastically Restrained Eccentrically Loaded Columns", A. E. Shabaan

"Determination of the Buckling Load for Columns of Variable Stiffness", C. C. Miesse

"Effect of Initial Eccentricities on Column Performance and Capacity", John M. Hayes

"German Buckling Specifications", T. V. Galambos and J. Jones

"German Buckling Specifications"—DIN 4114, Vol. 1—German Version

"German Buckling Specifications"—DIN 4114, Vol. 2—German Version

"Japanese Handbook on Elastic Stability" (in Japanese)

"Lateral Buckling of Eccentrically Loaded I- and H-Section Columns", H. N. Hill and J. W. Clark

"Notes on Compression Testing of Metals"—Technical Memorandum No. 2

"The Philosophy of Column Design"—Column Research Council

"The Stability of Bridge Chords Without Lateral Bracing", R. M. Barnoff and W. G. Mooney

"Study of Columns with Perforated Cover Plates", M. W. White and B. Thurlimann

"A Survey of Progress 1944-1951", B. G. Johnston and the Project Supervisors

"Tests and Analysis of Eccentrically Loaded Columns", R. E. Mason, G. P. Fisher and G. Winter

EARLY TRANSACTIONS VOLUMES OBTAINABLE

The feasibility of reproducing the first ten volumes of ASCE Transactions (1872-1881) has been studied. It has been decided that these historic volumes could be reproduced at a cost that would permit a top price of $150 for the ten-volume set. If more than 100 engineers, or libraries, indicate an interest in obtaining such a set, the project will be undertaken. If the endeavor is successful, other rare volumes of Transactions will be reprinted.

Engineers interested in obtaining the ten-volume set should write to the Executive Secretary of ASCE, 33 West 39th Street, New York 18, N. Y.

NEWS ITEMS FOR OCTOBER LETTER

Items to be considered for the EMD Newsletter circulated with the July Journal must be on your editor's desk not later than August 25, 1959.

Donald L. Dean, Newsletter Editor, EMD
Department of Civil Engineering
University of Kansas
Lawrence, Kansas